EFFECTS OF PRIOR AGING AT 260 °C IN ARGON ON INELASTIC DEFORMATION BEHAVIOR OF PMR-15 POLYMER AT 260 °C: EXPERIMENT AND MODELING

THESIS

Bradley K. Diedrick, Second Lieutenant, USAF
AFIT/GAE/ENY/10-M08

DEPARTMENT OF THE AIR FORCE
AIR UNIVERSITY

AIR FORCE INSTITUTE OF TECHNOLOGY

Wright-Patterson Air Force Base, Ohio

AFIT/GAE/ENY/10-M08

EFFECTS OF PRIOR AGING AT 260 °C IN ARGON ON INELASTIC DEFORMATION BEHAVIOR OF PMR-15 POLYMER AT 260 °C: EXPERIMENT AND MODELING

THESIS

Presented to the Faculty

Department of Aeronautics and Astronautics

Graduate School of Engineering and Management

Air Force Institute of Technology

Air University

Air Education and Training Command

In Partial Fulfillment of the Requirements for the

Degree of Master of Science in Aeronautical Engineering

Bradley Diedrick, BAE

Second Lieutenant, USAF

March 2010

AFIT/GAE/ENY/10-M08

EFFECTS OF PRIOR AGING AT 260 °C IN ARGON ON INELASTIC DEFORMATION BEHAVIOR OF PMR-15 POLYMER AT 260 °C: EXPERIMENT AND MODELING

Bradley K. Diedrick, BAE
Second Lieutenant, USAF

Approved:

Dr. Marina B. Ruggles-Wrenn (Chairman)	date
Richard B. Hall (Member)	date
Greg A. Schoeppner (Member)	date

Abstract

The purpose of this research was to investigate the inelastic deformation behavior of PMR-15 neat resin, a high-temperature polymer, at 260 °C. The experimental program was designed to explore the influence of strain rate on loading and unloading behaviors. In addition, the effect of prior strain rate on creep, relaxation, and recovery responses was evaluated. The material exhibits positive, nonlinear strain rate sensitivity in monotonic loading. Early failures occur before fully establishing inelastic flow. The creep, relaxation, and recovery responses are significantly influenced by prior strain rate.

The experimental results suggest the behavior of PMR-15 at 260 °C can be effectively modeled using a unified constitutive model with an overstress dependence of inelastic rate deformation. The experimental data were modeled using the Viscoplasticity Based on Overstress for Polymers (VBOP) theory. The lack of data in the inelastic region inhibited the application of the VBOP. The deformation behavior of PMR-15 at 260 °C was modeled well despite this lack of data. The effects of prior aging in argon at 260 °C on the time (rate)-dependent behavior of the PMR-15 polymer were evaluated in a series of strain controlled experiments. Several of the VBO material parameters were expanded as functions of prior aging time. The resulting model was used to predict the behavior of PMR-15 subjected to various prior aging durations.

Acknowledgements

I would like to extend my sincerest thanks to my faculty advisor, Dr. Marina Ruggles-Wrenn. This thesis would not have been possible without her assistance and guidance. I would also like to thank my committee members: Dr. Hall and Dr. Schoeppner. I owe a special thanks to the AFIT Materials Testing Laboratory staff consisting of Jay Anderson and Barry Page for ensuring my testing equipment was working properly at all times, and for fixing it when necessary. I would like to thank John Hixenbaugh for his assistance with everything needed for the aging process. I would like to convey my gratitude to Amber McClung for her willingness to assist with the modeling process. And finally, I would be remiss if I did not thank my friends and family for their support throughout this process. Without them, my sanity and production would have been lost.

Bradley K Diedrick

Table of Contents

Page

Abstract iv

Acknowledgements v

Table of Contents vi

List of Figures x

List of Tables xvii

List of Symbols xviii

I. Introduction 1

II. Background 3

Polymer Matrix Composites 3
Polymer Aging 4
Problem Statement 6
Thesis Objective 6
Methodology 7
Previous Research: Experimental Investigations 8
PMR-15 – Mechanical Behavior *8*
PMR-15 - Mechanical Behavior at 288 °C 8
PMR-15 – Mechanical Behavior at 316 °C 9
Prior Aging – Effects on Mechanical Behavior *10*
PMR-15- Effect of Prior Aging at 288 °C 10
PMR-15- Effect of Prior Aging at 316 °C 12
Previous Research: Constitutive Modeling 13
Viscoplasticity Based on Overstress *13*
Viscoplasticity Based on Overstress for Polymers *17*
Viscoplasticity Based on Overstress for Polymers with Prior Aging *21*

III. Theoretical Formulation of Viscoplasticity Based on Overstress for Polymers 24

Basis of Viscoplasticity Based on Overstress – Standard Linear Solid 24
Viscoplasticity Based on Overstress 25
Viscoplasticity Based on Overstress for Polymers 27

IV. Material and Test Specimen 31

PMR-15 (Polymerization of Monomeric Reactants – 15) 31
Specimen Geometry 32
Specimen Preparation 33

V. Experimental Setup and Testing Procedures 34

Mechanical Testing Equipment 34
Test Procedures 34
Room Temperature Elastic Modulus *34*
Temperature Calibration *35*
Monotonic Tensile Test at Constant Strain Rate *35*
Loading Followed by Unloading at Constant Strain Rate *36*
Recovery of Strain at Zero Stress *36*
Constant Strain Rate Test with a Period of Relaxation *37*
Creep Test *37*
Strain Rate Jump Test *37*
Isothermal Aging 38
Weight Measurements 38

VI. Unaged PMR-15 Neat Resin: Experimental Observations 39

Assessment of Specimen-to-Specimen Variability 39
Monotonic Stress-Strain Behavior at Various Constant Strain Rates at Room Temperature 39
Monotonic Stress-Strain Behavior at Various Constant Strain Rates at 230 °C 40
Deformation Behavior at 260 °C 41
Monotonic Tension to Failure *42*
Loading and Unloading *43*
Recovery of Strain at Zero Stress *46*
Constant Strain Rate Test with a Period of Relaxation *47*
Creep Test *50*
Strain Rate Jump Test *51*
Comparison of Deformation Behavior at Different Temperatures 53

VII. Unaged PMR-15 Neat Resin: Constitutive Modeling 56

Phenomenological Aspects of Deformation Behavior and Implications for Modeling 56
Review of Model Formulation 57
Model Characterization Procedure 59
Elastic Modulus and Tangent Modulus *59*

Equilibrium Stress and Isotropic Stress *60*
Viscosity Function *61*
Shape Function *62*
Model Verification 64

VIII. Aged PMR-15 Neat Resin: Experimental Observations 70

Weight Loss Measurements 70
Deformation Behavior at 260 °C of PMR-15 Subjected to Prior Aging 71
Monotonic Tension to Failure *71*
Constant Strain Rate Test with a Period of Relaxation *81*
Creep Test *84*
Strain Rate Jump Test *89*
Summary of Key Effects of Prior Aging at 260 °C on Deformation Behavior at 260 °C 90
Comparison of the Effects of Prior Aging at 260 °C with the Effects of Prior Aging at Other Temperatures 91

IX. Aged PMR-15 Neat Resin: Constitutive Modeling 93

Implications for Modeling the Effects of Prior Aging at 260 °C 93
Characterization of Model Parameters for PMR-15 Neat Resin Subjected to Prior Aging at 260 °C 94
Prior Aging for 100 h *95*
Prior Aging for 250 h *100*
Model Parameters as Functions of Aging Time 104
Predictions of Deformation Behavior of the PMR-15 Neat Resin Subjected to Prior Aging 109
Prior Aging for 500 h *109*
Prior Aging for 1000 h *113*
Prior Aging for 2000 h *117*

X. Conclusions and Recommendations 122

Concluding Remarks 122
Comparison with Previous Efforts 125
Recommendations 127

Appendix A: MATLAB Scripts for Optimizing Viscosity Function 128

Appendix B: MATLAB Scripts for Optimizing Shape Function 135

Appendix C: MATLAB Scripts for Power Law Curve Fitting of Model Parameters 140

Bibliography 141

List of Figures

Page

Figure II.1: Creep Strain Versus Time at 20 MPa and 288 °C for PMR-15 Aged at 288 °C in Argon. Reproduced from Broeckert [6]. 11

Figure II.2: Stress-Strain Curves Obtained in Monotonic Tension to Failure Tests Conducted at a Strain Rate of 10^{-6} s^{-1} for PMR-15 Aged in Argon at 288 °C. Reproduced from McClung [23]. 12

Figure II.3: Stress-Strain Curves Obtained in Monotonic Tension to Failure Tests Conducted at a Strain Rate of 10^{-6} s^{-1} for PMR-15 Aged in Argon at 316 °C. Reproduced from Ozmen [24]. 13

Figure II.4: Viscoelastic and Viscoplastic Stress-Strain Behavior. Reproduced from Ozmen [24]. 14

Figure II.5: Standard Linear Solid Stress-Strain Behavior. Equilibrium Stress and Overstress Concepts are Depicted. Reproduced from Ozmen [24]. 16

Figure II.6: Relaxation Behavior of Unaged PMR-15 at 288 °C Described by Experimentation and the VBOP. Reproduced from McClung [21]. 18

Figure II.7: Stress-Strain Behavior of Unaged PMR-15 at 288 °C in Monotonic Tension to Failure Tests Described by Experimentation and the VBOP. Reproduced from McClung [21]. 19

Figure II.8: Stress-Strain Behavior of Unaged PMR-15 at 288 °C in the Strain Rate Jump Test Described by Experimentation and the VBOP. Reproduced from McClung [21]. 19

Figure II.9: Stress-Strain Behavior of Unaged PMR-15 at 288 °C in Loading Followed by Unloading Described by Experimentation and the VBOP. Reproduced from McClung [21]. 20

Figure II.10: Creep Behavior of Unaged PMR-15 at 288 °C Described by Experimentation and the VBOP. Reproduced from McClung [21]. 20

Figure II.11: Creep Behavior of Unaged PMR-15 at 316 °C Described by Experimentation and the VBOP. Reproduced from Ozmen [24]. 21

Figure II.12: Comparison Between Experimental Results and Predicted Stress-Strain Curves for PMR-15 Aged at 288 °C for 2000 h in Tension to Failure Test. Reproduced from McClung [23]. 23

Figure II.13: Comparison Between Experimental Results and Predicted Creep Response for PMR-15 Aged at 288 °C for 2000 h in Creep Test. Reproduced from McClung [23]. 23

Figure III.1: Standard Linear Solid (SLS). Reproduced from Ozmen [24]. 24

Figure IV.1: Nominal Test Specimen Geometry 32

Figure V.1: Stress-Strain Curves Obtained for PMR-15 in Tension to Failure Tests and Loading/Unloading Tests at 288 °C. Reproduced from McClung and Ruggles-Wrenn [22]. 36

Figure VI.1: Stress-Strain Curves Obtained for Unaged PMR-15 in Tensile Test to Failure Conducted at Constant Strain Rates of 10^{-3}, 10^{-4}, 10^{-5}, and 10^{-6} s^{-1} at Room Temperature. 40

Figure VI.2: Stress-Strain Curves Obtained for Unaged PMR-15 in Tensile Test to Failure Conducted at Constant Strain Rates of 10^{-3}, 10^{-4}, 10^{-5}, and 10^{-6} s^{-1} at 230 °C 41

Figure VI.3: Stress-Strain Curves Obtained for Unaged PMR-15 in Tensile Test to Failure Conducted at Constant Strain Rates of 10^{-3}, 10^{-4}, 10^{-5}, and 10^{-6} s^{-1} at 260 °C 43

Figure VI.4: Stress-Strain Curves Obtained for Unaged PMR-15 in Loading/Unloading Tests Conducted at Constant Strain Rates of 10^{-3}, 10^{-4}, 10^{-5}, and 10^{-6} s^{-1} at 260 °C Compared to Tension to Failure Results. 44

Figure VI.5: Stress-Strain Curves Obtained for PMR-15 in Loading/Unloading Tests Conducted at Constant Strain Rates of 10^{-3}, 10^{-4}, 10^{-5}, and 10^{-6} s^{-1} at 288 °C Compared to Tension to Failure Results. Reproduced from McClung [23]. 45

Figure VI.6: Stress-Strain Curves Obtained for PMR-15 in Loading/Unloading Tests Conducted at Constant Strain Rates of 10^{-3}, 10^{-5}, and 10^{-6} s^{-1} at 316 °C Compared to Tension to Failure Results. Reproduced from Ozmen [24]. 45

Figure VI.7: Recovery at Zero Stress at 260 °C (Following Loading and Unloading in Strain Control). Recovered Strain is Shown as a Percentage of the Initial Value (Inelastic Strain Value Measured Immediately After Reaching Zero Stress). 47

Figure VI.8: Stress-Strain Curves Obtained for PMR-15 Polymer in Constant Strain Rate Tests with a Period of Relaxation at 2% Strain at 260 °C. 48

Figure VI.9: Stress Decrease vs Relaxation Time for the PMR-15 Polymer at 260 °C 49

Figure VI.10: Creep Strain vs Time at 25 MPa and 260 °C. 50

Figure VI.11: Stress-Strain Curves Obtained for Unaged PMR-15 Polymer in Strain Rate Jump Tests and in Constant Strain Rate Tests at 260 °C. 52

Figure VI.12: Effect of Test Temperature on Deformation Behavior of PMR-15 in Tension to Failure Test Loaded at a Strain Rate of 10^{-3} s^{-1}. Experimental Data at 316 °C from Ozmen[24]. Experimental Data at 288 °C from McClung [23]. 54

Figure VI.13: Effect of Test Temperature on Deformation Behavior of PMR-15 in Tension to Failure Test Loaded at a Strain Rate of 10^{-4} s^{-1}. Experimental Data at 316 °C from Ozmen[24]. Experimental Data at 288 °C from McClung [23]. 54

Figure VI.14: Effect of Test Temperature on Deformation Behavior of PMR-15 in Tension to Failure Test Loaded at a Strain Rate of 10^{-5} s^{-1}. Experimental Data at 316 °C from Ozmen[24]. Experimental Data at 288 °C from McClung [23]. 55

Figure VI.15: Effect of Test Temperature on Deformation Behavior of PMR-15 in Tension to Failure Test Loaded at a Strain Rate of 10^{-6} s^{-1}. Experimental Data at 316 °C from Ozmen[24]. Experimental Data at 288 °C from McClung [23]. 55

Figure VII.1: A Comparison Between Experimental and Predicted Stress Drop vs Relaxation Time for Unaged PMR-15 Polymer at 260 °C. 62

Figure VII.2: A Comparison Between Experimental and Predicted Stress-Strain Curves Obtained for Unaged PMR-15 Polymer at Constant Strain Rates of 10^{-3}, 10^{-4}, and 10^{-6} s^{-1} at 260 °C. 63

Figure VII.3: Comparison Between the Experimental and Predicted Strain vs Time Curves Obtained for Unaged PMR-15 Polymer at 260 °C in Creep at 25 MPa. 65

Figure VII.4: A Comparison Between Experimental and Predicted Stress-Strain Curves Obtained for Unaged PMR-15 Polymer in Loading and Unloading at Two Constant Strain Rates at 260 °C..... 67

Figure VII.5: A Comparison Between Experimental and Predicted Stress-Strain Curves Obtained for Unaged PMR-15 Polymer in the Strain Rate Jump Test at 260 °C with Fast Loading First. 68

Figure VII.6: A Comparison Between Experimental and Predicted Stress-Strain Curves Obtained for Unaged PMR-15 Polymer in the Strain Rate Jump Test at 260 °C with Slow Loading First. 69

Figure VIII.1: Comparison of Percent Weight Loss for PMR-15 Neat Resin Aged in Argon at 260 °C, 288 °C, and 316 °C. Experimental Data at 316 °C from Ozmen[24]. Experimental Data at 288 °C from Broeckert [7]. 71

Figure VIII.2: Stress-Strain Curves for PMR-15 Specimens Aged for 50 h at 260 °C in Argon Obtained in Monotonic Tension to Failure Tests Conducted at Constant Strain Rates of 10^{-3}, 10^{-4}, 10^{-5}, and 10^{-6} s^{-1} at 260 °C. 72

Figure VIII.3: Stress-Strain Curves for PMR-15 Specimens Aged for 100 h at 260 °C in Argon Obtained in Monotonic Tension to Failure Tests Conducted at Constant Strain Rates of 10^{-3}, 10^{-4}, 10^{-5}, and 10^{-6} s^{-1} at 260 °C. 73

Figure VIII.4: Stress-Strain Curves for PMR-15 Specimens Aged for 250 h at 260 °C in Argon Obtained in Monotonic Tension to Failure Tests Conducted at Constant Strain Rates of 10^{-3}, 10^{-4}, 10^{-5}, and 10^{-6} s^{-1} at 260 °C. 74

Figure VIII.5: Stress-Strain Curves for PMR-15 Specimens Aged for 500 h at 260 °C in Argon Obtained in Monotonic Tension to Failure Tests Conducted at Constant Strain Rates of 10^{-3}, 10^{-4}, 10^{-5}, and 10^{-6} s^{-1} at 260 °C. 75

Figure VIII.6: Stress-Strain Curves for PMR-15 Specimens Aged for 1000 h at 260 °C in Argon Obtained in Monotonic Tension to Failure Tests Conducted at Constant Strain Rates of 10^{-3}, 10^{-4}, 10^{-5}, and 10^{-6} s^{-1} at 260 °C. 76

Figure VIII.7: Stress-Strain Curves for PMR-15 Specimens Aged for 2000 h at 260 °C in Argon Obtained in Monotonic Tension to Failure Tests Conducted at Constant Strain Rates of 10^{-3}, 10^{-4}, 10^{-5}, and 10^{-6} s^{-1} at 260 °C. 77

Figure VIII.8: Stress-Strain Curves for PMR-15 Specimens Aged at 260 °C in Argon Obtained in Monotonic Tension to Failure Tests at 260 °C Conducted at a Strain Rate of 10^{-3} s^{-1}. 78

Figure VIII.9: Stress-Strain Curves for PMR-15 Specimens Aged at 260 °C in Argon Obtained in Monotonic Tension to Failure Tests at 260 °C Conducted at a Strain Rate of 10^{-4} s^{-1}. 79

Figure VIII.10: Stress-Strain Curves for PMR-15 Specimens Aged at 260 °C in Argon Obtained in Monotonic Tension to Failure Tests at 260 °C Conducted at a Strain Rate of 10^{-5} s^{-1}. 80

Figure VIII.11: Stress-Strain Curves for PMR-15 Specimens Aged at 260 °C in Argon Obtained in Monotonic Tension to Failure Tests at 260 °C Conducted at a Strain Rate of 10^{-6} s^{-1}. 81

Figure VIII.12: Stress Drop During Relaxation for PMR-15 Specimens Aged at 260 °C in Argon Obtained at Constant Prior Strain Rate of 10^{-4} s^{-1}. 82

Figure VIII.13: Stress Drop During Relaxation for PMR-15 Specimens Aged at 260 °C in Argon Obtained at Constant Prior Strain Rate of 10^{-5} s^{-1}. 83

Figure VIII.14: Stress Drop During Relaxation for PMR-15 Specimens Aged at 260 °C in Argon Obtained at Constant Prior Strain Rate of 10^{-6} s^{-1}. 83

Figure VIII.15: Creep Strain vs Time at 25 MPa and 260 °C for Specimens Aged in Argon at 260 °C for 100 h. 84

Figure VIII.16: Creep Strain vs Time at 25 MPa and 260 °C for Specimens Aged in Argon at 260 °C for 250 h. 85

Figure VIII.17: Creep Strain vs Time at 25 MPa and 260 °C for Specimens Aged in Argon at 260 °C for 500 h. 86

Figure VIII.18: Creep Strain vs Time at 25 MPa and 260 °C for Specimens Aged in Argon at 260 °C for 1000 h. 86

Figure VIII.19: Creep Strain vs Time at 25 MPa and 260 °C for Specimens Aged in Argon at 260 °C for 2000 h. 87

Figure VIII.20: Creep Strain Accumulation for PMR-15 Specimens Aged at 260 °C in Argon Obtained in Creep Tests at 260 °C Conducted at 25 MPa after a Prior Loading Strain Rate of 10^{-4} s^{-1}. 88

Figure VIII.21: Creep Strain Accumulation for PMR-15 Specimens Aged at 260 °C in Argon Obtained in Creep Tests at 260 °C Conducted at 25 MPa after a Prior Loading Strain Rate of 10^{-6} s^{-1}. 89

Figure VIII.22: Stress-Strain Curves Obtained for PMR-15 Polymer Subjected to Prior Aging in Argon at 260 °C in Strain Rate Jump Tests and in Constant Strain Rate Tests at 260 °C. 90

Figure IX.1: A Comparison Between Experimental and Predicted Stress Drop vs Relaxation Time for the PMR-15 Polymer at 260 °C Aged in Argon at 260 °C for 100 h. 96

Figure IX.2: A Comparison Between Experimental and Predicted Stress-Strain Curves Obtained for PMR-15 Polymer at Constant Strain Rates of 10^{-3}, 10^{-4}, and 10^{-6} s^{-1} at 260 °C Aged in Argon at 260 °C for 100 h. 97

Figure IX.3: Comparison Between the Experimental and Predicted Creep Strain vs Time Curves Obtained for PMR-15 Polymer at 260 °C in Creep at 25 MPa Aged in Argon at 260 °C for 100 h. 98

Figure IX.4: A Comparison Between Experimental and Predicted Stress-Strain Curves Obtained for PMR-15 Polymer in the Strain Rate Jump Test at 260 °C with Fast Loading First Aged in Argon at 260 °C for 100 h. 99

Figure IX.5: A Comparison Between Experimental and Predicted Stress-Strain Curves Obtained for PMR-15 Polymer in the Strain Rate Jump Test at 260 °C with Slow Loading First Aged in Argon at 260 °C for 100 h. 99

Figure IX.6: A Comparison Between Experimental and Predicted Stress Drop vs Relaxation Time for the PMR-15 Polymer at 260 °C Aged in Argon at 260 °C for 250 h. 101

Figure IX.7: A Comparison Between Experimental and Predicted Stress-Strain Curves Obtained for PMR-15 Polymer at Constant Strain Rates of 10^{-3}, 10^{-4}, and 10^{-6} s^{-1} at 260 °C Aged in Argon at 260 °C for 250 h. 101

Figure IX.8: Comparison Between the Experimental and Predicted Creep Strain vs Time Curves Obtained for PMR-15 Polymer at 260 °C in Creep at 25 MPa Aged in Argon at 260 °C for 250 h. 102

Figure IX.9: A Comparison Between Experimental and Predicted Stress-Strain Curves Obtained for PMR-15 Polymer in the Strain Rate Jump Test at 260 °C with Fast Loading First Aged in Argon at 260 °C for 250 h. 103

Figure IX.10: A Comparison Between Experimental and Predicted Stress-Strain Curves Obtained for PMR-15 Polymer in the Strain Rate Jump Test at 260 °C with Slow Loading First Aged in Argon at 260 °C for 250 h. 104

Figure IX.11: Elastic Modulus E at 260 °C as a Continuous Function of Prior Aging Time for the PMR-15 Neat Resin Aged at 260 °C in Argon. 105

Figure IX.12: Tangent Modulus E_t at 260 °C as a Continuous Function of Prior Aging Time for the PMR-15 Neat Resin Aged at 260 °C in Argon. 106

Figure IX.13: Isotropic Stress A at 260 °C as a Continuous Function of Prior Aging Time for the PMR-15 Neat Resin Aged at 260 °C in Argon. 107

Figure IX.14: Shape Function Parameter, C_2, at 260 °C as a Continuous Function of Prior Aging Time for the PMR-15 Neat Resin Aged at 260 °C in Argon. 108

Figure IX.15: Shape Function Parameter, C_3, at 260 °C as a Continuous Function of Prior Aging Time for the PMR-15 Neat Resin Aged at 260 °C in Argon. 109

Figure IX.16: A Comparison Between Experimental and Predicted Stress-Strain Curves Obtained for PMR-15 Polymer at Constant Strain Rates of 10^{-3}, 10^{-4}, and 10^{-6} s^{-1} at 260 °C Aged in Argon at 260 °C for 500 h. 111

Figure IX.17: A Comparison Between Experimental and Predicted Stress Drop vs Relaxation Time for the PMR-15 Polymer at 260 °C Aged in Argon at 260 °C for 500 h. 111

Figure IX.18: Comparison Between the Experimental and Predicted Creep Strain vs Time Curves Obtained for PMR-15 Polymer at 260 °C in Creep at 25 MPa Aged in Argon at 260 °C for 500 h. 112

Figure IX.19: A Comparison Between Experimental and Predicted Stress-Strain Curves Obtained for PMR-15 Polymer in the Strain Rate Jump Test at 260 °C with Fast Loading First Aged in Argon at 260 °C for 500 h. 113

Figure IX.20: A Comparison Between Experimental and Predicted Stress-Strain Curves Obtained for PMR-15 Polymer at Constant Strain Rates of 10^{-3}, 10^{-4}, 10^{-5}, and 10^{-6} s^{-1} at 260 °C Aged in Argon at 260 °C for 1000 h. 115

Figure IX.21: A Comparison Between Experimental and Predicted Stress Drop vs Relaxation Time for the PMR-15 Polymer at 260 °C Aged in Argon at 260 °C for 1000 h. 116

Figure IX.22: Comparison Between the Experimental and Predicted Creep Strain vs Time Curves Obtained for PMR-15 Polymer at 260 °C in Creep at 25 MPa Aged in Argon at 260 °C for 1000 h. 117

Figure IX.23: A Comparison Between Experimental and Predicted Stress-Strain Curves Obtained for PMR-15 Polymer at Constant Strain Rates of 10^{-3}, 10^{-4}, 10^{-5}, and 10^{-6} s^{-1} at 260 °C Aged in Argon at 260 °C for 2000 h. 119

Figure IX.24: A Comparison Between Experimental and Predicted Stress Drop vs Relaxation Time for the PMR-15 Polymer at 260 °C Aged in Argon at 260 °C for 2000 h. Experimental Data is for Prior Strain Rate 10^{-6} s^{-1}. 120

Figure IX.25: Comparison Between the Experimental and Predicted Creep Strain vs Time Curves Obtained for PMR-15 Polymer at 260 °C in Creep at 25 MPa Aged in Argon at 260 °C for 2000 h. 121

Figure X.1: Stress- Strain Behavior of Viscoplastic Material 123

List of Tables

Page

Table IV-1: Standard Post Cure Cycle for PMR-15 Neat Resin Panels 32

Table VII-1: Model Parameters Used in the VBOP Predictions of the Deformation Behavior of the Unaged PMR-15 Neat Resin at 260 °C. 64

Table IX-1: Model Parameters Used in the VBOP Predictions of the Deformation Behavior of the PMR-15 Neat Resin at 260 °C Aged in Argon at 260 °C for 100 h. 95

Table IX-2: Model Parameters Used in the VBOP Predictions of the Deformation Behavior of the PMR-15 Neat Resin at 260 °C Aged in Argon at 260 °C for 250 h. 100

Table IX-3: Model Parameters Used in the VBOP Predictions of the Deformation Behavior of the PMR-15 Neat Resin at 260 °C Aged in Argon at 260 °C for 500 h. 110

Table IX-4: Model Parameters Used in the VBOP Predictions of the Deformation Behavior of the PMR-15 Neat Resin at 260 °C Aged in Argon at 260 °C for 1000 h. 114

Table IX-5: Model Parameters Used in the VBOP Predictions of the Deformation Behavior of the PMR-15 Neat Resin at 260 °C Aged in Argon at 260 °C for 2000 h. 117

List of Symbols

Symbol	Definition
Γ	overstress
ϵ	strain
$\dot{\epsilon}^{el}$	elastic strain rate
$\dot{\epsilon}^{in}$	inelastic strain rate
η	viscosity constant
σ	stress
Ψ	shape function
A	isotropic stress
A_f	saturated value of isotropic stress
C_1, C_2, C_3	shape function parameters
E	modulus of elasticity
E_t	tangent modulus
f	kinematic stress
g	equilibrium stress
h	hours
k	viscosity function
k_1, k_2, k_3	viscosity function parameters
T_g	glass transition temperature
t	time
t_a	prior aging time
s	seconds

Superscript dot means it is a time derivative (i.e. $\dot{\epsilon}$ is strain rate)

EFFECTS OF PRIOR AGING AT 260 °C IN ARGON ON INELASTIC DEFORMATION BEHAVIOR OF PMR-15 POLYMER AT 260 °C: EXPERIMENT AND MODELING

I. Introduction

The aerospace industry is in constant pursuit of lighter, stronger materials to improve efficiency of the aircraft. Cost is another driving factor in material selection. Composites have taken off as the material of choice. Several structures on aircraft also have the capability to perform at high temperatures. This is where the choice to use polyimide resins as a matrix material becomes an intelligent choice. Specifically, polymerization of monomeric reactants-15 (PMR-15) has become the most common of these resins and has been used in aircraft components, like engine casings, that are subjected to elevated temperatures [1].

When dealing with a composite it is necessary to understand the material properties of the matrix. This information can be combined with the material properties of the reinforcing material to determine the overall properties of the composite. The Air Force Institute of Technology (AFIT) has conducted extensive experiments on PMR-15 [7, 11, 23, 24, 28]. It has been proven that this polymer exhibits rate-dependent behavior [23, 24, 28]. Generally elastic or linear viscoelastic models are used to predict behavior of polymers [23]. However, these models lose their usefulness when large regions of inelastic flow exist, resulting in large safety factors and the inability to use the material to

its fullest capacity [23]. Even a nonlinear viscoelastic model was proven inappropriate for PMR-15 [28]. This model was unable to account for the effect of prior loading histories on creep and recovery response [23]. Models do exist that are able to handle the effect of these prior loading histories. The Viscoplasticity Based on Overstress (VBO) model, in particular, is an excellent choice to model a majority of the behaviors of PMR-15 revealed through experimentation. More specifically, the Viscoplasticity Based on Overstress for Polymers (VBOP) model accurately describes the behavior of PMR-15 and has been developed in previous efforts [23].

Since one of the intended uses for this material is on aircraft components that may be subjected to elevated temperatures it is necessary to understand the effect of these high temperatures. The material will behave differently at different temperatures as seen in previous analyses of PMR-15 at 316 °C and 288 °C respectively [24, 23]. It is also necessary to understand the effect of maintaining this material at the elevated temperatures for extended durations. Thus the concept of thermal aging is introduced.

The subsequent sections will provide more details about the procedure and results of this research. Background information on composites, specifically High Temperature Polymer Matrix Composites (HTPMCs), will be provided. This will be followed by information on constitutive modeling of these composites. The theory behind the VBOP will also be discussed before defining the test material and experimental procedures to be used. Experimental results will be presented before concluding remarks and suggestions for the future are made.

II. Background

Polymer Matrix Composites

The combination of two or more significantly different materials constitutes a composite. Two phase composites consist of a matrix and a reinforcement phase. Daniel [9] identifies the four most common matrix types for fiber reinforced composites as polymer, metal, ceramic, and carbon. A polymer is a "macromolecule that contains many groups of atoms, called monomeric units" that are covalently bonded together [25]. Polymer matrix composites (PMCs) are generally reinforced with glass, carbon, aramid, or boron fibers [9]. PMCs can be subdivided into elastomers, thermoplastics, and thermosets [9].

Elastomers have the ability to stretch to several times their original length and return to their original state [14]. Rubber is a classic example of an elastomer.

Thermoplastics consist of monomers connected by intermolecular forces instead of covalent bonds [14]. Thermoplastics become fluid when heated and are thus easily formed into their desired shapes through injection molding or extrusion [25]. This process can be repeated without loss of its properties [12]. Thermoplastics have significant toughness and temperature resistance, but are not as good as thermosets in overall composite performance [12].

Thermosets are much less able to deform once processed. Thermosets are "polymeric materials that in their final state cannot be fused, are insoluble, and degrade before melting" [14]. Many covalent bonds are formed between the monomers in

thermosets making their cured state permanent [14]. Thermosets can be broken into three subgroups: polyesters, epoxies, and polyimides [9]. Polyesters cure quickly and are therefore great for commercial products [9]. Epoxies tend to have the best mechanical properties of the thermosets [24], but they are better served in low or moderate temperature applications. Polyimides, on the other hand, are great for high temperature applications and can be used in temperatures up to 370 °C [9].

PMR-15 is a polyimide resin. So, it is a thermosetting polymer which is capable of performing in temperatures up to its glass transition temperature of 348 °C [8]. The glass transition temperature is the temperature at which the polymer changes from brittle behavior, often deemed "glassy," to a soft state, termed "rubbery." Chuang [8] describes PMR-15 as "a high-temperature polyimide developed in the mid-1970's at the NASA Lewis Research Center, [that] offers the combination of low cost, easy processing, and good high-temperature performance and stability." Dr. Ruth Pater, a senior polymer scientist at NASA's Langley Research Center, also noted the thermal and mechanical properties of PMR-15 are very good [2]. When coupled with carbon as a reinforcing fiber, PMR-15 becomes a good choice for use in aircraft engine components [8].

Polymer Aging

Material properties change over the lifespan of the material. This could be due to the high temperatures or loads the material is exposed to for extended periods of time. It therefore becomes important to understand the change in behavior of the material due to its history in order to use it safely. Aging can affect a polymer's properties such as

strength, toughness, density, and reactivity toward other chemicals [24]. Several modes of aging exist, but this work will assume the following definitions for aging:

- Strain aging: mechanical property or material behavior changes caused by deformation [24, 23, 16]
- Prior thermal aging: mechanical property or material behavior changes caused by exposure to elevated temperature prior to deformation

Prior thermal aging causes degradation in polymers due to the breakdown of covalent bonds. Additional crosslinking also occurs during aging at high temperatures [5]. Degradation occurs quickly in polymers exposed to temperatures well beyond their glass transition temperature [24, 23, 5]. Degradation still occurs in polymers exposed to temperatures below the glass transition temperature, it just occurs more slowly. This degradation has been shown to effect the mechanical behavior, i.e. creep and recovery response, in PMR-15 [7, 23].

The different modes of aging can exist simultaneously. In order to determine exactly how a material will behave in a given environment it becomes necessary to know how each form of aging effects the material independently. The focus of this research will be to determine the effect of prior aging at 260 °C on the mechanical behavior of PMR-15 neat resin. Strain aging will not be introduced. It has been shown that strain aging for less than 50 hours has a negligible effect on the mechanical behavior of PMR-15 [6, 7]. Since all tests conducted in this effort last for less than 50 hours, the assumption of no strain aging effects is valid.

Problem Statement

High Temperature Polymer Matrix Composites (HTPMCs) are obviously intended for use in high temperature applications such as turbine engines and high-speed aircraft skins. These materials must exhibit consistent and long term durability in their designed applications. Failure to meet these requirements could be costly. Thus it is of paramount importance to fully understand the capabilities of these materials before they are put to use. This can be accomplished through experiment-based life-prediction methods. The development of predictive models heavily relies on the understanding of aging and deformation mechanisms and their effects on the mechanical behavior of HTPMCs. One major issue is the effect of long term exposure to elevated temperatures on the strength, stiffness, and dimensional stability of HTPMCs.

Thesis Objective

This research focuses on the effect of prior aging at 260 °C in an inert environment on the mechanical behavior of PMR-15 high-temperature polymer at 260 °C. Monotonic constant strain rate tension to failure, constant strain rate loading and unloading, constant strain rate loading to failure with a period of relaxation, creep and strain rate jump tests will be performed on unaged PMR-15 at 260 °C. These same tests will be repeated on samples aged at 260 °C in argon for various durations. The results of these tests will be used to determine the parameters of the Viscoplasticity Based on Overstress for Polymers (VBOP) constitutive model at 260 °C. The effect of aging on

model parameters will be determined and used to predict the behavior of the material aged for 2000 hours. Model predictions will be compared to experimental results.

Methodology

The key issues identified in the problem statement were evaluated through the following steps:

1. Determine the room temperature elastic modulus to determine specimen to specimen variability.
2. Age samples for various durations in argon environment at 260 °C.
3. Determine the effect of strain rate on monotonic stress-strain behavior on unaged PMR-15.
4. Determine the existence of strain rate history effect through experimentation on unaged PMR-15.
5. Determine the effect of prior strain rate on recovery behavior on unaged PMR-15.
6. Determine the effect of prior strain rate on creep behavior on unaged PMR-15.
7. Study the relaxation behavior in monotonic test with single period of relaxation on unaged PMR-15.
8. Determine model parameters for the VBOP applied to unaged PMR-15 at 260 °C.
9. Verify the VBOP model qualitatively matches the unaged PMR-15 behavior.
10. Determine the effect of prior aging on deformation behavior of PMR-15.
11. Determine the model parameters for the VBOP for PMR-15 aged for 50, 100, 250, 500, and 1000 h.

12. Develop equations to determine model parameters as functions of prior aging time.
13. Demonstrate VBOP with prior aging constitutive model qualitatively predicts deformation behavior of PMR-15 aged for 2000 hours at 260 °C.

Previous Research: Experimental Investigations

PMR-15 – Mechanical Behavior

PMR-15 - Mechanical Behavior at 288 °C

Westberry [28], Falcone [11], and McClung [23] studied the time-dependent behavior of PMR-15 at 288 °C. Westberry conducted tests using varying stress rates and concluded PMR-15 exhibits rate dependent behavior in creep and recovery tests at 288 °C [28]. From these results, Westberry concluded a rate history dependent constitutive model is needed to describe the behavior of PMR-15 at elevated temperatures. Falcone [11] also conducted tests with varying stress rates and concluded PMR-15 exhibits rate dependent behavior in creep and relaxation tests at 288 °C.

McClung [23] conducted tests on PMR-15 with varying strain rates at 288 °C. McClung reached several conclusions on the behavior of PMR-15 at 288 °C. These conclusions [23] are listed below:

1. A linear, quasi-elastic behavior upon initial loading exists. This behavior transitions to the region of inelastic deformation which is characterized by the tangent modulus.

2. PMR-15 exhibits nonlinear strain rate sensitivity in monotonic loading. The flow stress increases nonlinearly with increasing load rate.
3. Each strain rate has a unique stress-strain curve. There is no strain rate history effect.
4. Strain recovery is strongly influenced by prior strain rate.
5. Creep behavior is strongly influenced by prior strain rate.
6. Relaxation behavior is strongly influenced by prior strain rate. Stress drop is independent of stress and strain at the beginning of relaxation. Stress drop during relaxation only depends on time and prior strain rate.

PMR-15 – Mechanical Behavior at 316 °C

Ozmen [24] studied the time-dependent behavior of PMR-15 at 316 °C. The observations made at 316 °C are similar to those made at 288 °C. Listed below are the conclusions Ozmen [24] reached on the deformation behavior of PMR-15 at 316 °C:

1. PMR-15 exhibits positive nonlinear strain rate sensitivity in monotonic loading and unloading. The flow stress region is not achieved at the faster strain rates due to early failures. The flow stress level increases with strain rate.
2. There is no strain rate history effect.
3. Strain recovery is strongly influenced by prior strain rate. The recovery rate increases with prior strain rate.
4. Creep behavior is strongly influenced by prior strain rate. Creep rate increases with prior strain rate.

5. Relaxation behavior is strongly influenced by prior strain rate. The existence of an equilibrium stress curve is suggested.

Prior Aging – Effects on Mechanical Behavior

Materials intended for high temperature applications will be exposed to these high temperatures for extended periods of time. Therefore, it becomes necessary to understand the effect of these high temperatures on the mechanical behavior of the material being used. Krempl [20] suggests prior aging must be singled out in order to identify its effects and correctly incorporate them into a constitutive model. It is known that an oxidative surface layer forms which has different properties from the unoxidized inner material when aged in air [27]. Thus, recent efforts at AFIT have conducted prior aging in an inert environment such as argon [23, 24].

PMR-15- Effect of Prior Aging at 288 °C

Broeckert [7, 6] examined the effects of prior aging on PMR-15 at 288 °C in both air and argon environments. He concluded prior aging increases the elastic modulus, decreases the creep strain, and increases the glass transition temperature. Creep response at 288 °C for various aging times at 288 °C is reproduced from Broeckert [6] in Figure II.1. The effect of prior aging on creep response is readily apparent.

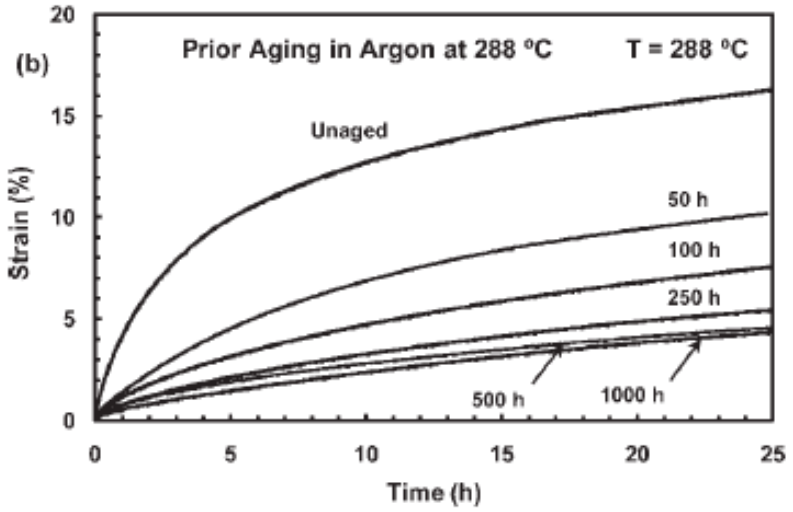

Figure II.1: Creep Strain Versus Time at 20 MPa and 288 °C for PMR-15 Aged at 288 °C in Argon. Reproduced from Broeckert [6].

McClung [23] examined the effects of prior aging on PMR-15 at 288 °C in an argon environment. She determined prior aging has a significant effect on the mechanical behavior of PMR-15 at 288 °C. The following results were reported by McClung [23] and can be clearly seen in Figure II.2, a reproduction of the effect of prior aging on the monotonic tension to failure test at a strain rate of 10^{-6} s^{-1}.:

1. Elastic modulus increases with increasing aging time.
2. Tangent modulus increases with increasing aging time.
3. Flow stress increases with increasing aging time.

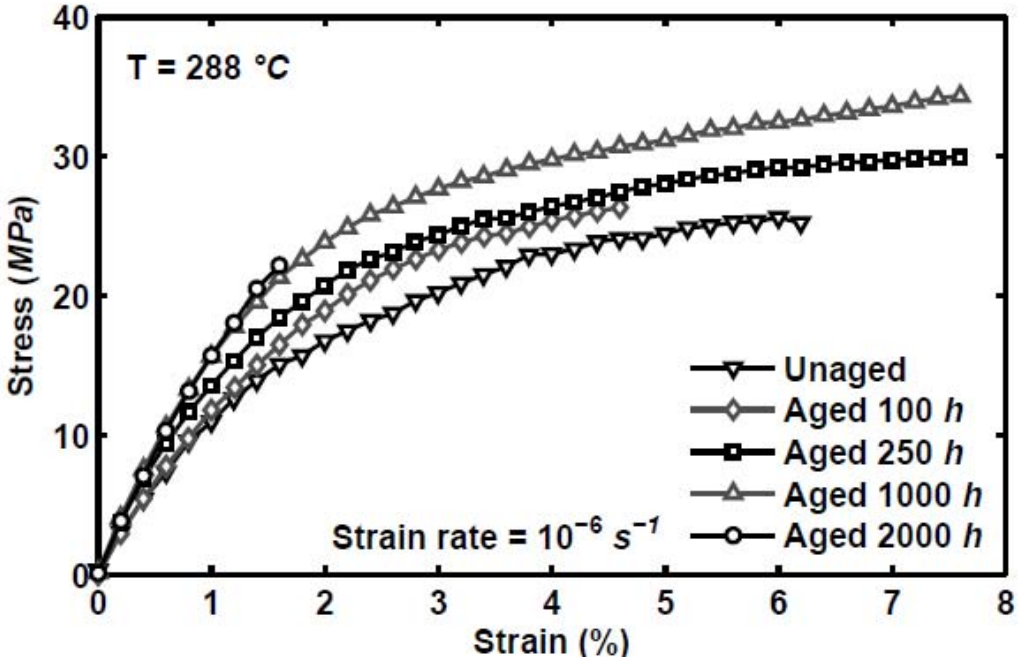

Figure II.2: Stress-Strain Curves Obtained in Monotonic Tension to Failure Tests Conducted at a Strain Rate of 10^{-6} s^{-1} for PMR-15 Aged in Argon at 288 °C. Reproduced from McClung [23].

PMR-15- Effect of Prior Aging at 316 °C

Ozmen [24] examined the effects of prior aging on PMR-15 at 316 °C in an argon environment. He determined prior aging has a significant effect on the mechanical behavior of PMR-15 at 316 °C. The following results were reported by Ozmen [24]:

1. Elastic modulus increases with prior aging time.
2. Tangent modulus increases with prior aging time.
3. Flow stress increases with prior aging time.

These trends are consistent with those seen at 288 °C. These results can be clearly seen in Figure II.3, a reproduction from reference [24] of the effect of prior aging on the monotonic tension to failure test at a strain rate of 10^{-6} s^{-1}.

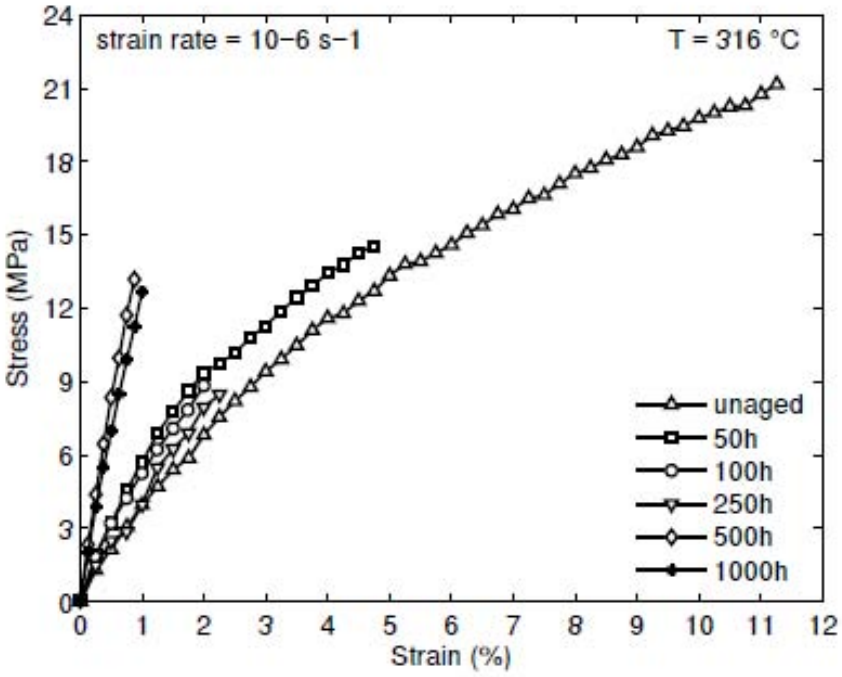

Figure II.3: Stress-Strain Curves Obtained in Monotonic Tension to Failure Tests Conducted at a Strain Rate of 10^{-6} s^{-1} for PMR-15 Aged in Argon at 316 °C. Reproduced from Ozmen [24].

Previous Research: Constitutive Modeling

Viscoplasticity Based on Overstress

Many constitutive models exist, so it becomes necessary to determine which model most closely matches the specific material at hand. Early attempts at modeling PMR-15 used a viscoelastic model [11] developed by Schapery [26]. However, this

model was too basic and did not account for the rate dependence of the material. So, McClung [23] tried a viscoplastic model for PMR-15. It has been determined that a viscoplastic model is the best choice to describe the behavior of PMR-15[23]. A comparison of (a) viscoelastic and (b) viscoplastic behavior is shown in Figure II.4 reproduced from Ozmen [24].

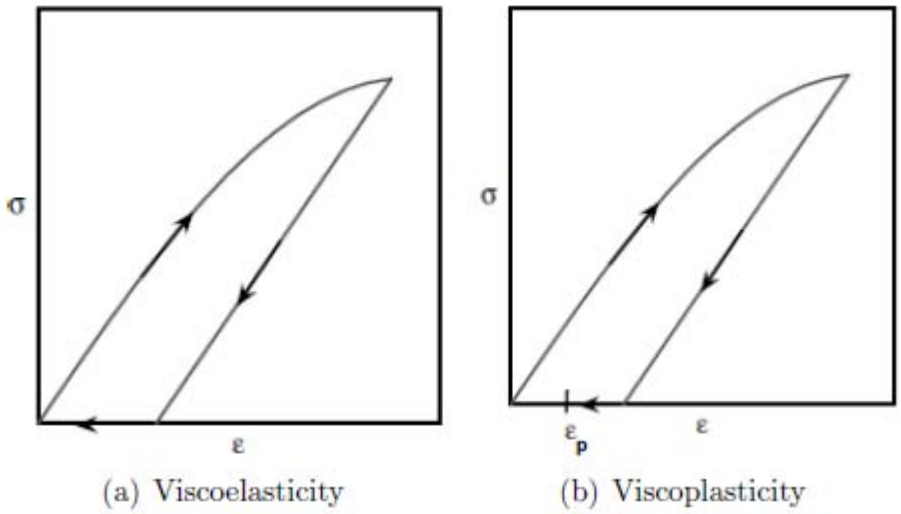

Figure II.4: Viscoelastic and Viscoplastic Stress-Strain Behavior. Reproduced from Ozmen [24].

Viscoelastic and viscoplastic behavior are very similar. The difference lies in the strain recovery upon unloading to zero stress. Viscoelastic materials will recover all of the strain, while viscoplastic materials will never recover all of the strain. Thus, viscoplastic materials have a permanent, plastic strain that results from loading and unloading. Numerous viscoplastic models exist. McClung [23] has identified the Viscoplasticity Based on Overstress (VBO) model as the most applicable to PMR-15.

Krempl and colleagues have developed a unified viscoplastic constitutive model based on overstress. The terms "unified viscoplastic constitutive model" imply a model that separates creep strain and plastic strain into their own terms. As the name implies, the VBO incorporates an overstress concept. Overstress is defined as the difference between the flow stress and equilibrium stress in the region of fully established inelastic flow, known as the flow stress region. The equilibrium stress is the stress that lies on a theoretical stress-strain curve produced from loading a specimen at an infinitesimally small strain rate. Krempl defined the equilibrium stress as the stress that exists at rest [17]. A graphical representation of these terms is shown in Figure II.5. Also note the strain rate dependence generated by this model; specimens load at a fast strain rate result in different stress-strain curves than those loaded at slower rates. The flow stress region can also be seen in Figure II.5 at high strains. Krempl describes the flow stress region as the "steady inelastic flow with a tangent modulus much smaller than the elastic modulus measured at the origin" [18]. The tangent modulus is the slope of the stress-strain curve in the flow stress region.

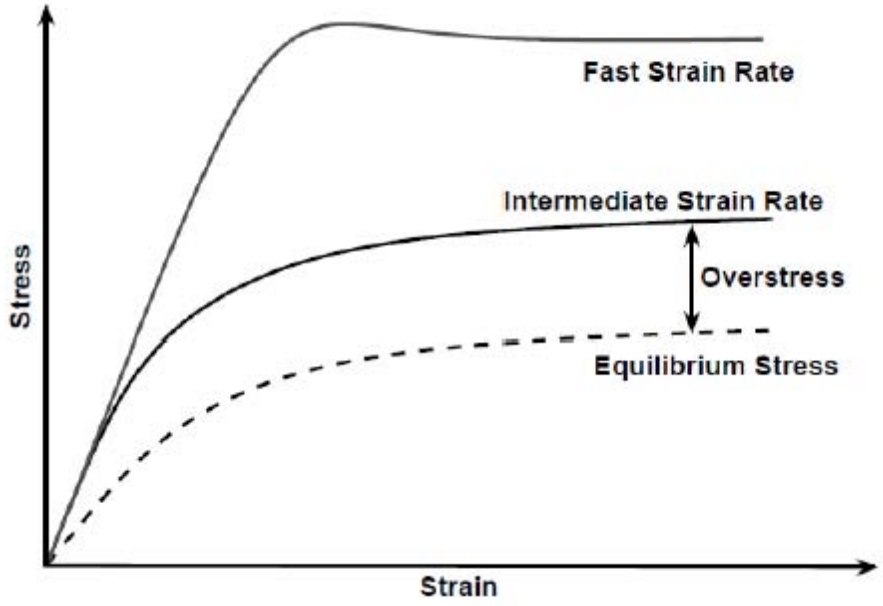

Figure II.5: Standard Linear Solid Stress-Strain Behavior. Equilibrium Stress and Overstress Concepts are Depicted. Reproduced from Ozmen [24].

Viscoplastic models incorporate the inelastic strain as a function of the overstress. This can be seen in the equations listed below. The VBO is described by two coupled nonlinear differential equations [15]

$$\dot{\epsilon} = \dot{\epsilon}^{el} + \dot{\epsilon}^{in} = \frac{\dot{\sigma}}{E} + \frac{\sigma - g}{Ek[\sigma - g]} \tag{2.1}$$

$$\dot{g} = \Psi[\,]\dot{\epsilon} - \frac{g - f[\,]}{b[\,]}\left|\dot{\epsilon}^{in}\right| \tag{2.2}$$

where σ denotes engineering stress, ϵ denotes engineering strain, E denotes elastic modulus, k denotes the viscosity function, g denotes the equilibrium stress and Ψ, f, b are positive functions. A superscript dot denotes a time derivative and the vertical bars denote the absolute value of the argument. The brackets immediately following a symbol

denote the variable is a function of whatever is inside the brackets. These functions will be discussed in Chapter 3.

Viscoplasticity Based on Overstress for Polymers

The standard VBO applies well to metals and alloys such as 304 Stainless Steel and a Ti-alloy studied by Krempl [15]. However, Bordonaro [4] and Krempl and Bordonaro [3] showed that some polymers exhibited behavior that could not be described by the VBO alone. Among these behaviors are high relaxation rates, increased strain recovery after unloading to zero stress, curved loading in stress control, reduced rate-dependence in unloading, and merging of the stress strain curves produced at different strain rates [24]. The Viscoplasticity Based on Overstress for Polymers (VBOP) was introduced by Ho to incorporate these behaviors into a model [13].

McClung successfully applied the VBOP to PMR-15 [23]. McClung reported several key features of the deformation behavior of the unaged PMR-15 neat resin at 288 °C [23]:

1. Linear, quasi-elastic behavior observed upon initial loading transitions into the region of inelastic deformation which is characterized by a low tangent modulus.
2. The unaged PMR-15 neat resin exhibits significant nonlinear strain rate sensitivity in monotonic loading. The flow stress increases nonlinearly with increase in the loading rate.
3. A unique stress-strain curve is obtained for a given strain rate. There is a lack of a strain rate history effect.

4. Recovery of strain is strongly influenced by prior strain rate. The recovery rate increases with prior strain rate.
5. Creep rate at a given stress increases with prior strain rate.
6. Relaxation behavior is influenced by prior strain rate. Stress drop in relaxation depends only on time and prior strain rate. Stress drop in relaxation is independent of stress and strain at the beginning of relaxation.

These experimental results led McClung to choose the VBOP to model the behavior of PMR-15 at 288 °C. McClung [23] developed a procedure to determine the necessary parameters in the VBOP. This procedure will be outlined in Chapter VII. The model accurately predicted the behavior of the unaged PMR-15 at 288 °C as can be seen in Figure II.6 - Figure II.10 [21].

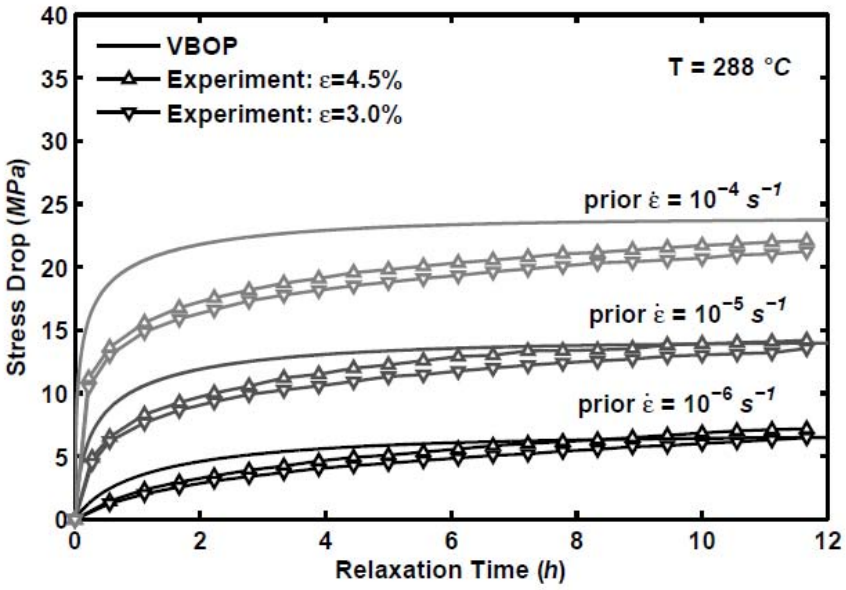

Figure II.6: Relaxation Behavior of Unaged PMR-15 at 288 °C Described by Experimentation and the VBOP. Reproduced from McClung [21].

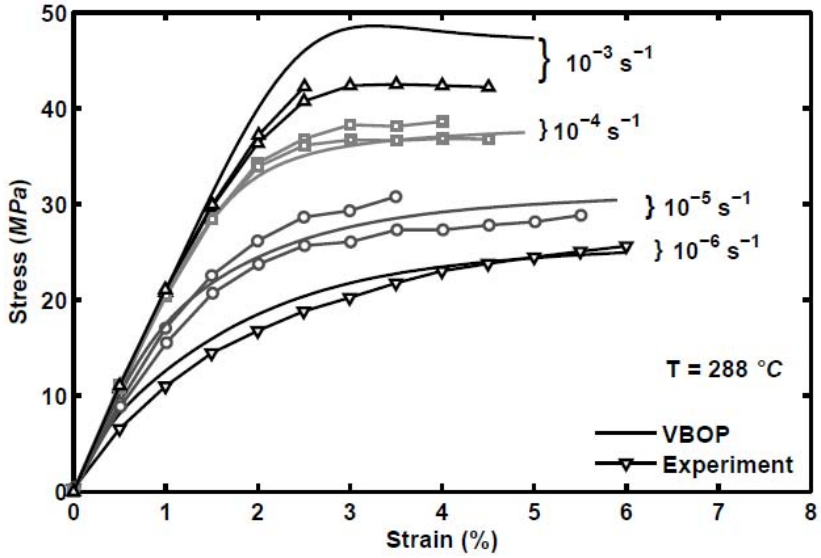

Figure II.7: Stress-Strain Behavior of Unaged PMR-15 at 288 °C in Monotonic Tension to Failure Tests Described by Experimentation and the VBOP. Reproduced from McClung [21].

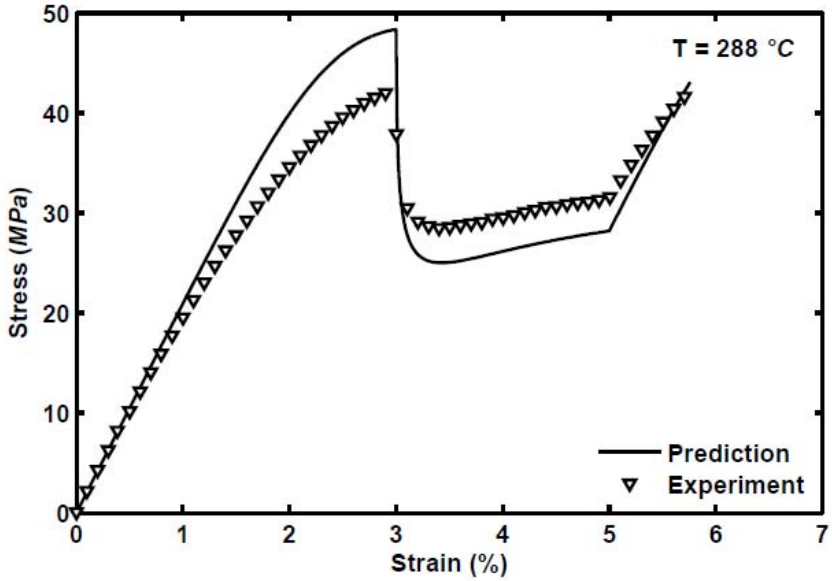

Figure II.8: Stress-Strain Behavior of Unaged PMR-15 at 288 °C in the Strain Rate Jump Test Described by Experimentation and the VBOP. Reproduced from McClung [21].

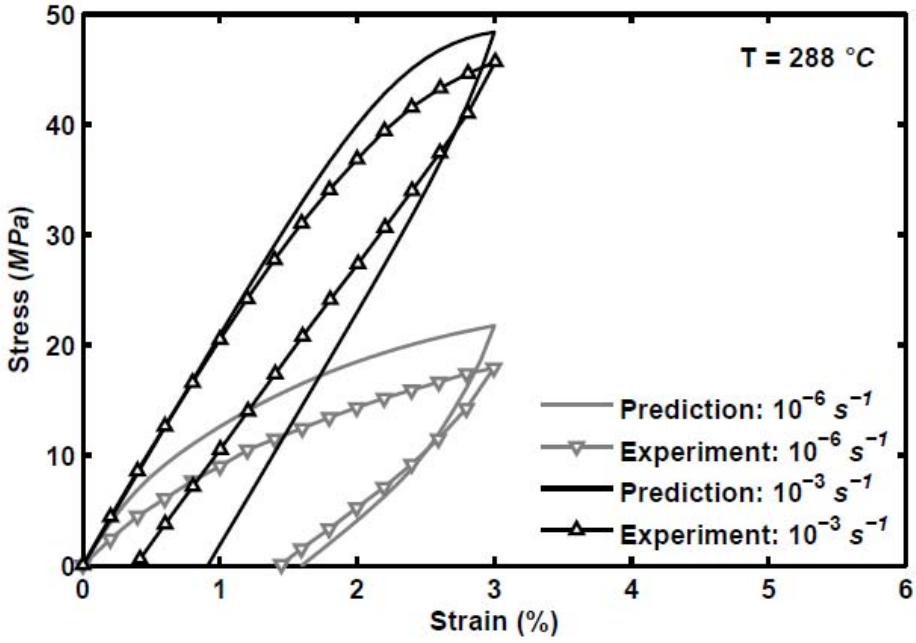

Figure II.9: Stress-Strain Behavior of Unaged PMR-15 at 288 °C in Loading Followed by Unloading Described by Experimentation and the VBOP. Reproduced from McClung [21].

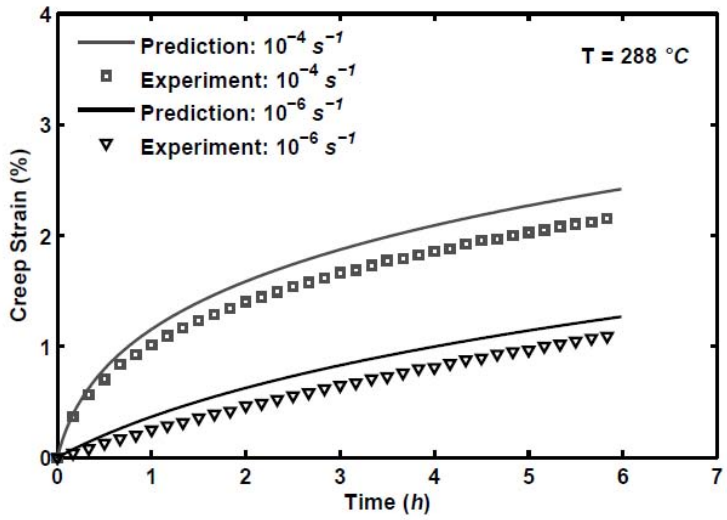

Figure II.10: Creep Behavior of Unaged PMR-15 at 288 °C Described by Experimentation and the VBOP. Reproduced from McClung [21].

Ozmen [24] successfully applied McClung's model characterization procedure to unaged PMR-15 at 316 °C. He also used the creep behavior to verify the model. Creep behavior of PMR-15 at 316 °C is shown in Figure II.11.

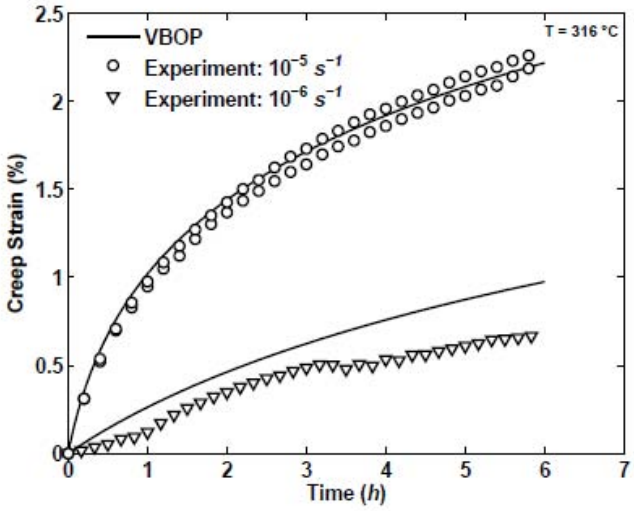

Figure II.11: Creep Behavior of Unaged PMR-15 at 316 °C Described by Experimentation and the VBOP. Reproduced from Ozmen [24].

Viscoplasticity Based on Overstress for Polymers with Prior Aging

McClung [23] also analyzed the effect of prior aging at 316 °C on the deformation behavior of PMR-15 at 316 °C. She reported the following results as the impact of an increase in prior aging:

1. Initial slope of stress-strain curve increases.
2. Final slope of stress-strain curve increases
3. Flow stress increases.
4. Departure from quasi-linear behavior is delayed.

Each of these effects of prior aging resulted in a correlating change in the model parameters of the VBOP. McClung [23] reported the following changes in parameters due to an increase in prior aging:

1. Elastic modulus, E, increases
2. Tangent modulus, E_t, increases.
3. Isotropic stress, A, increases.
4. Shape parameter, C_2, increases.

Each altered model parameter was best fitted to a function of aging time. The group of specimens aged for 2000 h was then analyzed using the parameters found through the aging functions instead of the model characterization procedure previously described. A comparison of the experimental results and the VBOP determined through the aging functions is shown in Figure II.12- Figure II.13. The VBOP successfully predicts the behavior.

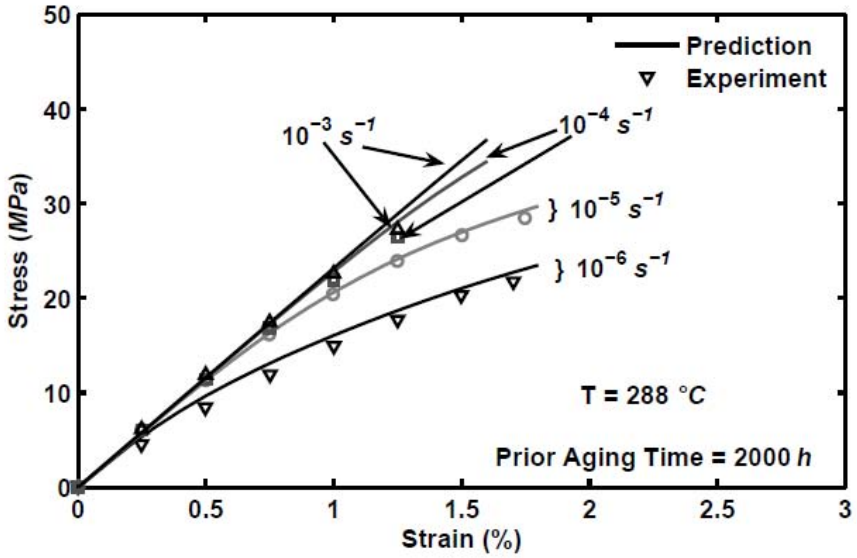

Figure II.12: Comparison Between Experimental Results and Predicted Stress-Strain Curves for PMR-15 Aged at 288 °C for 2000 h in Tension to Failure Test. Reproduced from McClung [23].

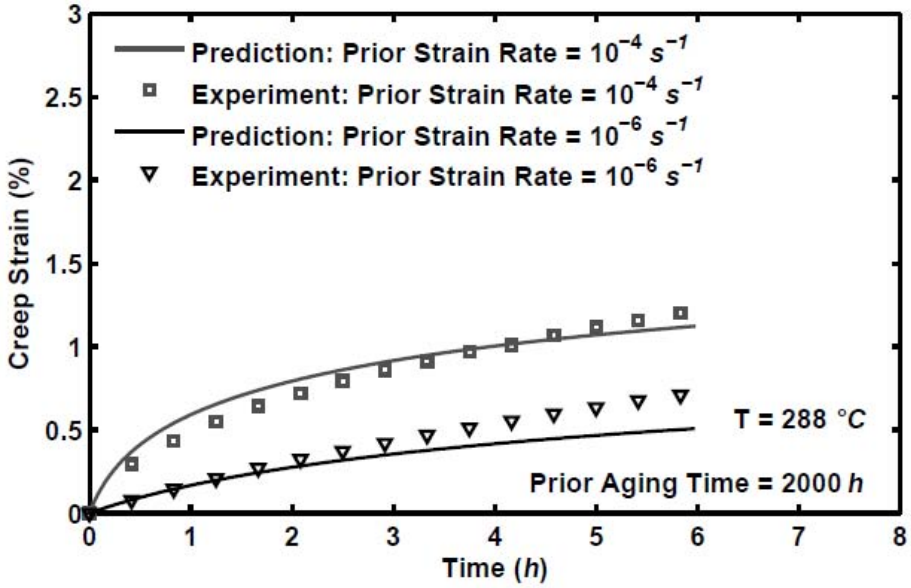

Figure II.13: Comparison Between Experimental Results and Predicted Creep Response for PMR-15 Aged at 288 °C for 2000 h in Creep Test. Reproduced from McClung [23].

III. Theoretical Formulation of Viscoplasticity Based on Overstress for Polymers

This chapter is devoted to the development of the theory of Viscoplasticity Based on Overstress for Polymers (VBOP). The VBOP will be used to model the behavior of PMR-15 at 260 °C. The VBOP will be expanded to include prior aging. The VBOP is a unified viscoplastic constitutive model.

Basis of Viscoplasticity Based on Overstress – Standard Linear Solid

The Standard Linear Solid (SLS) is the basis of the VBO. The SLS, shown in Figure III.1, consists of a spring in series with a Kelvin-Voigt element (spring and dashpot elements in parallel). This is a simple linear viscoelastic solid.

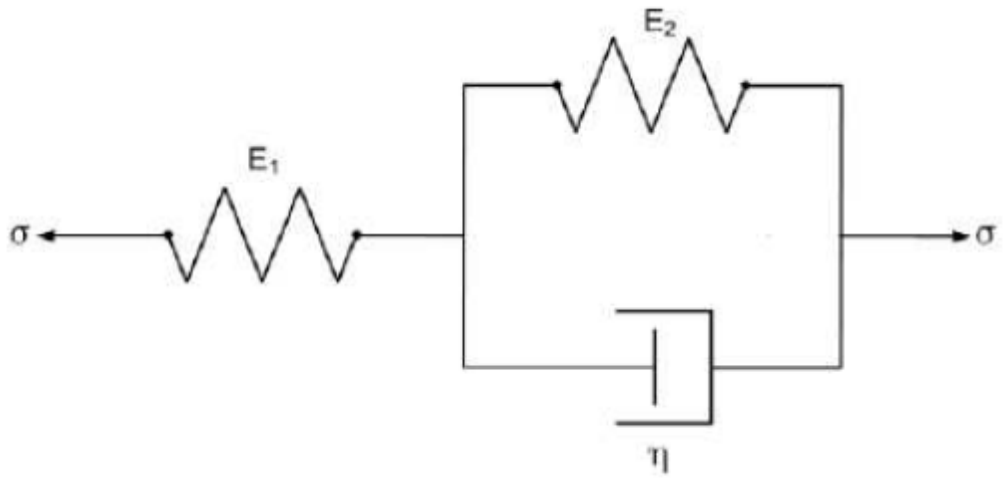

Figure III.1: Standard Linear Solid (SLS). Reproduced from Ozmen [24].

The constitutive equation for the SLS is given in Equation 3.1

$$\dot{\epsilon} + \frac{E_2}{\eta}\epsilon = \frac{\dot{\sigma}}{E_1} + \left(\frac{E_1 + E_2}{E_1}\right)\frac{\sigma}{\epsilon} \tag{3.1}$$

Where E_i is the elastic constant of spring "i" and η is the viscosity constant of the dashpot. Stress and strain are denoted by σ and ϵ, respectively. The SLS can describe both creep and relaxation [19].

Viscoplasticity Based on Overstress

The overstress form of Equation 3.1 can be obtained by rearranging the equation into its elastic and inelastic components.

$$\dot{\epsilon} = \dot{\epsilon}^{el} + \dot{\epsilon}^{in} = \frac{\dot{\sigma}}{E_1} + \frac{\sigma - aE_2\epsilon}{an} \tag{3.2}$$

where

$$a = \frac{E_1}{E_1 + E_2} \tag{3.3}$$

The term $\sigma - aE_2\epsilon$ is called the overstress, thus giving the constitutive model its name. The second term of the overstress is referred to as the equilibrium stress, g. Therefore,

$$g = aE_2\epsilon \tag{3.4}$$

The equilibrium stress is the stress the material exhibits when all rates approach zero.

The behavior of PMR-15 varies according to strain rate as illustrated in Figure II.7. Slow load rates exhibit behavior similar to the equilibrium stress-strain curve and are governed by the two springs in series $\frac{E_1E_2}{E_1+E_2}$ [24, 23]. Rapid loading provides an upper bound on the behavior of the material and is governed by E_1 [24, 23].

Nonlinear effects can be described by the SLS by forcing E_2 to be a nonlinear function of strain and forcing η to vary with the overstress [19]. The final change needed

to develop the standard VBO involves changing the equilibrium stress to allow for "hysteretic behavior" [19].

The governing equation for the VBO is

$$\dot{\epsilon} = \frac{\dot{\sigma}}{E} + \frac{\sigma - g}{Ek} \tag{3.5}$$

where E is the Elastic modulus, g is the equilibrium stress, and k is the viscosity function.

The evolution of the equilibrium stress is defined as

$$\dot{g} = \Psi \frac{\dot{\sigma}}{E} + \frac{\Psi}{E}\left[\frac{\sigma - g}{k} - \frac{g - f}{A}\frac{(\sigma - g)}{k}\right] + \left(1 - \frac{\Psi}{E}\right)\dot{f} \tag{3.6}$$

where A is the isotropic (rate independent) stress, Ψis the shape function and f is the kinematic (rate dependent) stress.

The viscosity function has the basic form

$$k = k_1\left(1 + \frac{|\sigma - g|}{k_2}\right)^{-k_3} \tag{3.7}$$

where $k_1, k_2,$ and k_3 are material constants.

The isotropic stress A establishes the difference between the kinematic stress and the equilibrium stress [23]. The evolution of the isotropic stress is

$$\dot{A} = A_c\left[A_f - A\right]\left|\frac{\sigma - g}{Ek}\right| \tag{3.8}$$

where A_c is a constant that controls how quickly saturation of cyclic hardening or softening is reached and A_f is the saturated value of A [23].

The shape function Ψ governs the shape of the "knee" in the stress-strain curve. The "knee" is the portion of the stress-strain curve where the quasi-elastic behavior transitions to inelastic behavior. The shape function takes the form

$$\Psi = C_1 + (C_2 - C_1)e^{-C_3|\epsilon^{in}|} \tag{3.9}$$

where C_1, C_2, and C_3 are shape function parameters.

The region of inelastic flow is governed by the kinematic stress, f. The evolution of the kinematic stress is defined as

$$\dot{f} = E_t \frac{(\sigma - g)}{Ek} \tag{3.10}$$

where E_t is the slope of the stress-strain curve in the region of fully established inelastic flow.

The concept of a yield surface is not employed in the VBO. This implies that inelastic strain, however small, is always present.

Several versions of the VBO exist. All of them, however, utilize the equilibrium stress, kinematic stress, and isotropic stress variables.

Viscoplasticity Based on Overstress for Polymers

The VBOP is an extension of the VBO. It was developed by Ho [13] to describe the behavior of several polymers. The governing equation of the VBO is still valid:

$$\dot{\epsilon} = \frac{\dot{\sigma}}{E} + \frac{\sigma - g}{Ek} \tag{3.11}$$

with a growth law for the equilibrium stress described by:

$$\dot{g} = \Psi \frac{\dot{\sigma}}{E} + \frac{\Psi}{E}\left[\frac{\sigma - g}{k} - \frac{g - f}{A}\frac{(\sigma - g)}{k} + (\dot{\sigma} - \dot{g})\right] + \left(1 - \frac{\Psi}{E}\right)\dot{f} \tag{3.12}$$

Comparing Equation 3.12 with Equation 3.6 one will find an additional term of $\frac{\Psi}{E}(\dot{\sigma} - \dot{g})$ included in the growth law for the equilibrium stress for the VBOP. This term shows the growth law for the equilibrium stress is dependent on the overstress rate. The

additional term allows high relaxation rates, which are commonly found in polymers, to be modeled. However, this additional term is optional. McClung [23] found the overstress rate term was not necessary to model PMR-15 at 288 °C. Thus, the current research does not incorporate this additional term. Instead, the growth law for the equilibrium stress will take the form found in Equation 3.6.

The viscosity function for the VBOP is

$$k = k_1 \left[1 + \left(1 + \frac{A_0 - A}{A_0 - A_f}\right)\frac{\Gamma}{k_2}\right]^{-k_3} \tag{3.13}$$

where A_0 is the initial value of the isotropic stress, and k_1, k_2, and k_3 are material constants. The term Γ is the overstress invariant and is defined as

$$\Gamma = |\sigma - g| \tag{3.14}$$

The evolution of the isotropic stress remains the same as was seen in the VBO:

$$\dot{A} = A_c\left[A_f - A\right]\left|\frac{\sigma - g}{Ek}\right| \tag{3.15}$$

Many solid polymers can be successfully modeled by setting $A_c = 0$ resulting in a constant isotropic stress value. This can be accomplished for cyclically neutral polymers. PMR-15 is a cyclically neutral polymer; therefore the isotropic stress is constant. Constant isotropic stress allows the viscosity function to be simplified to:

$$k = k_1 \left[1 + \frac{\Gamma}{k_2}\right]^{-k_3} \tag{3.16}$$

The shape function takes the form

$$\Psi = C_1^* + (C_2 - C_1^*)e^{-C_3|\epsilon^{in}|} \tag{3.17}$$

where

$$C_1^* = C_1\left[1 + C_4\left(\frac{|g|}{A+|f|+\Gamma^2}\right)\right] \tag{3.18}$$

and C_1 and C_4 are material constants. The C_1^* term is also optional. McClung [23] deemed this term to be complicated while not contributing much to the predictive capability of the model. Thus, the term was not used and the shape function retained the form from the VBO as seen in Equation 3.9.

The evolution of the kinematic stress takes the form

$$\dot{f} = \left(\frac{|\sigma|}{\Gamma+|g|}\right) E_t \frac{(\sigma-g)}{Ek} \tag{3.19}$$

This form differs from the VBO evolution of the kinematic stress by the inclusion of the term $\left(\frac{|\sigma|}{\Gamma+|g|}\right)$ which increases the strain recovery by slowing the rate at which the equilibrium stress decreases after unloading to zero stress [23]. McClung pointed out this term is optional depending on the material. This term is included in the model formulation for PMR-15.

The VBOP is an appropriate choice for constitutive modeling of PMR-15 at 260 °C. The necessary equations, as used in the model formulation, are listed below.

Uniaxial Flow Law

$$\dot{\epsilon} = \dot{\epsilon}^{el} + \dot{\epsilon}^{in} = \frac{\dot{\sigma}}{E} + \frac{\sigma-g}{Ek} \tag{3.20}$$

Equilibrium Stress Evolution

$$\dot{g} = \Psi\frac{\dot{\sigma}}{E} + \frac{\Psi}{E}\left[\frac{\sigma-g}{k} - \frac{g-f}{A}\left|\frac{(\sigma-g)}{k}\right|\right] + \left(1-\frac{\Psi}{E}\right)\dot{f} \tag{3.21}$$

Kinematic Stress Evolution

$$\dot{f} = \left(\frac{|\sigma|}{\Gamma+|g|}\right) E_t \frac{(\sigma-g)}{Ek} \tag{3.22}$$

Shape Function

$$\Psi = C_1 + (C_2 - C_1)e^{-C_3|\epsilon^{in}|} \tag{3.23}$$

Viscosity Function

$$k = k_1\left[1 + \frac{\Gamma}{k_2}\right]^{-k_3} \tag{3.24}$$

Overstress Invariant

$$\Gamma = |\sigma - g| \tag{3.25}$$

IV. Material and Test Specimen

PMR-15 (Polymerization of Monomeric Reactants – 15)

The focus of this research centers on PMR-15 solid polymer. It is a highly cross-linked thermosetting polyimide used as a matrix in High Temperature Polymer Matrix Composites (HTPMCs). PMR-15 was first developed by the NASA Lewis Research Center in the 1970's [8]. It has become the "leading polymer matrix resin for carbon-fiber-reinforced composites used in aircraft engines" [8]. PMR-15 received its name from the type of reaction used to make this material. The number 15 refers to the average molecular weight of 1500 g/mol of the oligomers before it is cured for the final time [7]. PMR-15 has a glass transition temperature, T_g, of 348 °C and a "long-term use temperature" of 288 °C [8]. The "long-term use temperature" is necessary since polymers must be used at temperatures far from their glass transition temperature. Broeckert, however, reported a glass transition temperature of 331 °C. This discrepancy was attributed by differences in the exact material used, sample geometries, or heating rates [7].

The PMR-15 neat resin panels were supplied by HyComp Inc. (Cleveland, OH). The standard post cure cycle for PMR-15 neat resin used by the Air Force Research Laboratory is shown in Table IV-1. Each panel is assumed to have been exposed to this cure cycle.

Table IV-1: Standard Post Cure Cycle for PMR-15 Neat Resin Panels

Step	Description
1	Heat to 204 °C in 2 h and hold for 1 h
2	Heat to 260 °C in 1 h and hold for 1 h
3	Heat to 316 °C in 2 h and hold for 16 h
4	Cool to room temperature at a rate of 1 °C/min

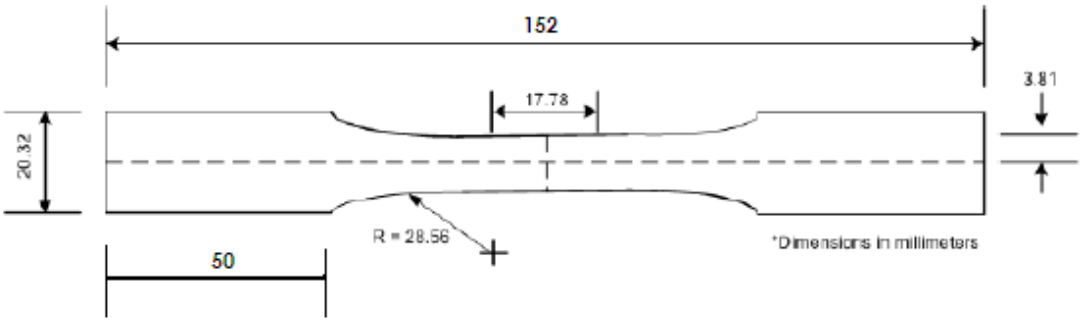

Figure IV.1: Nominal Test Specimen Geometry

Specimen Geometry

Reduced gage section, or dog bone shaped, specimens were used in all tests to ensure failure occurred in a known location. Clearly, this location would be in the middle of the specimen where the cross section is the smallest. The dimensions of the specimens used are shown in Figure IV.1. The gage section length of 17.78 mm allowed enough room for placement of the high temperature extensometer to gather strain data. The

average cross sectional area of the gage section was 24.12 mm^2 with a range in gage section cross sectional area from 17.85 to 31.34 mm^2.

Specimen Preparation

All specimens were washed using common hand soap and rinsed with distilled water to remove contaminates that may have been introduced during diamond grinding or any other process. The specimens were then handled by gloves to prevent oils from the hands from contaminating the specimens. The washed specimens were then dried in a Blue M vacuum oven at 105 °C for 26 hours to remove all moisture. All specimens were then stored in a desiccator continuously purged with dry air unless they were being aged or tested. A silver colored permanent marker was used to mark each specimen.

The surface of PMR-15 was not rough enough to prevent slippage of the high temperature extensometer used for strain measurements. Thus, small dimples were made on each specimen prior to aging through a metal punch and hammer provided by MTS. The depth of the dimples was kept to a minimum to prevent crack propagation. The effect of dimples on ultimate tensile strength (UTS) was studied by Falcone [11] and taken into consideration in this effort.

The gripping section of each specimen was tabbed with a fiber glass composite to protect it from the rough surface of the wedge grips. The tabs were applied to the specimens by the room temperature cure epoxy adhesive M-Bond 200.

V. Experimental Setup and Testing Procedures

This chapter describes the procedures necessary to analyze the strain-rate effect and effect of aging of PMR-15 at 260 °C.

Mechanical Testing Equipment

All mechanical testing was conducted using a Material Test Systems (MTS) servo-hydraulic model 810 with a 3 KIP load cell and a vertically configured MTS model 318.10 load unit equipped with a FlexTest 40 digital controller for signal generation and data acquisition. The gage section of each specimen was heated via a MTS single zone furnace model 653.01A with a MTS model 409.83 temperature controller. The wedge grips, MTS model 647.02B, on the hydraulic machine were cooled by water throughout the testing process to prevent overheating. A grip pressure of 8 MPa was used to ensure the specimen neither slipped nor was crushed during testing. A high-temperature MTS model 632.53E-14 axial extensometer was used for strain measurements.

Test Procedures

Room Temperature Elastic Modulus

The room temperature elastic modulus of each specimen was experimentally determined to view specimen to specimen variability. This test was conducted prior to any aging or testing of specimens. Each specimen was loaded to 3 MPa at a rate of 1 MPa/s and unloaded to zero stress at the same rate in room temperature air. Previous research has indicated this load and load rate guarantee a quasi linear response and no permanent strain [7].

Temperature Calibration

The temperature controller was calibrated to find the set point corresponding to 260 °C. Temperature calibration was accomplished using two k-type thermocouples attached to a PMR-15 sample. The thermocouples were attached to a two-channel temperature sensor to monitor the gage section temperature of the specimen. The input temperature was increased slowly as the output temperature was monitored. A furnace set point of 230 °C was found to maintain a temperature of 260 °C ± 3 °C. The left and right thermocouples remained within 3 °C of each other. Validation of the furnace set point was accomplished by heating the furnace to the set point to 230 °C at a rate of 2 °C/min and then holding the temperature at the set point for 45 minutes to ensure a temperature of 260 °C was maintained on the specimen. This is the same procedure that was used to heat each specimen during each test. The set point was also validated after maintaining its temperature for 3 hours.

Monotonic Tensile Test at Constant Strain Rate

Specimens from each age group were subjected to monotonic tensile tests until failure was reached. These tests were conducted at constant strain rates of 10^{-3}, 10^{-4}, 10^{-5}, and 10^{-6} s^{-1}. This test provided the information necessary to determine when the flow stress region was reached. The elastic modulus and tangent elastic modulus were also determined from this test. The different strain rates allowed the dependence on load rate to be determined. An example of the dependency of PMR-15 on strain rate is shown in Figure V.1 reproduced from McClung and Ruggles-Wrenn [22].

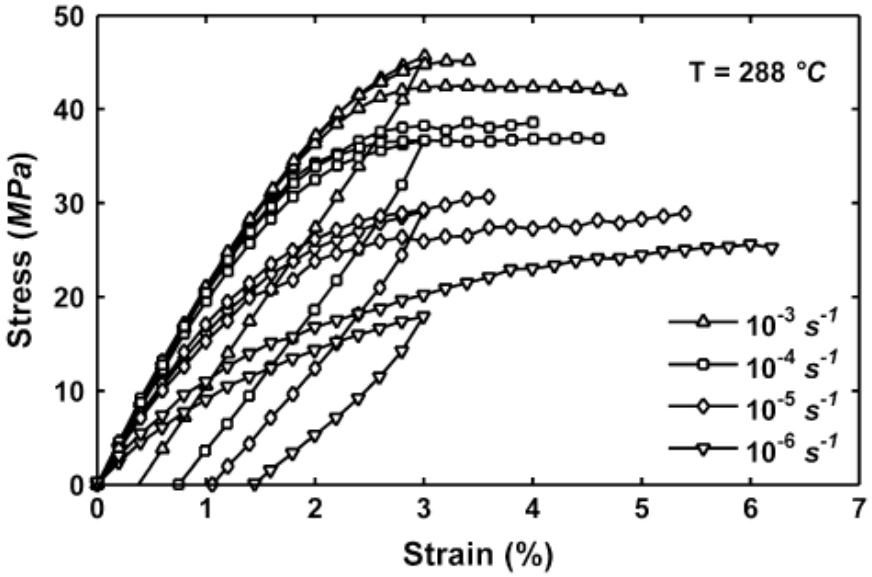

Figure V.1: Stress-Strain Curves Obtained for PMR-15 in Tension to Failure Tests and Loading/Unloading Tests at 288 °C. Reproduced from McClung and Ruggles-Wrenn [22].

Loading Followed by Unloading at Constant Strain Rate

Specimens from each age group were also loaded at a constant strain rate to 2% strain and then unloaded at the same constant strain rate to zero stress. These tests were conducted at constant strain rates of 10^{-3}, 10^{-4}, 10^{-5}, and 10^{-6} s^{-1}. These tests provided the strain rate effects upon unloading of PMR-15.

Recovery of Strain at Zero Stress

Recovery tests were performed immediately following the loading and unloading at constant strain rate tests. After unloading to zero stress, each specimen was held at zero stress for a maximum of 25 h or until saturation was achieved. A recovery test was performed for each age group and prior loading rate of 10^{-3}, 10^{-4}, 10^{-5}, and 10^{-6} s^{-1}.

Again, the varying load rates provided the effect of strain rate on the recovery of PMR-15.

Constant Strain Rate Test with a Period of Relaxation

Specimens from each age group were loaded to 2% strain at a constant strain rate. A period of relaxation was then introduced by holding the specimen at 2% strain for 12 h. At the conclusion of the relaxation period the specimen was loaded to failure at the constant strain rate used prior to relaxation. These tests were conducted at strain rates of 10^{-3}, 10^{-4}, 10^{-5}, and 10^{-6} s^{-1}. The effect of strain rate on relaxation can be determined from these tests.

Creep Test

Specimens from each age group were subjected to creep tests at 25 MPa. Each specimen was loaded at a constant strain rate to a stress of 25 MPa. The stress was then held at 25 MPa for 6 h. At the conclusion of the creep period the specimen was loaded to failure at the constant strain rate used prior to creep. These tests were conducted at strain rates of 10^{-4} and 10^{-6} s^{-1}. The effect of strain rate on creep can be determined from these tests.

Strain Rate Jump Test

The strain rate history effect was analyzed using the strain rate jump test. Specimens in the unaged group were loaded at a constant strain rate to 2% strain and then subjected to a different constant strain rate to failure. The strain rates of 10^{-3} and 10^{-5} s^{-1}

were used. For example, one specimen was loaded at a strain rate of 10^{-3} s^{-1} to 2% and then loaded at a strain rate of 10^{-5} s^{-1} to failure.

Isothermal Aging

The specimens were aged in an argon environment at 260 °C for various lengths of time in a Blue M oven. The age groups were 0, 50, 100, 250, 500, 1000, and 2000 h. The 0 h age group will be referred to as the unaged group. The Blue M oven provided a flow rate of 30 standard cubic feet per hour (SCFH) of argon during steady state operation. The oven door was opened and closed without cooling when removing specimens from each age group. The oven would enter a purge cycle each time the oven door was opened. The flow rate of argon during the purge cycle was approximately 150 SCFH. Each specimen was placed in a dry-air-purged dessicator upon removal from the oven. The dessicator was kept at a relative humidity of less than 10% at all times to avoid moisture effects. It is assumed the effect of the aging of each specimen at room temperature is negligible compared to the effect of aging at 260 °C.

Weight Measurements

Each age group included a rectangular blank sample of PMR-15 to analyze the effect of aging. Each rectangular sample was weighed prior to aging using a Voyager Pro VP214CN microbalance with a resolution of 0.1 mg. After aging, each sample was allowed to cool before being weighed again.

VI. Unaged PMR-15 Neat Resin: Experimental Observations

Assessment of Specimen-to-Specimen Variability

Each specimen may exhibit slightly different characteristics. The room temperature elastic modulus of each specimen was measured prior to thermal aging and testing to ensure the differences in mechanical behavior were not too drastic. This procedure was described in Chapter V. The mean elastic modulus was 3.63 GPa with a standard deviation of 0.22 GPa. As expected, some variability in the elastic moduli existed, but the deviations were insignificant. Thus, no specimen was deemed untestable due to its initial room temperature elastic modulus.

Monotonic Stress-Strain Behavior at Various Constant Strain Rates at Room Temperature

The monotonic tension to failure test described in Chapter V was conducted at room temperature on PMR-15 at several constant strain rates. These results provide a baseline of the tensile behavior of the neat resin. The strain rates used were 10^{-3}, 10^{-4}, 10^{-5}, and 10^{-6} s^{-1}. The results are shown in Figure VI.1. Note the material exhibits near-glassy behavior at this low temperature. The stress-strain curves are all quasi elastic. The flow stress region is never reached. However, the strain rate dependence is readily apparent. Faster strain rates produce steeper stress-strain curves. Slower strain rates result in greater ductility. A clear distinction between the deformation behavior of PMR-15 tested at strain rates of 10^{-3} s^{-1} and 10^{-6} s^{-1} can be seen. The rate dependence is not as obvious between the strain rates of 10^{-4} s^{-1} and 10^{-5} s^{-1}. The rate sensitivity of PMR-15 at

room temperature should not be ignored. This is a phenomenon that must be taken into account when modeling the material behavior.

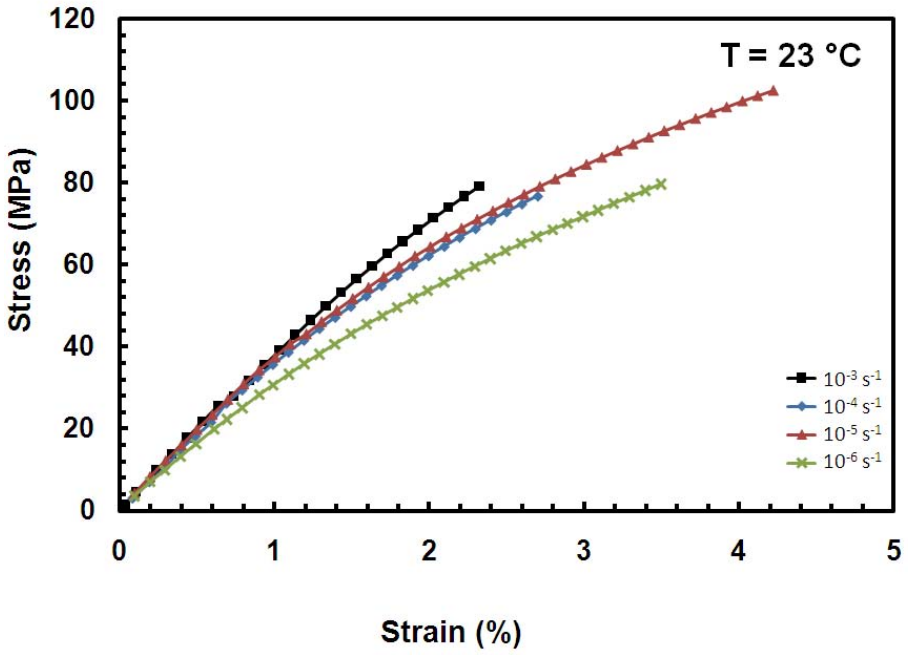

Figure VI.1: Stress-Strain Curves Obtained for Unaged PMR-15 in Tensile Test to Failure Conducted at Constant Strain Rates of 10^{-3}, 10^{-4}, 10^{-5}, and 10^{-6} s^{-1} at Room Temperature.

Monotonic Stress-Strain Behavior at Various Constant Strain Rates at 230 °C

The monotonic tension to failure test described in Chapter V was also conducted at 230 °C on PMR-15 at several constant strain rates. The results of the monotonic tension to failure tests conducted at 230 °C are shown in Figure VI.1.

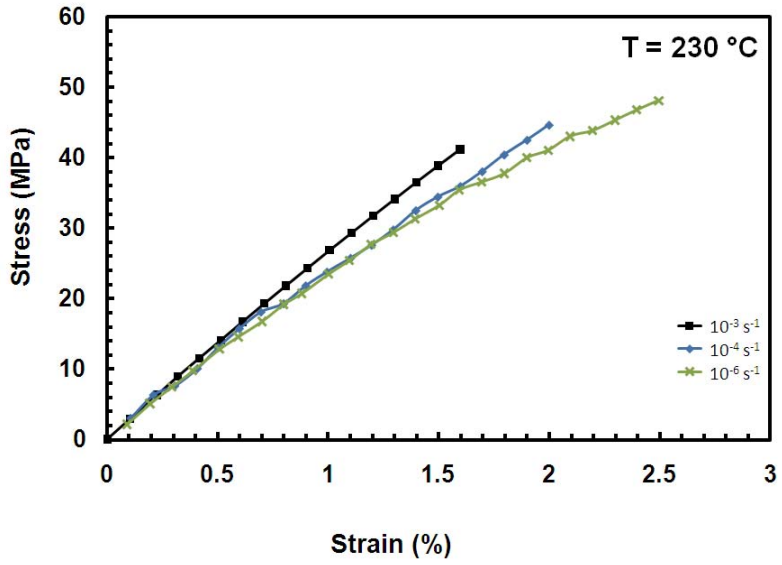

Figure VI.2: Stress-Strain Curves Obtained for Unaged PMR-15 in Tensile Test to Failure Conducted at Constant Strain Rates of 10^{-3}, 10^{-4}, 10^{-5}, and 10^{-6} s^{-1} at 230 °C.

The rate dependence is evident. It is also noteworthy that the material fails before entering the flow stress region for all loading rates.

Deformation Behavior at 260 °C

The tests outlined in Chapter V were conducted on PMR-15 neat resin with no prior thermal aging. The goal of these experiments is to investigate the strain rate (time)-dependent deformation behavior of the PMR-15 polymer at 260 °C. The tests conducted include monotonic tension to failure, loading and unloading, recovery of strain at zero stress, constant strain rate test with a period of relaxation, creep, and strain rate jump test. All tests, with the exception of creep tests, were conducted in strain control with varying strain rates.

Monotonic Tension to Failure

Monotonic tension to failure tests were conducted at constant strain rates of 10^{-3}, 10^{-4}, 10^{-5}, and 10^{-6} s^{-1} to observe the effect of strain rate. The results are shown in Figure VI.3. A distinct linear range is not apparent as the slope of each curve decreases with increasing stress. Strain rate dependence is not seen initially as all four curves exhibit a quasi-elastic slope of 2.3 GPa upon leaving the origin. The strain rate dependence becomes apparent as the material enters the inelastic region. A clear distinction between the strain rate of 10^{-3} s^{-1} and 10^{-6} s^{-1} can be seen. However, the dependence on strain rate is not quite as obvious for the intermediate strain rates of 10^{-4} s^{-1} and 10^{-5} s^{-1}. The specimen loaded at a strain rate of 10^{-4} s^{-1} is the only one to reach the region of fully established inelastic flow, or the flow stress region. The other specimens failed before reaching the flow stress region. However, it can be seen that the flow stress level increases with increasing strain rate.

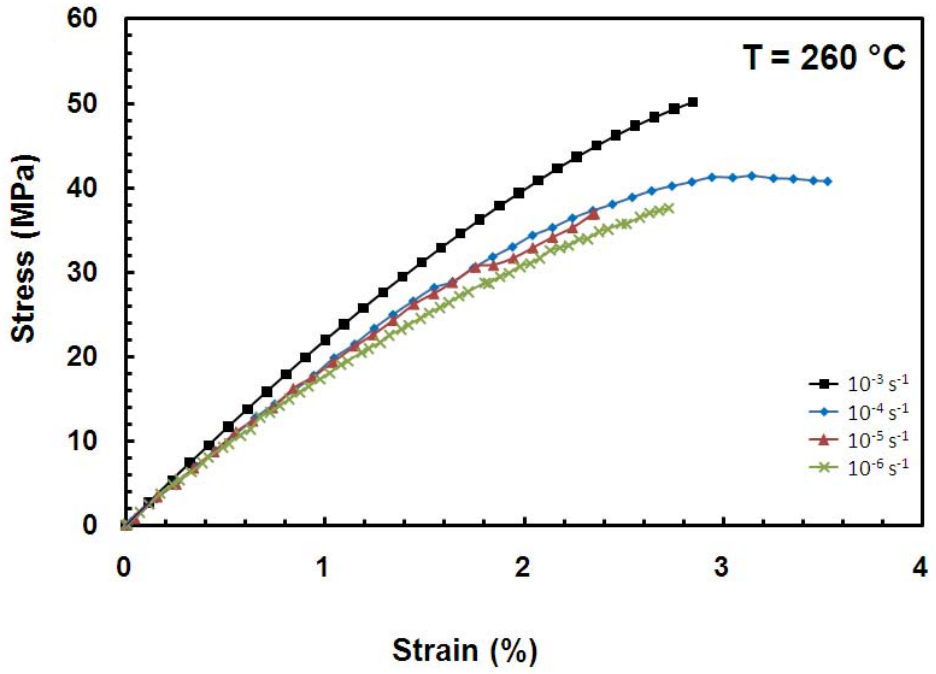

Figure VI.3: Stress-Strain Curves Obtained for Unaged PMR-15 in Tensile Test to Failure Conducted at Constant Strain Rates of 10^{-3}, 10^{-4}, 10^{-5}, and 10^{-6} s^{-1} at 260 °C.

Loading and Unloading

The effect of strain rate can also be seen in unloading. To show this effect, specimens were loaded at a constant strain rate to 2% strain and then unloaded at the same strain rate magnitude to zero stress as described in Chapter V. The results of this test are shown in Figure VI.4. The loading/unloading curves confirm the strain rate dependency in loading observed in the tension to failure tests. The maximum strain of 2% was chosen because it was the highest strain safely achieved at each strain rate in the tension to failure tests. Inelastic flow has not been fully established at 2% strain, therefore modeling may be difficult. It would have been ideal to load to a strain of 3%, but a limited supply of specimens led to the decision to use the "safer" value of 2% strain.

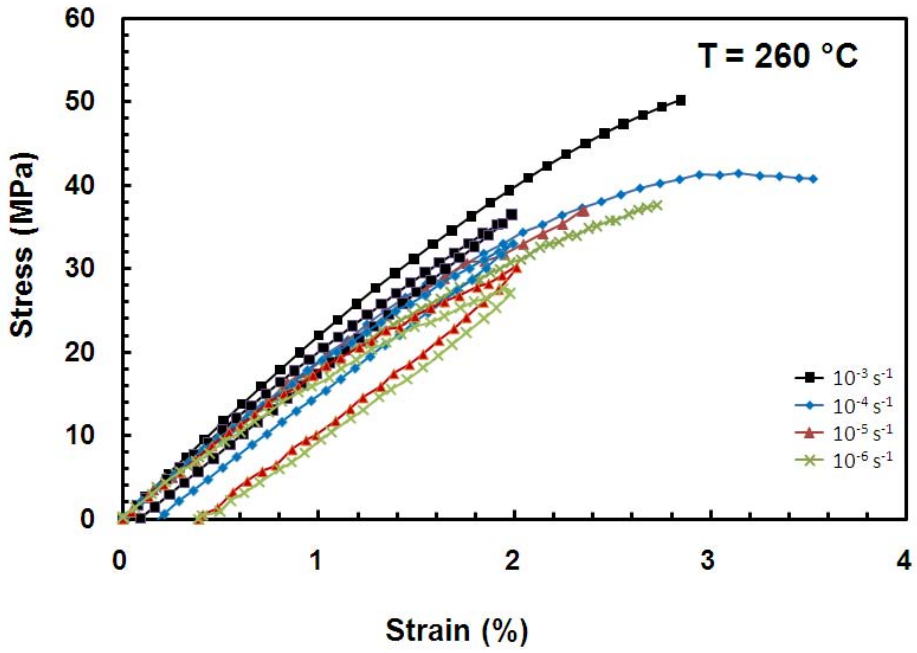

Figure VI.4: Stress-Strain Curves Obtained for Unaged PMR-15 in Loading/Unloading Tests Conducted at Constant Strain Rates of 10^{-3}, 10^{-4}, 10^{-5}, and 10^{-6} s^{-1} at 260 °C Compared to Tension to Failure Results.

The unloading paths are curved as has been seen in similar tests conducted at 288 °C and 316 °C [23, 24]. However, this curved unloading path is not nearly as pronounced at 260 °C as it is at 288 °C and 316 °C as shown in Figure VI.5 and Figure VI.6, respectively. This discrepancy is due to unloading the specimens while still in the quasi-elastic region. The unloading stress-strain curves still exhibit strain rate dependency. It is clear that the inelastic strain upon returning to zero stress decreases with increasing strain rate magnitude. This further confirms the strain rate dependency of PMR-15.

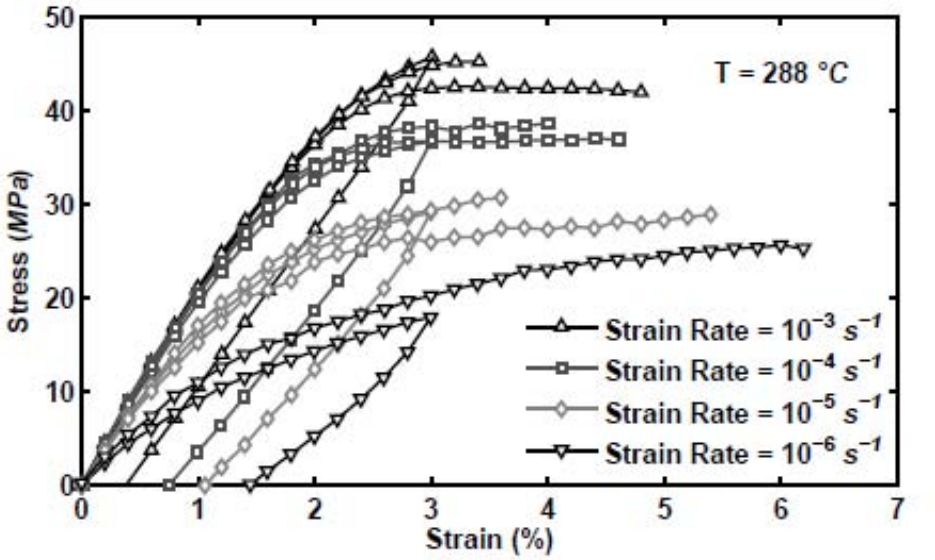

Figure VI.5: Stress-Strain Curves Obtained for PMR-15 in Loading/Unloading Tests Conducted at Constant Strain Rates of 10^{-3}, 10^{-4}, 10^{-5}, and 10^{-6} s^{-1} at 288 °C Compared to Tension to Failure Results. Reproduced from McClung [23].

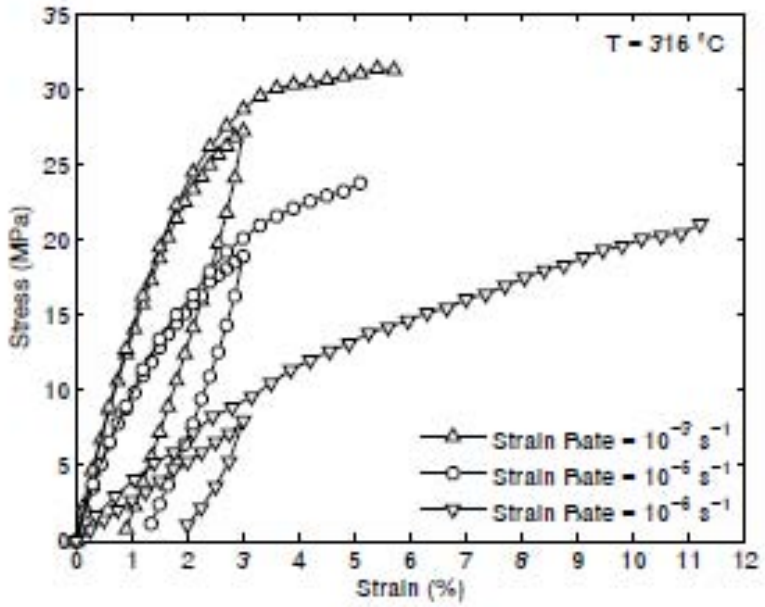

Figure VI.6: Stress-Strain Curves Obtained for PMR-15 in Loading/Unloading Tests Conducted at Constant Strain Rates of 10^{-3}, 10^{-5}, and 10^{-6} s^{-1} at 316 °C Compared to Tension to Failure Results. Reproduced from Ozmen [24].

Recovery of Strain at Zero Stress

Immediately following the loading and unloading process described in the previous section, the specimen was held at zero stress to allow for the recovery of strain. This procedure is described in greater detail in Chapter V. The recovery is plotted in Figure VI.7. Recovered strain is shown as a percentage of the inelastic strain measured immediately upon attaining zero stress. The prior strain rate used in loading and unloading dramatically affected the recovered strain. Strain was recovered much more rapidly with the fast prior strain rates. The specimen loaded at a strain rate of 10^{-3} s^{-1} recovered all of the inelastic strain within a half hour. In the case of 10^{-3} s^{-1} test the inelastic strain is minimal. Once the strain is fully recovered, the measurements reflect system noise. Because the strains are small, noise clouds the data and it appears that over 100% of strain is recovered. The specimen loaded at a strain rate of 10^{-4} s^{-1} recovered all of its inelastic strain within 2.5 h. The specimen loaded at a strain rate of 10^{-5} s^{-1} recovered nearly 75% of its inelastic strain. After 15 h of relaxation it became apparent this specimen would not recover any more strain. Therefore, it can be assumed that a permanent strain resulted from the prior loading. The specimen loaded at a strain rate of 10^{-6} s^{-1} also incurred a permanent strain. It was only able to recover about 35% of its inelastic strain even after 25 h of relaxation.

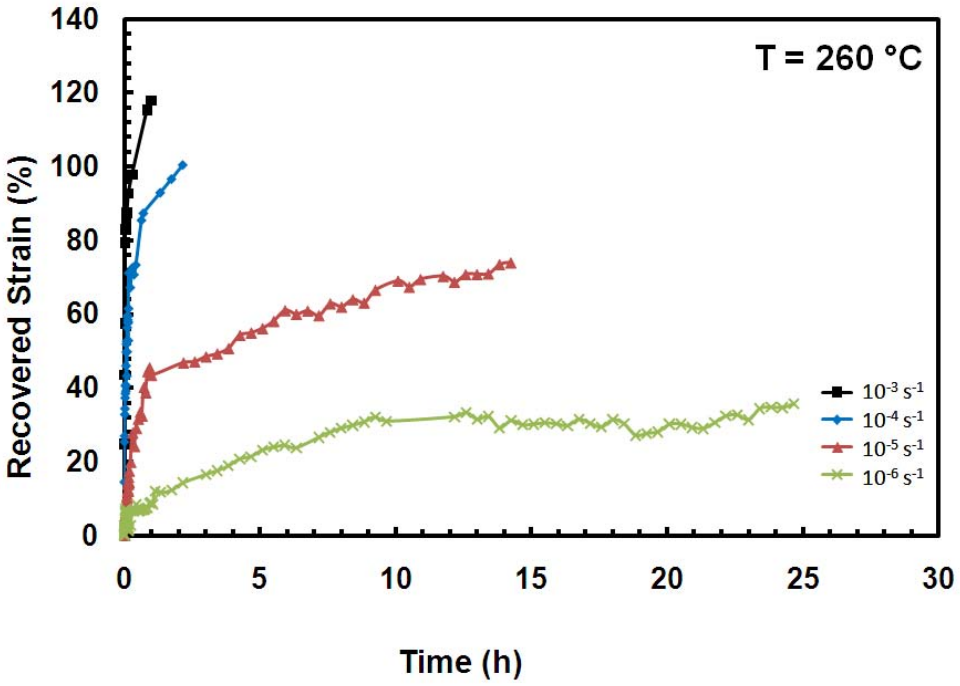

Figure VI.7: Recovery at Zero Stress at 260 °C (Following Loading and Unloading in Strain Control). Recovered Strain is Shown as a Percentage of the Initial Value (Inelastic Strain Value Measured Immediately After Reaching Zero Stress).

Constant Strain Rate Test with a Period of Relaxation

Specimens were also subjected to monotonic tensile tests with a period of relaxation. Each specimen was loaded at a constant strain rate to 2% strain and then held at 2% strain for 12 hours before being loaded to failure at the same strain rate. The strain rates used for this test were 10^{-3}, 10^{-4}, 10^{-5}, and 10^{-6} s^{-1}. Relaxation was performed at the strain of 2% because this was the highest strain comfortably reached at all strain rates in the tension to failure tests. Again note that inelastic flow has not been fully established at

2% strain, therefore modeling of these results may be difficult. The stress-strain behavior in the constant strain rate test with relaxation can be seen in Figure VI.8.

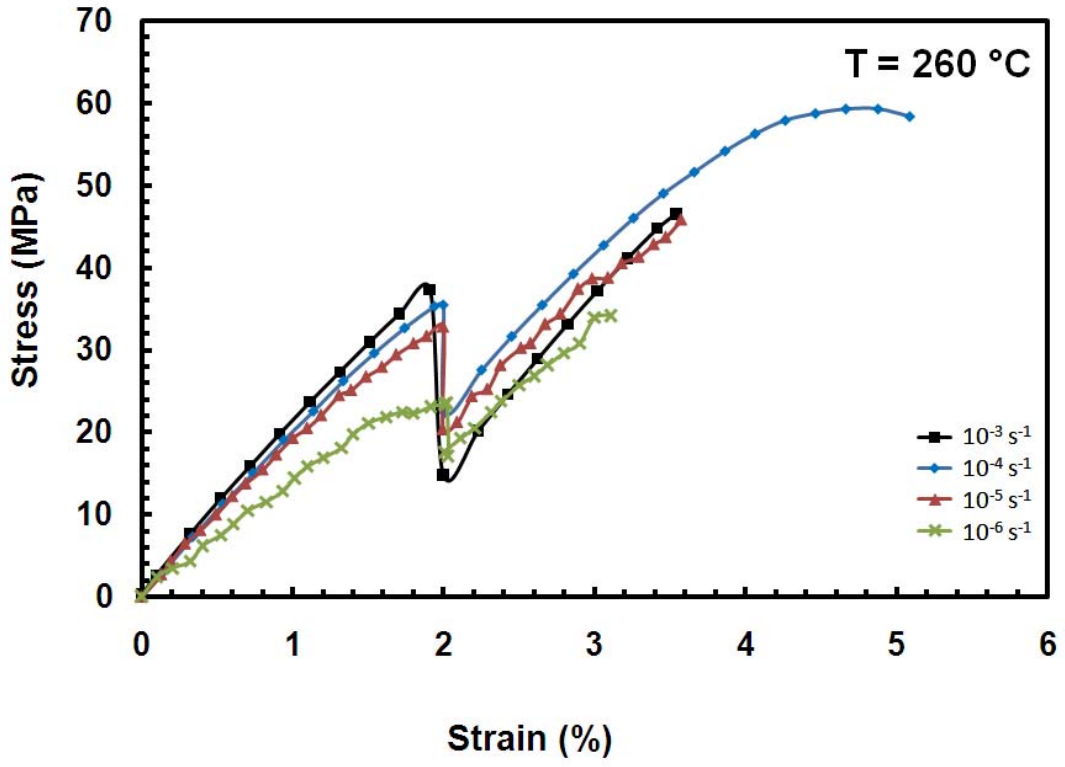

Figure VI.8: Stress-Strain Curves Obtained for PMR-15 Polymer in Constant Strain Rate Tests with a Period of Relaxation at 2% Strain at 260 °C.

The strain rate dependence is clear. The fastest loading rate achieved the highest stress before relaxation. The stress strain curve for the strain rate of 10^{-3} s^{-1} dropped to the lowest stress after relaxation. The strain rate dependence is also evident upon loading to failure after relaxation. It is assumed the stress strain curve for the strain rate of 10^{-3} s^{-1} would continue to a higher stress than for the strain rate of 10^{-4} s^{-1} had it not exhibited an early failure. It is also noteworthy that the stress strain curve for the strain rate of 10^{-4} s^{-1} exhibited the "overshoot" described by McClung [23]. It is assumed this same, and

probably more pronounced, overshoot would occur for the stress strain curve for the strain rate of 10^{-3} s^{-1} had it not exhibited an early failure. However, it cannot be assumed that an overshoot will exist for the strain rate of 10^{-5} s^{-1} or 10^{-6} s^{-1} since McClung and Ozmen both noted the overshoot becomes less pronounced at slower strain rates [24, 23].

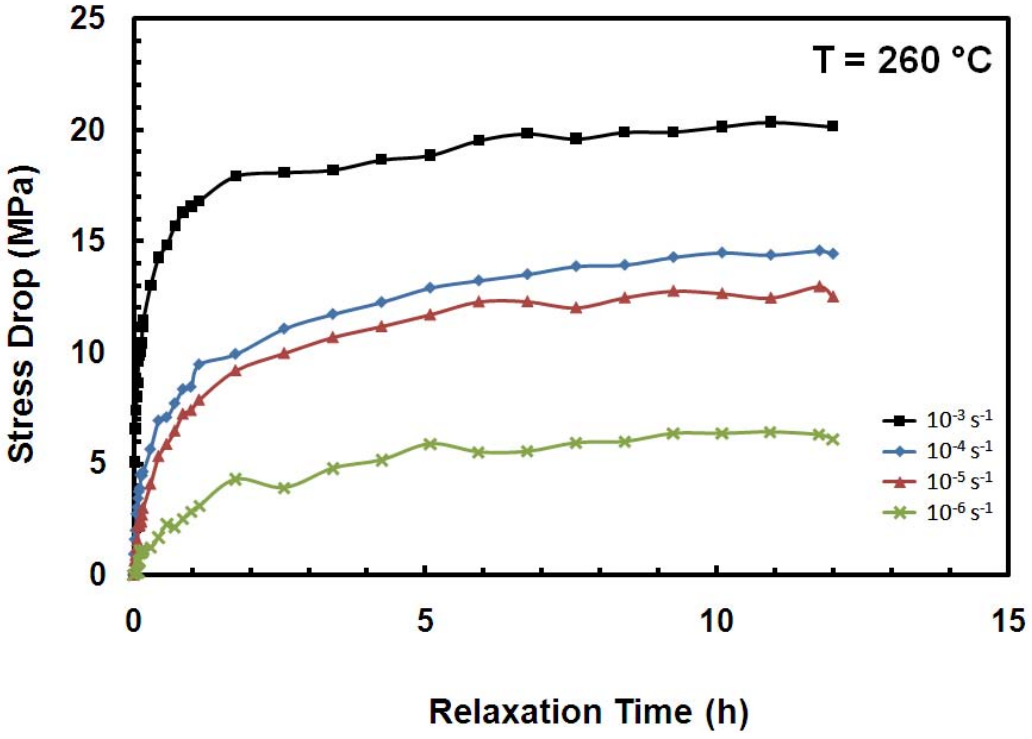

Figure VI.9: Stress Decrease vs Relaxation Time for the PMR-15 Polymer at 260 °C.

The stress drop during relaxation for each prior loading rate is shown in Figure VI.9. The influence of prior strain rate is very apparent. Faster prior loading rates lead to larger stress drops. As expected, most of the stress drop occurs within the first 2 hours of relaxation. The total stress drop levels off after about 10 hours of relaxation, and it is assumed that any further stress drop after 12 hours is negligible.

Creep Test

The effect of strain rate on creep behavior was studied. Specimens were loaded at a constant strain rate to a stress level of 25 MPa. The specimens were then held at a stress of 25 MPa for 6 hours allowing them to creep. The strain rates analyzed were 10^{-4} s^{-1} and 10^{-6} s^{-1}. This procedure is described in more detail in Chapter V. The stress level of 25 MPa was chosen as it was the highest stress safely achieved at all strain rates in tension to failure tests. It should be noted that the flow stress region is not attained at this stress level for any of the loading rates. The creep response is shown in Figure VI.10.

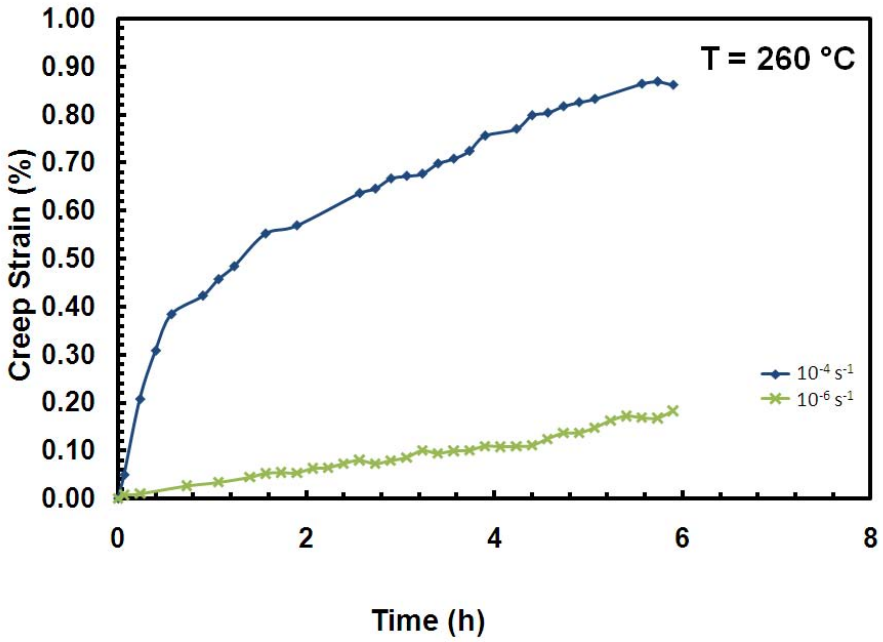

Figure VI.10: Creep Strain vs Time at 25 MPa and 260 °C.

The dependence of creep strain on prior strain rate is clear. Creep strain is accumulated more quickly for faster prior loading rates. Primary and secondary creep is exhibited in the test with a prior loading rate of 10^{-4} s^{-1} while only secondary creep

dominates in the test with a prior loading rate of 10^{-6} s^{-1}. Creep strain increases nonlinearly with increasing prior strain rate at a creep stress of 25 MPa. It is assumed this relation holds for all creep stress levels in the flow stress region.

Strain Rate Jump Test

The strain rate jump test is used to determine if a prior loading rate has an influence on the current loading behavior. This is known as strain rate history effect. One specimen was loaded at a strain rate of 10^{-3} s^{-1} to a strain of 2% and then loaded at a strain rate of 10^{-5} s^{-1} to failure. Another specimen was loaded in an opposite manner, first with 10^{-5} s^{-1} and then with 10^{-3} s^{-1}. This procedure was described in greater detail in Chapter V. The results from the strain rate jump test are shown in Figure VI.11. The monotonic tension to failure test results for strain rates of 10^{-3} s^{-1} and 10^{-5} s^{-1} are also included in this figure to provide a reference for comparison. The stress strain curve denoted by triangles is the tension to failure test at a strain rate of 10^{-3} s^{-1}. The stress strain curve denoted by diamonds is the tension to failure test at a strain rate of 10^{-5} s^{-1}. The stress strain curve denoted by squares is the strain rate jump test conducted with the strain rate of 10^{-3} s^{-1} first followed by the strain rate of 10^{-5} s^{-1}. The stress strain curve denoted by x's is the strain rate jump test conducted with the strain rate of 10^{-5} s^{-1} first followed by the strain rate of 10^{-3} s^{-1}.

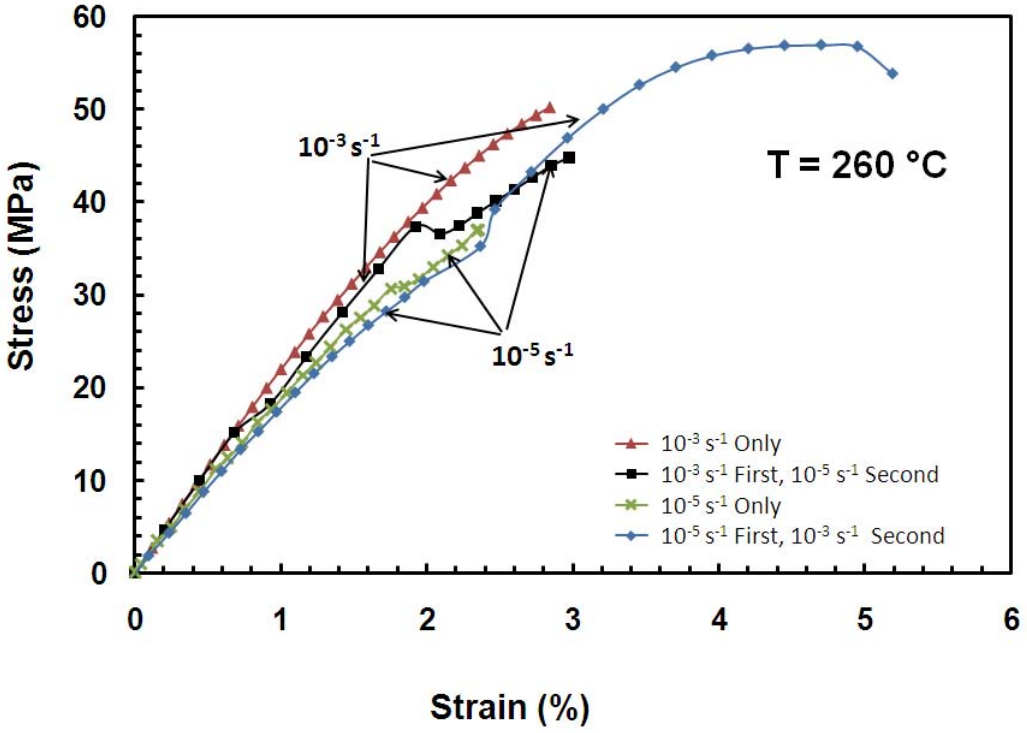

Figure VI.11: Stress-Strain Curves Obtained for Unaged PMR-15 Polymer in Strain Rate Jump Tests and in Constant Strain Rate Tests at 260 °C.

It is difficult to draw any conclusions from this test. The specimen loaded at a strain rate of 10^{-3} s^{-1} first does show a decrease in flow stress when it switches to a strain rate of 10^{-5} s^{-1}. It appears it would join up with the tension to failure specimen loaded at a constant strain rate of 10^{-5} s^{-1}. However, early failure occurred. These results would indicate the PMR-15 polymer exhibits no strain rate history effect.

No conclusions, however, can be drawn from the specimen loaded at a strain rate of 10^{-5} s^{-1} first. At first glance the stress strain curve for this specimen does appear to join up with that produced by the specimen loaded to failure at a constant strain rate of

10^{-3} s^{-1}, however this could just as easily be the same path as the specimen loaded to failure at a constant strain rate of 10^{-5} s^{-1} would have taken had it not failed early.

As a result, the strain rate jump test provided inconclusive results. Again, this can be attributed to the inability to reach the flow stress region at this temperature. This will complicate the use of the VBOP as a constitutive model.

Comparison of Deformation Behavior at Different Temperatures

PMR-15 has been shown to behave differently at different temperatures. Hence the reason the research did not terminate after modeling behavior of PMR-15 at 288 °C. Figure VI.12-Figure VI.15 show the dependence of PMR-15 tensile stress-strain response on test temperature. It is clear that the material exhibits greater ductility at higher temperatures. The flow stress region is successfully reached at all strain rates at temperatures of 288 °C and higher. For PMR-15 tested at 260 °C the flow stress region is generally not reached. It is clear that the flow stress level decreases with increasing temperature. The material gets noticeably stiffer as it approaches glassy behavior at decreasing temperature. This can be seen in Figure VI.12 - Figure VI.15.

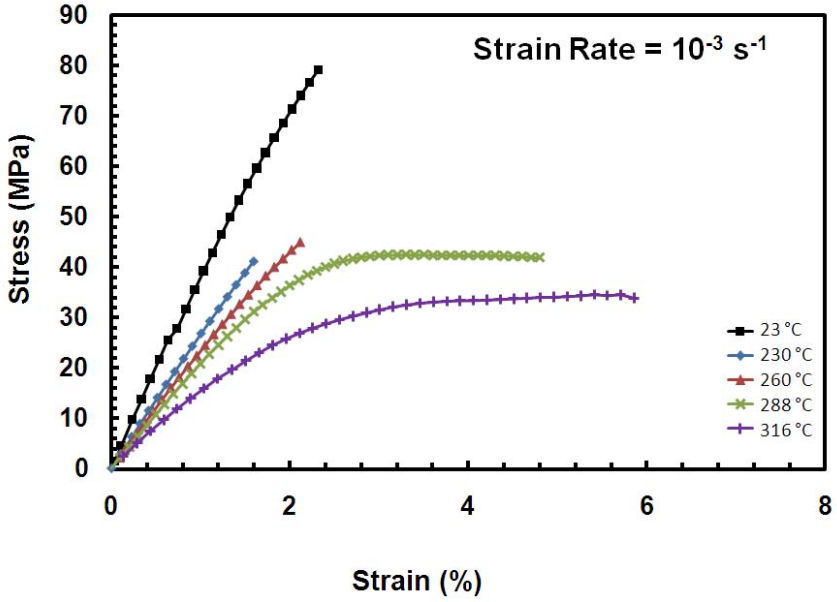

Figure VI.12: Effect of Test Temperature on Deformation Behavior of PMR-15 in Tension to Failure Test Loaded at a Strain Rate of 10^{-3} s^{-1}. Experimental Data at 316 °C from Ozmen[24]. Experimental Data at 288 °C from McClung [23].

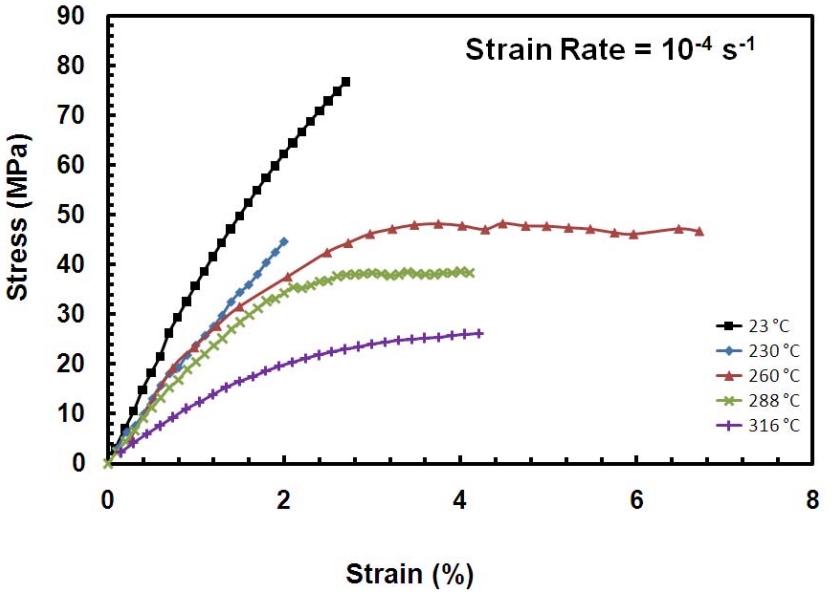

Figure VI.13: Effect of Test Temperature on Deformation Behavior of PMR-15 in Tension to Failure Test Loaded at a Strain Rate of 10^{-4} s^{-1}. Experimental Data at 316 °C from Ozmen[24]. Experimental Data at 288 °C from McClung [23].

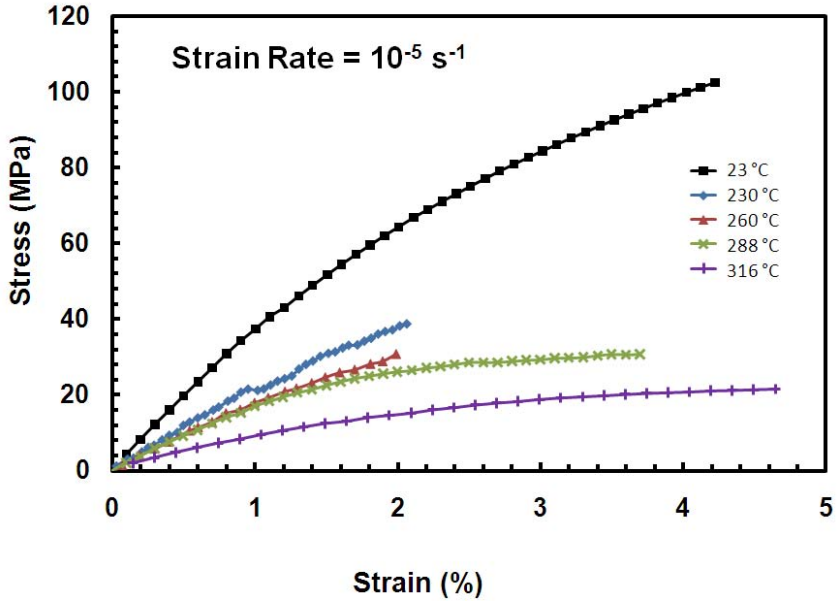

Figure VI.14: Effect of Test Temperature on Deformation Behavior of PMR-15 in Tension to Failure Test Loaded at a Strain Rate of 10^{-5} s^{-1}. Experimental Data at 316 °C from Ozmen[24]. Experimental Data at 288 °C from McClung [23].

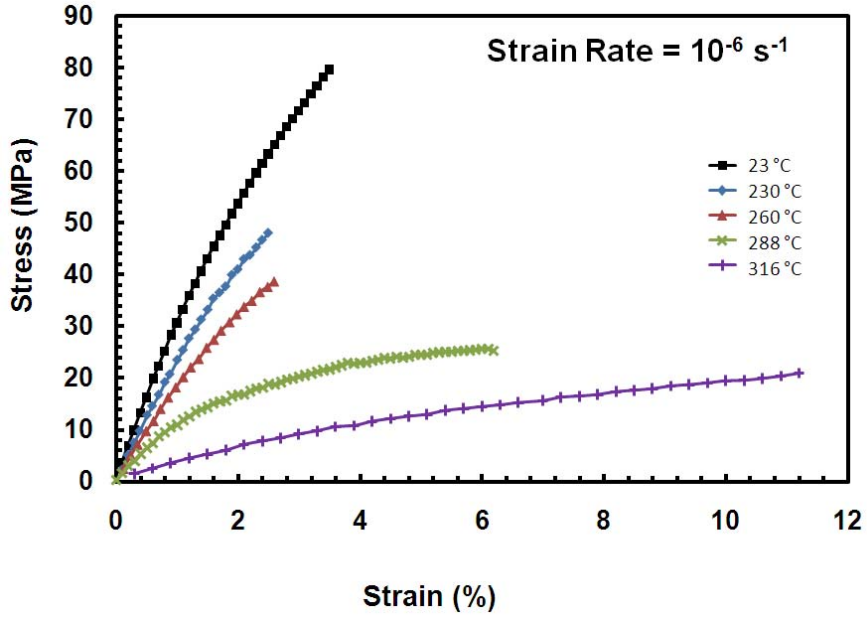

Figure VI.15: Effect of Test Temperature on Deformation Behavior of PMR-15 in Tension to Failure Test Loaded at a Strain Rate of 10^{-6} s^{-1}. Experimental Data at 316 °C from Ozmen[24]. Experimental Data at 288 °C from McClung [23].

VII. Unaged PMR-15 Neat Resin: Constitutive Modeling

McClung [23] and Ozmen [24] both successfully employed the Viscoplasticity Based on Overstress for Polymers (VBOP) to model the inelastic behavior of the unaged PMR-15 neat resin at 288 °C and 316 °C, respectively. It must be pointed out that the parameters of the VBOP are determined through data produced in the region of fully established inelastic flow. The tests performed at 260 °C revealed that the flow stress region was never successfully reached. Therefore, the VBOP model will be stretched to its limits in characterizing the behavior of PMR-15 at this temperature. The temperature of 260 °C is considerably below the glass transition temperature. This resulted in a near glassy behavior of the resin. In determining temperature dependence of the inelastic behavior of PMR-15 the results of the VBOP modeling efforts at 260 °C should be used with caution. These model parameters should only be used as auxiliary values. Tests at 275 °C may produce results that can be successfully modeled by the VBOP.

Phenomenological Aspects of Deformation Behavior and Implications for Modeling

The experimental results obtained for the unaged PMR-15 neat resin at 260 °C revealed the following characteristics:

1. Linear, quasi-elastic behavior upon initial loading.
2. Strain rate sensitivity in monotonic loading. The flow stress increases nonlinearly with increasing strain rate. A unique stress-strain curve exists for each strain rate.
3. Fully established inelastic flow is never reached due to early failure.

4. Prior load rate significantly effects recovery of strain. Recovery rate increases with prior strain rate.
5. Creep strain is strongly affected by prior strain rate. An increase in prior strain rate results in an increase in creep strain.
6. Relaxation behavior is influenced by prior strain rate. Higher prior strain rates result in larger stress drops during relaxation.

These characteristics follow the same trends as those seen at 288 °C and 316 °C [23, 24]. PMR-15 exhibits additional tendencies, such as the lack of a strain rate history effect seen in the strain rate jump tests, at these higher temperatures that are not seen as clearly at 260 °C due to the brittleness of the material at this lower temperature.

McClung [23] and Ozmen [24] demopnstrated the VBOP was able to model the characteristics listed above. Therefore, despite the lack of test data in the flow stress region at 260 °C, the VBOP will be used to model the behavior PMR-15 at this temperature. This will ensure consistency in the analysis of this material and provide the necessary information to determine the effect of temperature on the inelastic behavior of PMR-15.

Review of Model Formulation

The VBOP formulation for PMR-15 at 260 °C is summarized in this section. This is a reproduction of McClung's summary [23]. The uniaxial flow law is a combination of the elastic and inelastic strain rates

$$\dot{\epsilon} = \dot{\epsilon}^{el} + \dot{\epsilon}^{in} = \frac{\dot{\sigma}}{E} + \frac{\sigma - g}{Ek} \tag{7.1}$$

The growth law of the equilibrium stress is [23, 24]

$$\dot{g} = \Psi \frac{\dot{\sigma}}{E} + \Psi \left[\frac{\sigma - g}{Ek} - \frac{g - f}{A}\left|\frac{\sigma - g}{Ek}\right|\right] + \left[1 - \frac{\Psi}{E}\right]\dot{f} \tag{7.2}$$

The kinematic stress has the form

$$\dot{f} = \left[\frac{|\sigma|}{\Gamma + |g|}\right] E_t \frac{(\sigma - g)}{Ek} \tag{7.3}$$

The overstress invariant is defined as

$$\Gamma = |\sigma - g| \tag{7.4}$$

The isotropic stress evolution for polymers remains the same as that in the standard VBO

$$\dot{A} = A_c[A_f - A]\left|\frac{\sigma - g}{Ek}\right| \tag{7.5}$$

Equation 7.5 is simplified in the case of the PMR-15 at 260 °C by setting $A_c = 0$. Thus, A is a constant.

The shape function has the form

$$\Psi = C_1 + (C_2 - C_1)e^{-C_3|\epsilon^{in}|} \tag{7.6}$$

Since A is constant, the viscosity function for polymers reduces to

$$k = k_1\left[1 + \frac{\Gamma}{k_2}\right]^{-k_3} \tag{7.7}$$

Where k_1, k_2, and k_3 are material constants.

These equations were chosen based on the previous research accomplished for PMR-15 at 288 °C [23] and 316 °C [24]. These equations would also have been chosen based on the characteristics seen in the experiments on the unaged PMR-15 at 260 °C.

Model Characterization Procedure

McClung developed a systematic procedure to apply the VBOP to PMR-15. Her model characterization procedure is summarized as follows [23]

1) Determine elastic modulus and tangent modulus
2) Determine equilibrium stress
3) Determine isotropic stress
4) Assess viscosity function
5) Determine shape function parameters

The details of the procedure will be given in the subsequent sections, as well as the results of the procedure as it is applied to unaged PMR-15 tested at 260 °C.

Elastic Modulus and Tangent Modulus

The elastic modulus can easily be determined from the monotonic tension to failure data. The slope of the initial quasi-elastic region of the stress-strain curve is the elastic modulus. The stress-strain data acquired during the monotonic tension to failure of PMR-15 at 260 °C and a strain rate of 10^{-3} s^{-1} yielded an elastic modulus of $E = 2.304$ GPa.

The tangent modulus can also be easily determined from the monotonic tension to failure data. The slope of the stress-strain curve in the flow stress region is the tangent modulus. It is easiest to find the tangent modulus through the stress-strain curve that obtains the highest strains. For the unaged group the highest strain was achieved in the

monotonic tension to failure test conducted at a strain rate of 10^{-4} s^{-1}. Thus, this curve was used to find a tangent modulus of E_t = 23 MPa.

Equilibrium Stress and Isotropic Stress

It has been well documented [23, 24] that the stress and strain values at the end of relaxation for a given relaxation strain are the same value regardless of the prior strain rate. This suggests the existence of an equilibrium stress-strain curve. So, equilibrium stress values can be found at each value of strain to form an equilibrium curve. This equilibrium stress curve will have the same shape as the stress-strain curves obtained at higher loading rates. The easiest way to determine the equilibrium stress is to conduct relaxation at a strain in the flow stress region and record the stress value at the end of relaxation. Since unaged PMR-15 tested at 260 °C never enters the region of fully established inelastic flow, relaxation tests were performed at a strain value still in the quasi-linear region. Thus, the stress value at the end of relaxation may be much lower than the actual equilibrium stress. Experimental data suggests an equilibrium stress of $g = 15$ MPa for $\epsilon = 2\%$.

The isotropic stress is the difference between the equilibrium stress value and the kinematic stress value at a given strain. Kinematic stress, f, is defined as $f = E_t\epsilon$. Thus, the isotropic stress can be determined through the equation [23]

$$A = \{g - E_t\epsilon\} \tag{7.8}$$

Substituting the equilibrium stress value at the relaxation strain of 2% into Equation 7.8 yields an isotropic stress of $A = 14.54$ MPa. However, as stated before, the isotropic

stress may actually be higher since relaxation did not take place in the flow stress region. This turns out to be the case as the isotropic stress value that most accurately describes the behavior of unaged PMR-15 tested at 260 °C was found to be $A = 30$ MPa. This value was found through a "guess and check" method when determining the viscosity function described in the next section. This "guess and check" method was the very method McClung was attempting to avoid by developing her characterization procedure. However, since the flow stress region is never obtained at 260 °C the characterization procedure could not be blindly applied.

Viscosity Function

The viscosity function, given in Equation 7.7, controls the rate dependent aspects of the model. The values of k_1, k_2, and k_3 are obtained through the relaxation tests conducted at various prior strain rates. An optimization procedure in MATLAB was used to find the viscosity function parameters. This code is found in Appendix A. The resulting parameters were $k_1 = 1.09e + 04$ s, $k_2 = 31.18$ MPa, and $k_3 = 15.82$. The numerical simulations of the relaxation behavior at 2% strain are compared to the experimental results in Figure VII.1. The rate dependence is captured very well by the model. The model overestimates the stress drop early in relaxation of the higher prior strain rates, but begins to match up quite nicely as time progresses. The slowest strain rate is opposite: the model matches the experimental data very closely in the early stage of relaxation and begins to under predict the stress drop as time progresses. However, the discrepancy is not very large. The ability of the model to predict the relaxation behavior

this well is quite surprising as relaxation is not occurring in the flow stress region. It cannot be stressed enough that the model is not intended for use in the quasi-elastic region. McClung [23] clearly states that

> only relaxation data obtained at strain levels in the region where the plastic flow is fully established should be used to evaluate the viscosity function k. Relaxation results obtained at strain levels occurring before the "knee" in the stress-strain diagram can be influenced by the transients in the material behavior and therefore would not yield reliable characterization of the viscosity function k.

Thus, these results are very exciting.

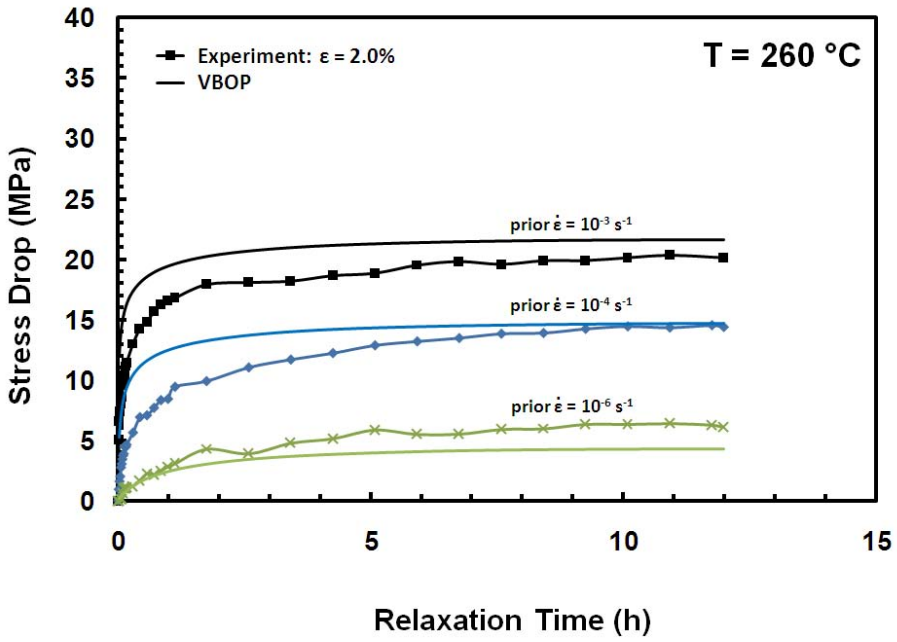

Figure VII.1: A Comparison Between Experimental and Predicted Stress Drop vs Relaxation Time for Unaged PMR-15 Polymer at 260 °C.

Shape Function

The shape function controls the shape of the "knee" in the stress-strain curve [23]. The values of C_1, C_2, and C_3 are obtained from the monotonic tension to failure tests

conducted at various strain rates. An optimization procedure in MATLAB is used to find the shape function parameters. This code is found in Appendix B. The resulting parameters were $C_1 = 100$ MPa, $C_2 = 1.33e + 03$ MPa, and $C_3 = 4.32e - 12$. It is interesting to note how small the C_3 value is. Equation 7.6 points to the fact that this coefficient is magnifying the effect of the inelastic strain. Since fully established inelastic flow is never established, it is not surprising that C_3 is small. The numerical simulations of the monotonic tension to failure tests are compared to the experimental results in Figure VII.2.

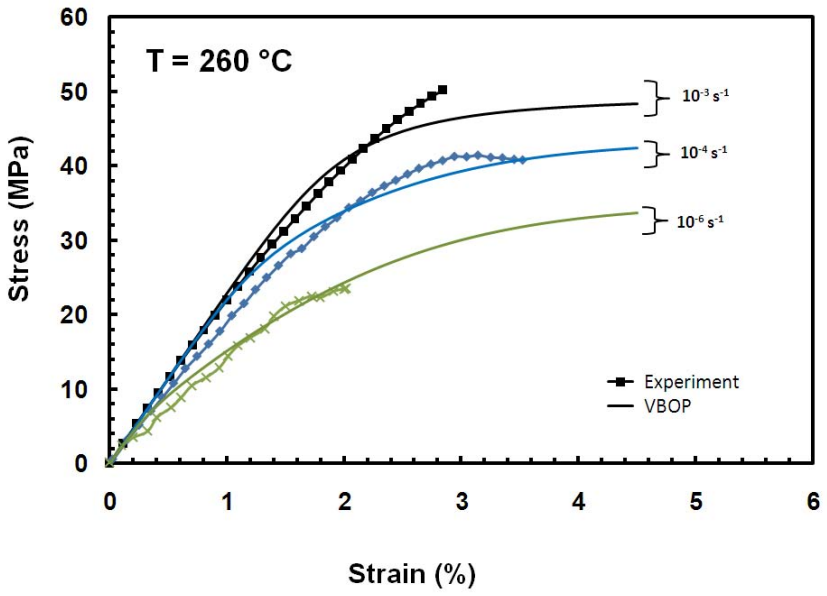

Figure VII.2: A Comparison Between Experimental and Predicted Stress-Strain Curves Obtained for Unaged PMR-15 Polymer at Constant Strain Rates of 10^{-3}, 10^{-4}, and 10^{-6} s^{-1} at 260 °C.

The results are adequate considering the viscosity function parameters were derived using data outside of the flow stress region. The rate dependency is represented by the model very well. The experimental and simulated curves obtained at a strain rate of 10^{-6} s^{-1}

match very well. The curves for the higher strain rates match well initially but depart from the quasi-elastic region at different strains. The experimental curve obtained at a strain rate of 10^{-4} s^{-1} merges with the simulated curve as the strain is increased beyond the knee. The experimental and simulated curves obtained at a strain rate of 10^{-3} s^{-1} match well in the quasi-elastic region. However, the simulated curve departs from the quasi-elastic region much earlier than the experimental curve. It is difficult to determine if the experimental curve would ever join back up with the simulated curves. It is possible that the specimen has failed right before the knee in the stress-strain curve was revealed and that the experimental curve would then flatten out as it meets up with the simulated curve.

The parameters as a result of the modeling effort are presented in Table VII-1.

Table VII-1: Model Parameters Used in the VBOP Predictions of the Deformation Behavior of the Unaged PMR-15 Neat Resin at 260 °C.

Moduli	E = 2304 MPa, E_t = 23 MPa
Isotropic Stress	A = 30 MPa
Viscosity Function	k_1 = 1.0857e+04 s, k_2 = 31.18 MPa, k_3 = 15.82
Shape Function	C_1 = 100 MPa, C_2 = 1.326e+03 MPa, C_3 = 4.32e-12

Model Verification

Since the optimization used to determine the model parameters incorporated the experimental values from the relaxation and monotonic tension to failure tests it becomes necessary to validate the model. This is accomplished by predicting the results of a test not used for model characterization, i.e. creep, and comparing predictions to the

experimental data. Figure VII.3 shows this comparison for a creep test. McClung notes that creep is a stress controlled test and is thus much more difficult for the VBOP, a strain controlled model, to produce accurate predictions [23]. The dependence on prior strain rate is captured qualitatively by the model. That is, more creep strain is accumulated at higher prior strain rates than at lower prior strain rates. However, the quantitative prediction of creep is not very accurate. Again, this can be attributed to the development of the model parameters using data from a region where inelastic flow is not fully established. These discrepancies can also be attributed to the fact that a creep test is conducted in stress control. This means creep is a rigorous validation of the model, which is originally defined through strain rates.

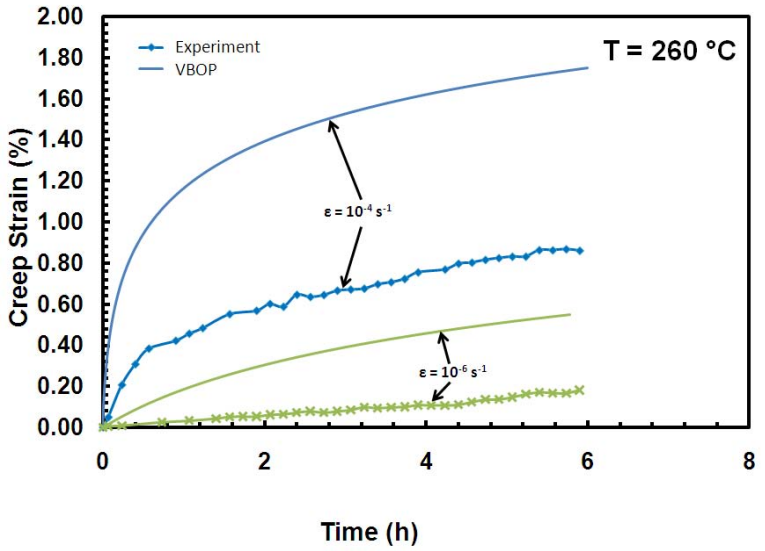

Figure VII.3: Comparison Between the Experimental and Predicted Strain vs Time Curves Obtained for Unaged PMR-15 Polymer at 260 °C in Creep at 25 MPa.

The viscosity function, k, is responsible for the time dependent behavior within the VBOP. Relaxation is one manifestation of this time dependent behavior. Creep is

another example of time dependent behavior for PMR-15. Previous work on the modeling of PMR-15 [23] used data obtained during relaxation to assess the viscosity function. However, it appears creep data could also be used with an optimization procedure to determine the viscosity function. It is assumed that relaxation behavior would not be accurately captured had creep data been used to determine the model parameters in the same way that creep is not accurately captured when using relaxation data to determine model parameters.

Another useful validation test is the loading followed by unloading at constant strain rate. The simulated results are compared to the experimental results in Figure VII.4. The strain rate dependence is definitely obvious in the loading portion. The unloading portion of the test is inconclusive. However, this is not surprising as McClung had difficulty in accurately describing unloading through the VBOP [23]. The behavior is almost entirely quasi-elastic in the experimental data. This is reproduced through the model quite well.

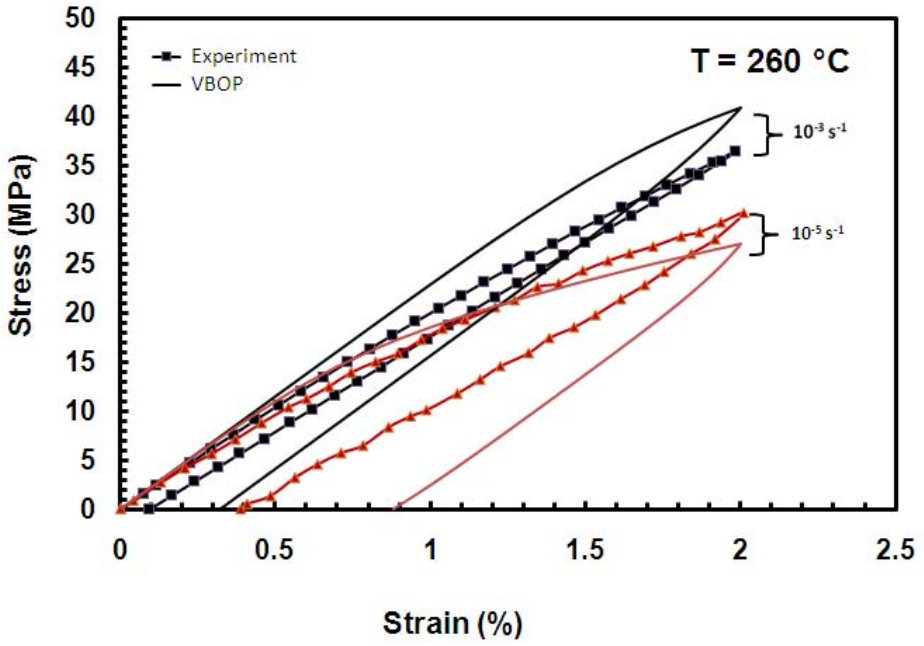

Figure VII.4: A Comparison Between Experimental and Predicted Stress-Strain Curves Obtained for Unaged PMR-15 Polymer in Loading and Unloading at Two Constant Strain Rates at 260 °C

The strain rate jump test can also be used to validate the model. The predictions of the VBOP are plotted against the experimental results in Figure VII.5 - Figure VII.6. The experiment loaded at 10^{-3} s^{-1} first is modeled well with the initial loading, but the second loading is not represented very accurately. The qualitative jump, however, is modeled.

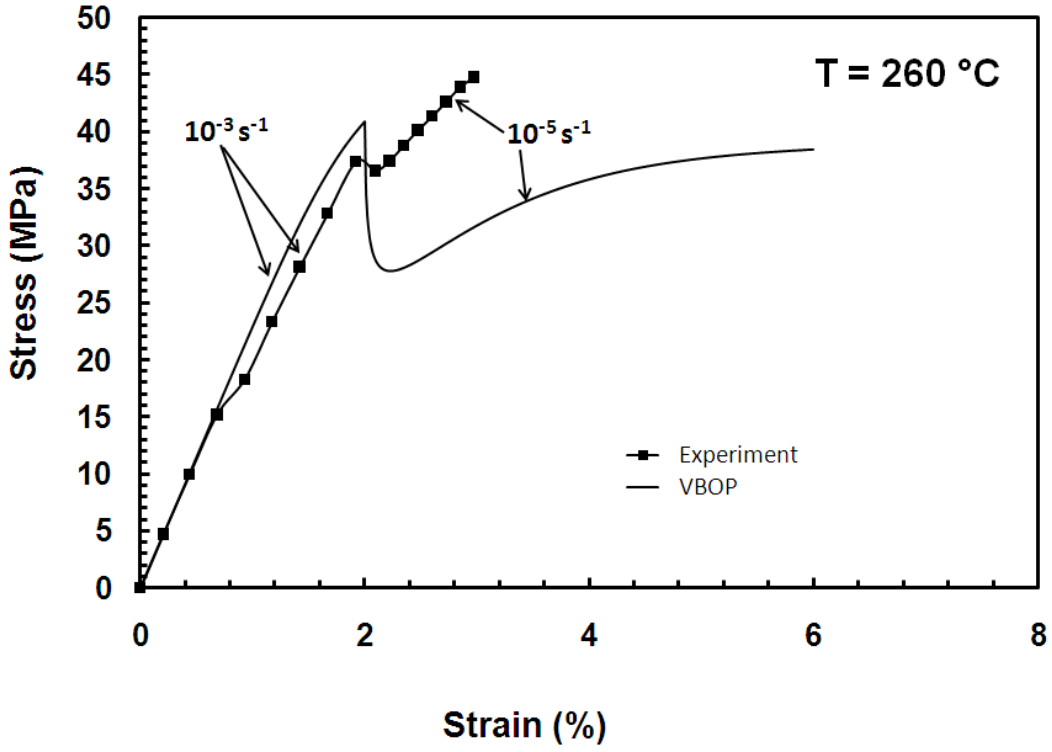

Figure VII.5: A Comparison Between Experimental and Predicted Stress-Strain Curves Obtained for Unaged PMR-15 Polymer in the Strain Rate Jump Test at 260 °C with Fast Loading First.

The experiment loaded at 10^{-5} s^{-1} first is modeled very accurately with the first loading. The experimental curve briefly hesitates upon changing strain rates but eventually matches the predicted curve all the way until the knee is reached. It does appear that the specimen has reached its maximum stress and that the stress might decrease had a failure not occurred. This would allow the experimental curve to more closely match the VBOP prediction. These discrepancies can all be attributed to the lack of data in the flow stress region. The VBOP must be characterized based on data obtained in the region of fully established inelastic flow which were not available at 260 °C. Therefore, the results that are obtained are remarkable. The VBOP has been

pushed to its limits in modeling the behavior of PMR-15 at 260 °C and has performed well.

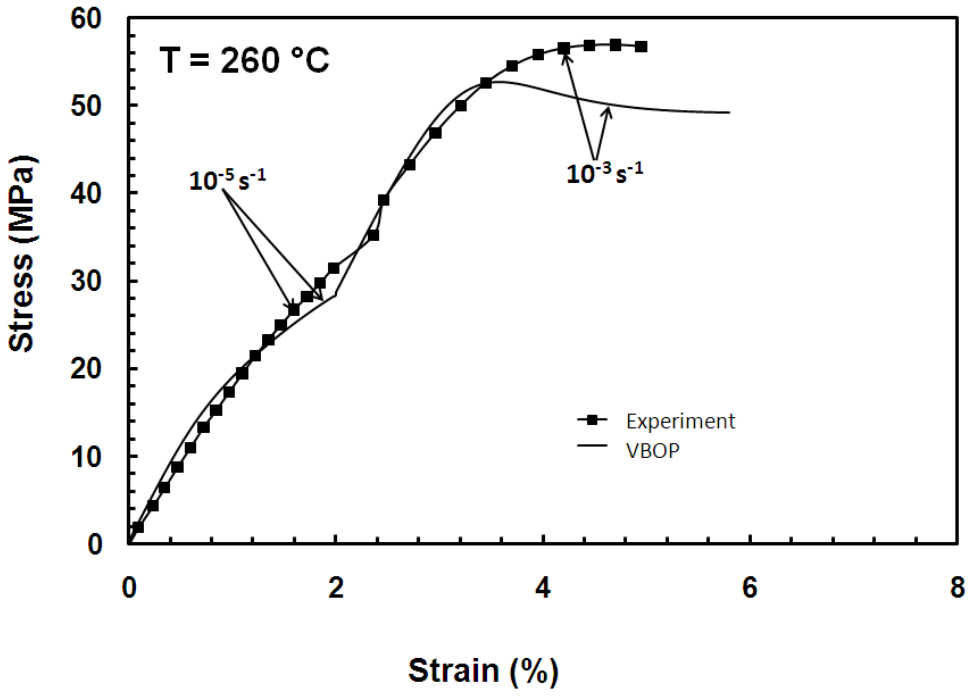

Figure VII.6: A Comparison Between Experimental and Predicted Stress-Strain Curves Obtained for Unaged PMR-15 Polymer in the Strain Rate Jump Test at 260 °C with Slow Loading First.

VIII. Aged PMR-15 Neat Resin: Experimental Observations

The objective of this chapter is to discuss the effects of prior aging at 260 °C in argon on the rate-dependent behavior of the PMR-15 neat resin at 260 °C. Specimens were tested according to the methods described in Chapter V.

Weight Loss Measurements

The weight of rectangular samples was measured prior to aging. These samples were then aged at 260 °C for 0 h, 100 h, 250 h, 500 h, 1000 h, and 2000 h. The weight of each sample was measured after aging as described in Chapter V. Weight loss was expected due to the loss of low molecular weight particles as the temperature degrades the polymer over time. The results of these measurements compared to the weight loss found at other temperatures can be seen in Figure VIII.1. Minimal weight loss at 260 °C is observed. The trend of increased weight loss due to an increase in temperature is seen.

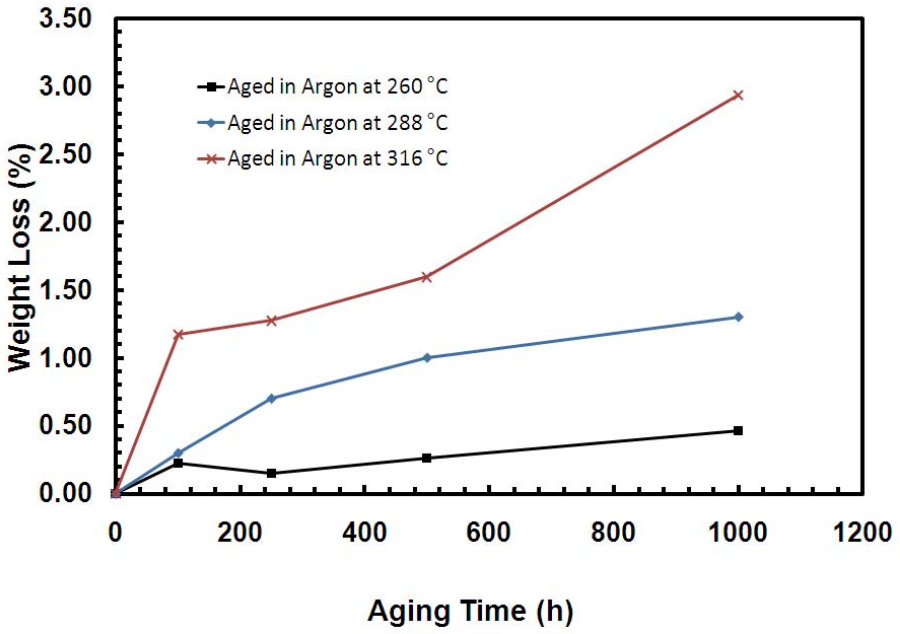

Figure VIII.1: Comparison of Percent Weight Loss for PMR-15 Neat Resin Aged in Argon at 260 °C, 288 °C, and 316 °C. Experimental Data at 316 °C from Ozmen[24]. Experimental Data at 288 °C from Broeckert [7].

Deformation Behavior at 260 °C of PMR-15 Subjected to Prior Aging

The procedures described in Chapter V were applied to the specimens aged in argon at 260 °C. Aging times were 50 h, 100 h, 250 h, 500 h, 1000 h, and 2000 h. The results of each test performed on each age group are presented here.

Monotonic Tension to Failure

Specimens from each age group were subjected to the monotonic tension to failure test described in Chapter V at strain rates of 10^{-3}, 10^{-4}, 10^{-5}, and 10^{-6} s^{-1}. The results of this test for the 50 h age group are shown in Figure VIII.2. There is no distinct linear region upon departure from the origin. However, all strain rates exhibit quasi-elastic behavior initially. Strain rate dependence is clearly seen. An increase in strain

rate leads to an increase in stress for a given strain. The test conducted at the strain rate of 10^{-6} s^{-1} is the only test to enter the region of fully established inelastic flow. Tests performed at the other three strain rates all exhibit early failures. It is assumed that the flow stress would increase with increasing strain rate had the early failures not occurred.

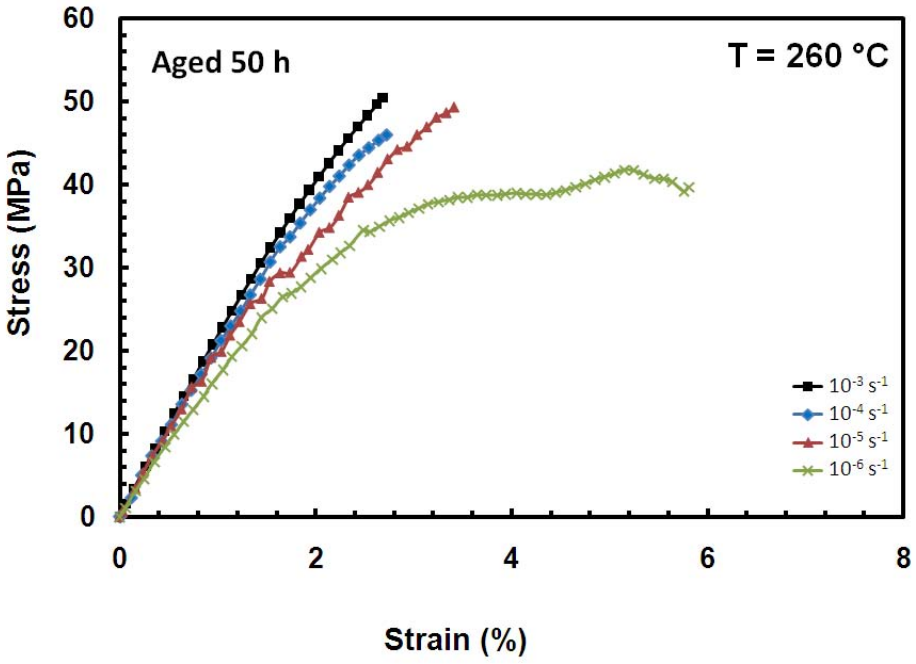

Figure VIII.2: Stress-Strain Curves for PMR-15 Specimens Aged for 50 h at 260 °C in Argon Obtained in Monotonic Tension to Failure Tests Conducted at Constant Strain Rates of 10^{-3}, 10^{-4}, 10^{-5}, and 10^{-6} s^{-1} at 260 °C.

The results of the monotonic tension to failure tests conducted on specimens aged for 100 h is shown in Figure VIII.3. The strain rate dependence is still seen; however, the specimen loaded at a strain rate of 10^{-5} s^{-1} fails before departing from the quasi-elastic region. For this age group, the specimen loaded at a strain rate of 10^{-4} s^{-1} is the only one to achieve fully established inelastic flow. All others fail before reaching the flow stress region.

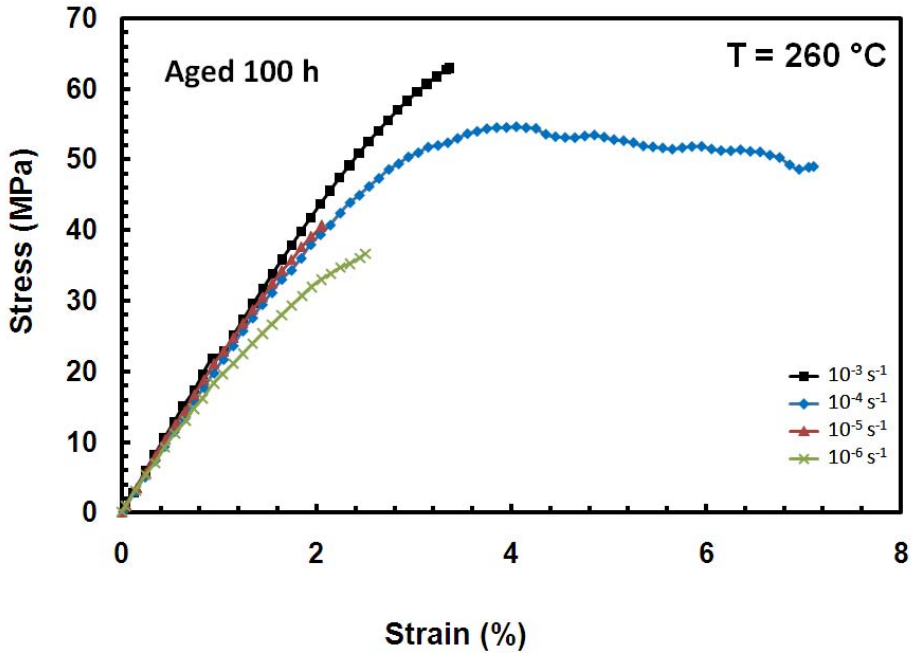

Figure VIII.3: Stress-Strain Curves for PMR-15 Specimens Aged for 100 h at 260 °C in Argon Obtained in Monotonic Tension to Failure Tests Conducted at Constant Strain Rates of 10^{-3}, 10^{-4}, 10^{-5}, and 10^{-6} s^{-1} at 260 °C.

The results of the monotonic tension to failure tests conducted on the specimens aged for 250 h is shown in Figure VIII.4. Again the strain rate dependence is obvious. The stress-strain curves for each strain rate in this age group show a very noticeable knee. This is the first clear appearance of this behavior. McClung also noted the "knee" of the stress-strain curves became more pronounced for increased aging times [23]. The specimen loaded at a strain rate of 10^{-5} s^{-1} is the only one to enter the region of fully established inelastic flow. Despite the early failures for the specimens loaded at the other strain rates, it is clear with this age group that the flow stress level increases with increasing strain rate.

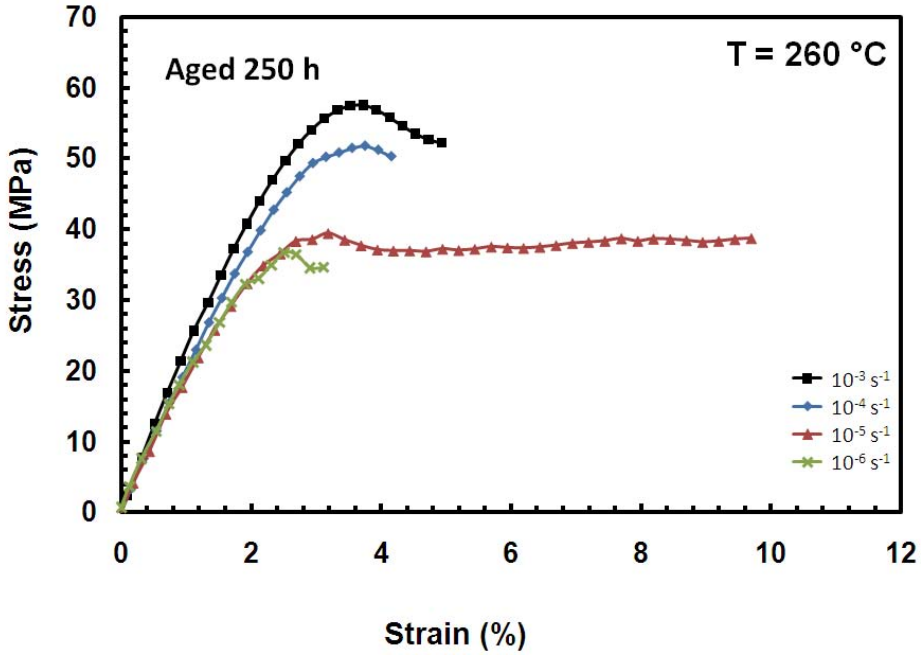

Figure VIII.4: Stress-Strain Curves for PMR-15 Specimens Aged for 250 h at 260 °C in Argon Obtained in Monotonic Tension to Failure Tests Conducted at Constant Strain Rates of 10^{-3}, 10^{-4}, 10^{-5}, and 10^{-6} s^{-1} at 260 °C.

The results of the monotonic tension to failure tests conducted on the specimens aged for 500 h are shown in Figure VIII.5. The specimens tested at strain rates of 10^{-4} and 10^{-6} s^{-1} failed very early. Thus, the rate dependence of those specimens is not seen. Their failures occurred in the quasi-elastic region. The rate dependence is still believed to exist, however, based on the results of the specimens tested at strain rates of 10^{-3} and 10^{-5} s^{-1}. These specimens lasted a bit longer, and the departure from quasi-elastic behavior can be seen in the specimen loaded at a strain rate of 10^{-5} s^{-1}. The specimen loaded at a strain rate of 10^{-3} s^{-1} continues on the quasi-elastic path after the specimen loaded at a strain rate of 10^{-5} s^{-1} enters inelastic flow.

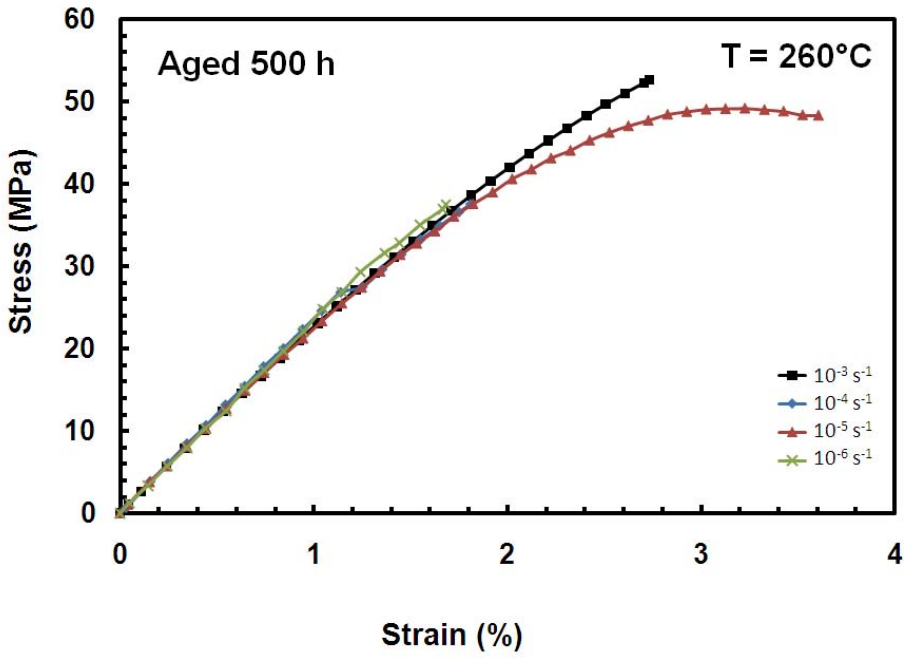

Figure VIII.5: Stress-Strain Curves for PMR-15 Specimens Aged for 500 h at 260 °C in Argon Obtained in Monotonic Tension to Failure Tests Conducted at Constant Strain Rates of 10^{-3}, 10^{-4}, 10^{-5}, and 10^{-6} s^{-1} at 260 °C.

The results of the monotonic tension to failure tests conducted on the specimens aged for 1000 h are shown in Figure VIII.6. Despite early failures in the specimens loaded at strain rates of 10^{-3}, 10^{-4}, and 10^{-5} s^{-1}, strain rate dependence is quite clear for this age group as each of the curves begin to depart from quasi-elastic behavior. The specimen loaded at a strain rate of 10^{-6} s^{-1} does enter the flow stress region.

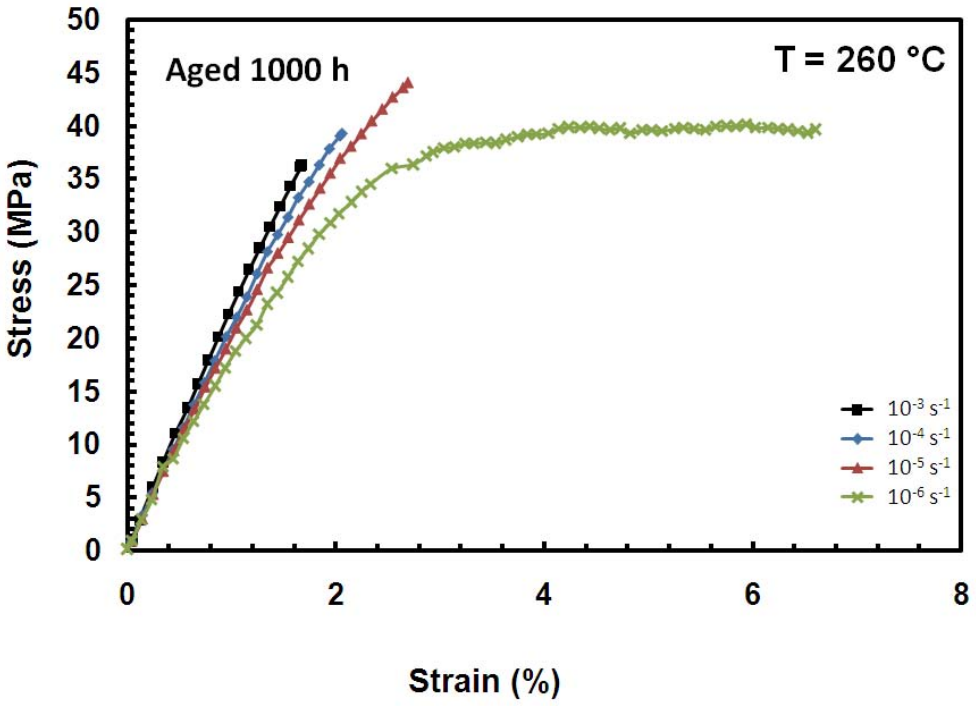

Figure VIII.6: Stress-Strain Curves for PMR-15 Specimens Aged for 1000 h at 260 °C in Argon Obtained in Monotonic Tension to Failure Tests Conducted at Constant Strain Rates of 10^{-3}, 10^{-4}, 10^{-5}, and 10^{-6} s^{-1} at 260 °C.

The results of the monotonic tension to failure tests conducted on the specimens aged for 2000 h are shown in Figure VIII.7. The PMR-15 samples have become much more brittle through aging. The specimen loaded at a strain rate of 10^{-6} s^{-1} did depart from quasi-elastic behavior, but inelastic flow is not fully established. The other specimens all failed before departing from the quasi-elastic region. Thus, the dependence on strain rate is only evidenced by the specimen loaded at a strain rate of 10^{-6} s^{-1}. With the failures at the faster strain rates occurring prior to 2% strain it is known that relaxation tests at 2% strain will be difficult to accomplish.

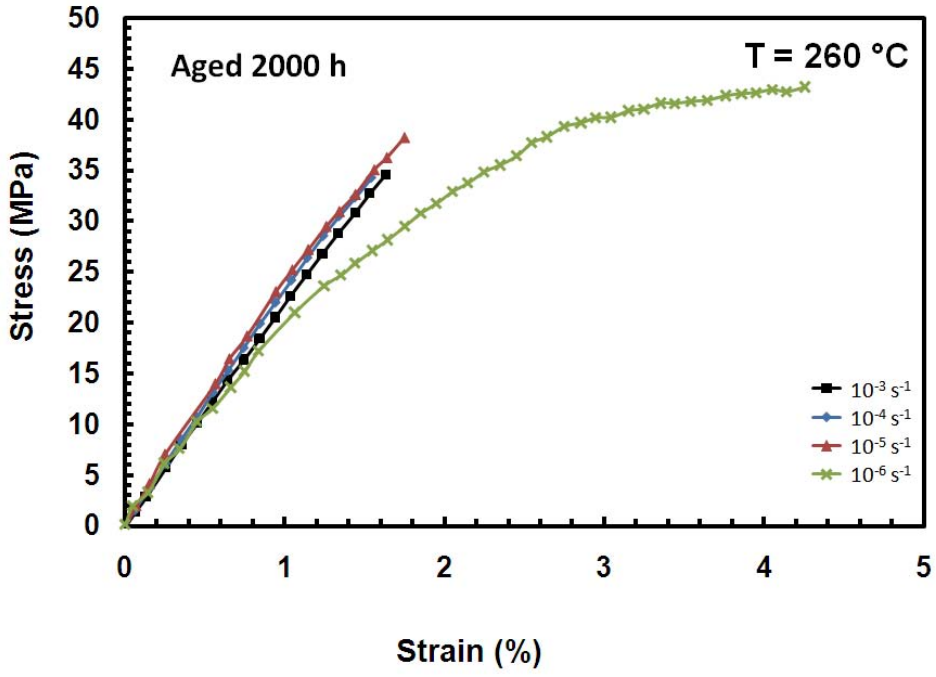

Figure VIII.7: Stress-Strain Curves for PMR-15 Specimens Aged for 2000 h at 260 °C in Argon Obtained in Monotonic Tension to Failure Tests Conducted at Constant Strain Rates of 10^{-3}, 10^{-4}, 10^{-5}, and 10^{-6} s^{-1} at 260 °C.

The results of the monotonic tension to failure tests conducted at a strain rate of 10^{-3} s^{-1} for all age groups are shown in Figure VIII.8 to further compare the effect of prior aging on the deformation behavior of PMR-15 at 260 °C. The unaged specimen is clearly the most ductile. All of the other age groups behave very similarly in the quasi-elastic region. The specimen aged for 250 h is the only one to enter the flow stress region. The specimen aged for 100 h appears to have a higher flow stress than the specimen aged for 250 h. This is not consistent with previous research. This may simply be an anomaly due to specimen-to-specimen variability.

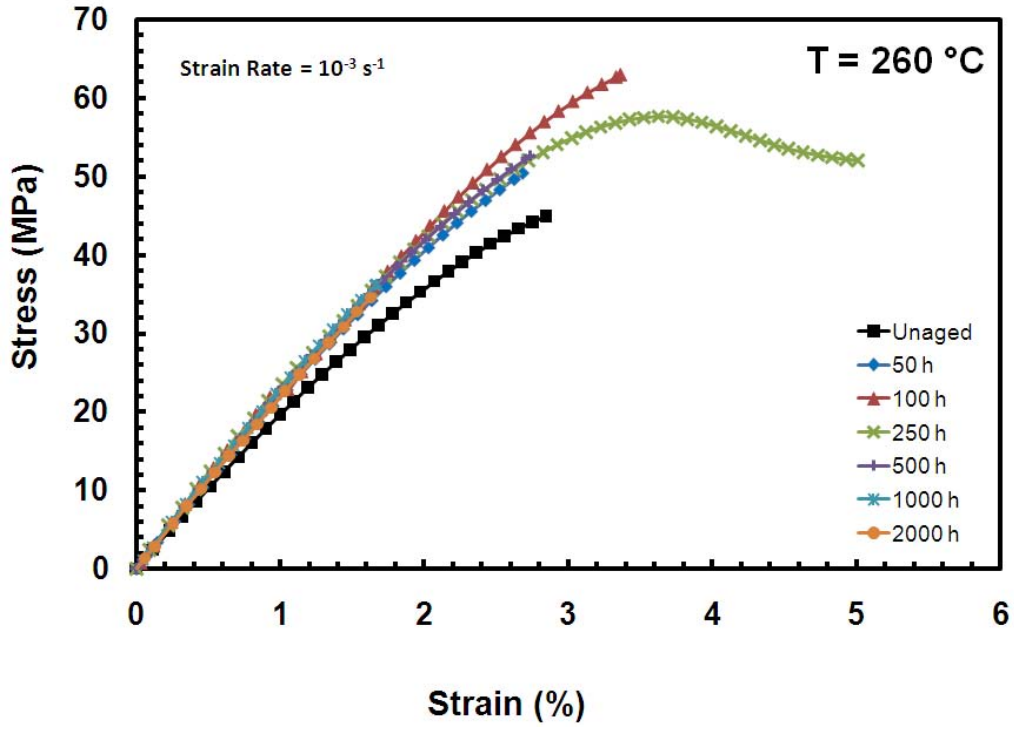

Figure VIII.8: Stress-Strain Curves for PMR-15 Specimens Aged at 260 °C in Argon Obtained in Monotonic Tension to Failure Tests at 260 °C Conducted at a Strain Rate of 10^{-3} s^{-1}.

The results of the monotonic tension to failure tests conducted at a strain rate of 10^{-4} s^{-1} for all age groups are shown in Figure VIII.9. Again, the unaged specimen is clearly the most ductile. Interestingly, the specimen aged for 250 h again appears to have a lower flow stress than the specimen aged for 100 h. Specimens aged for longer periods fail early. However, a general trend of increased brittleness and stiffness with increased aging time can be seen.

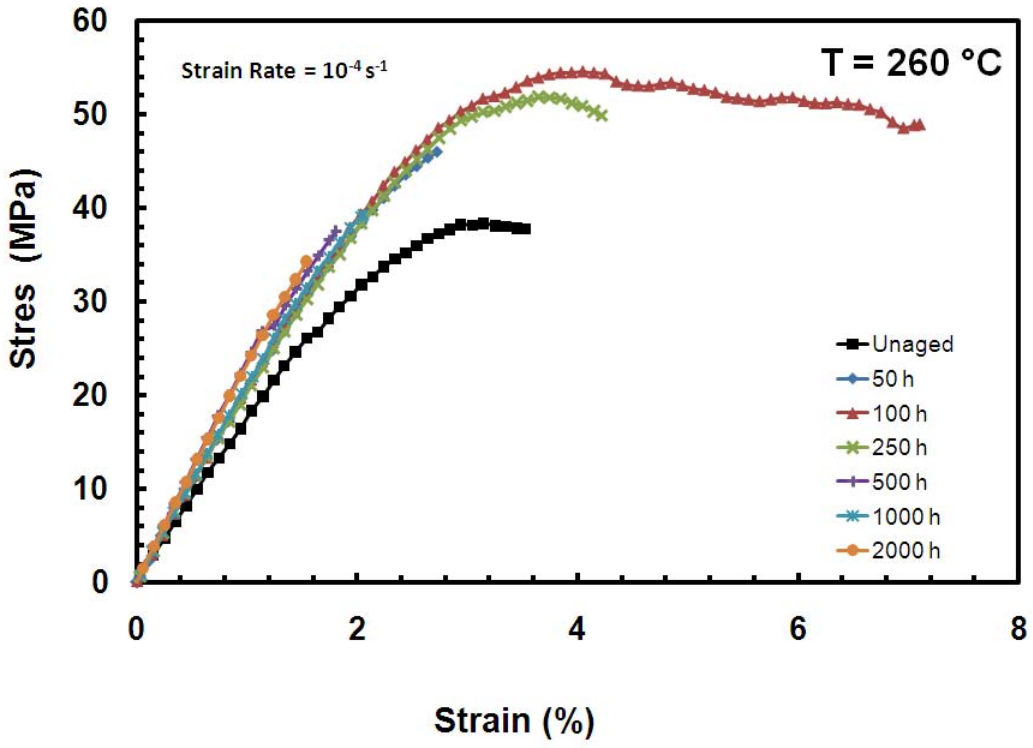

Figure VIII.9: Stress-Strain Curves for PMR-15 Specimens Aged at 260 °C in Argon Obtained in Monotonic Tension to Failure Tests at 260 °C Conducted at a Strain Rate of 10^{-4} s^{-1}.

The results of the monotonic tension to failure tests conducted at a strain rate of 10^{-5} s^{-1} for all age groups are shown in Figure VIII.10. The general trend of increased stiffness with increased aging time is seen. However, the specimen aged for 250 h is again an anomaly.

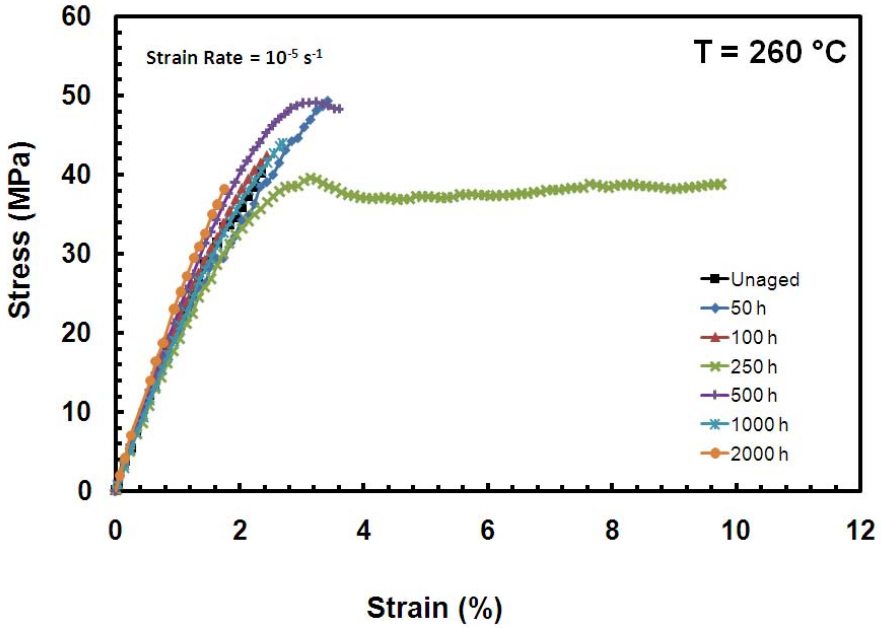

Figure VIII.10: Stress-Strain Curves for PMR-15 Specimens Aged at 260 °C in Argon Obtained in Monotonic Tension to Failure Tests at 260 °C Conducted at a Strain Rate of 10^{-5} s^{-1}.

The results of the monotonic tension to failure tests conducted at a strain rate of 10^{-6} s^{-1} for all age groups are shown in Figure VIII.11. The effect of aging is lost in this slow loading scenario. The specimen aged for 500 h does show increased stiffness. However, the specimens aged for 1000 h and 2000 h return back to properties similar to the unaged specimen. So, the specimen aged for 500 h probably exhibited uncharacteristic behavior. It is interesting to note that three of the specimens loaded at a strain rate of 10^{-6} s^{-1} enter the region of inelastic flow. Even more interesting to note is the fact that two of these three specimens that have inelastic flow are the specimens aged for the longest periods of time. This increase in ductility is not consistent with previous research. Longer aging

times were expected to lead to increased brittleness. Unfortunately, the number of specimens available did not allow for repeating the tests to confirm the results shown.

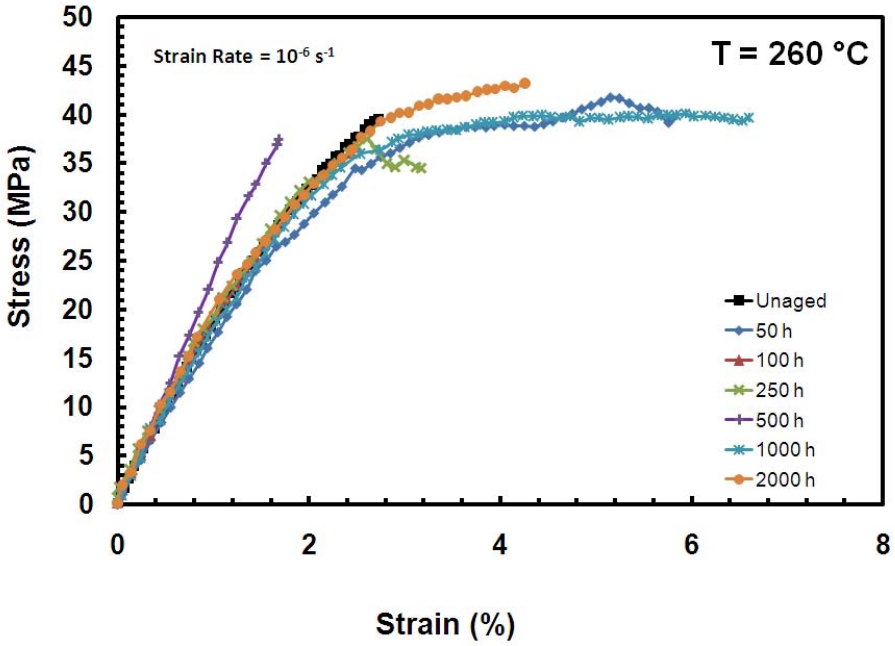

Figure VIII.11: Stress-Strain Curves for PMR-15 Specimens Aged at 260 °C in Argon Obtained in Monotonic Tension to Failure Tests at 260 °C Conducted at a Strain Rate of 10^{-6} s^{-1}.

Constant Strain Rate Test with a Period of Relaxation

Specimens from each age group were subjected to the constant strain rate test with a period of relaxation described in Chapter V. Strain rates were 10^{-3}, 10^{-4}, 10^{-5}, and 10^{-6} s^{-1} during loading. A comparison of the stress drop during relaxation for each age group subjected to loading with a given prior strain rate is shown in Figure VIII.12 - Figure VIII.14. It should be noted that prior aging appears to have no effect on relaxation behavior. Specimens aged for 2000 h were unable to achieve the 2% strain to start

relaxation for the prior strain rates of 10^{-3}, 10^{-4}, and 10^{-5} s^{-1}. However, 2% strain was achieved for the prior strain rate of 10^{-6} s^{-1} so relaxation data was obtained.

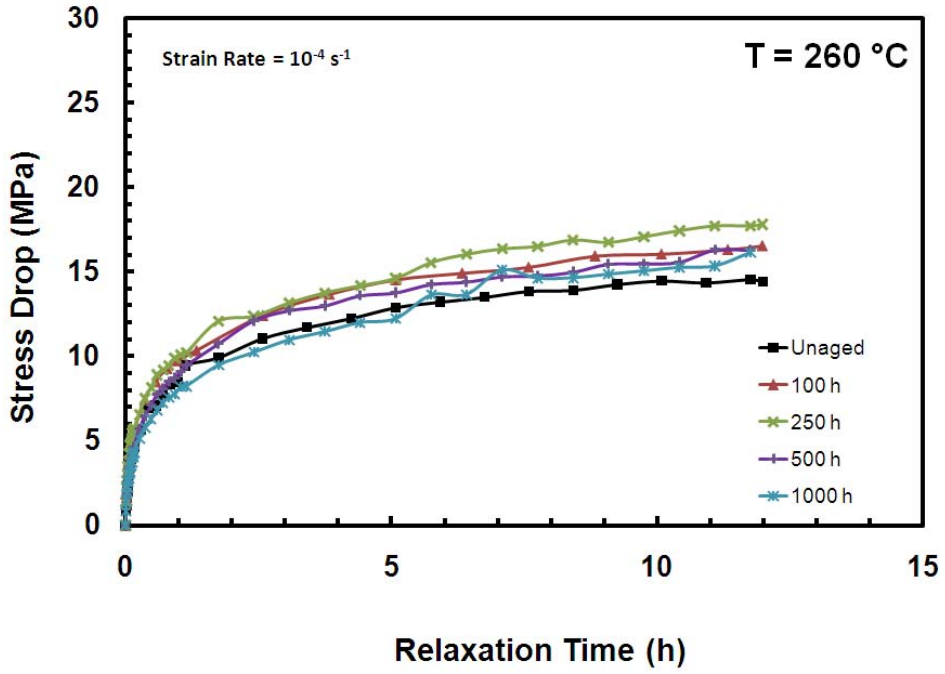

Figure VIII.12: Stress Drop During Relaxation for PMR-15 Specimens Aged at 260 °C in Argon Obtained at Constant Prior Strain Rate of 10^{-4} s^{-1}.

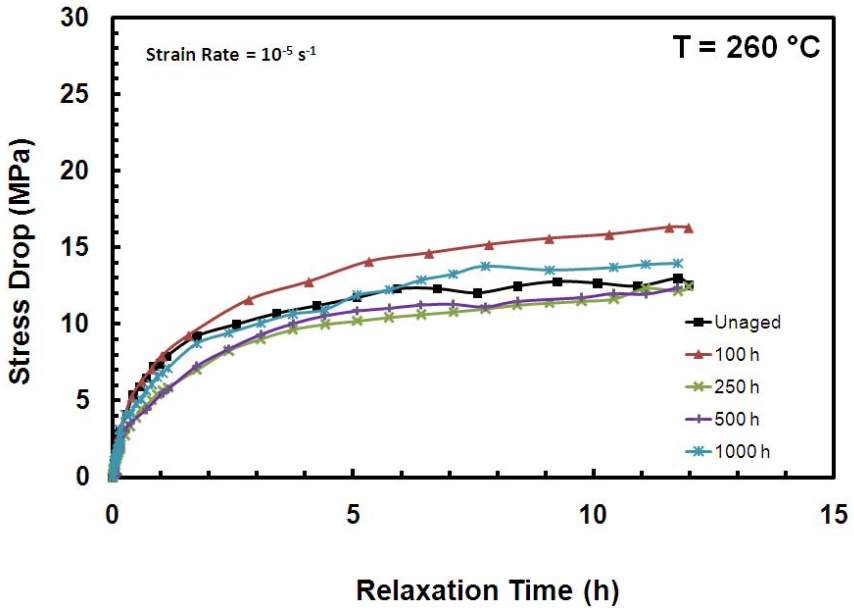

Figure VIII.13: Stress Drop During Relaxation for PMR-15 Specimens Aged at 260 °C in Argon Obtained at Constant Prior Strain Rate of 10^{-5} s^{-1}.

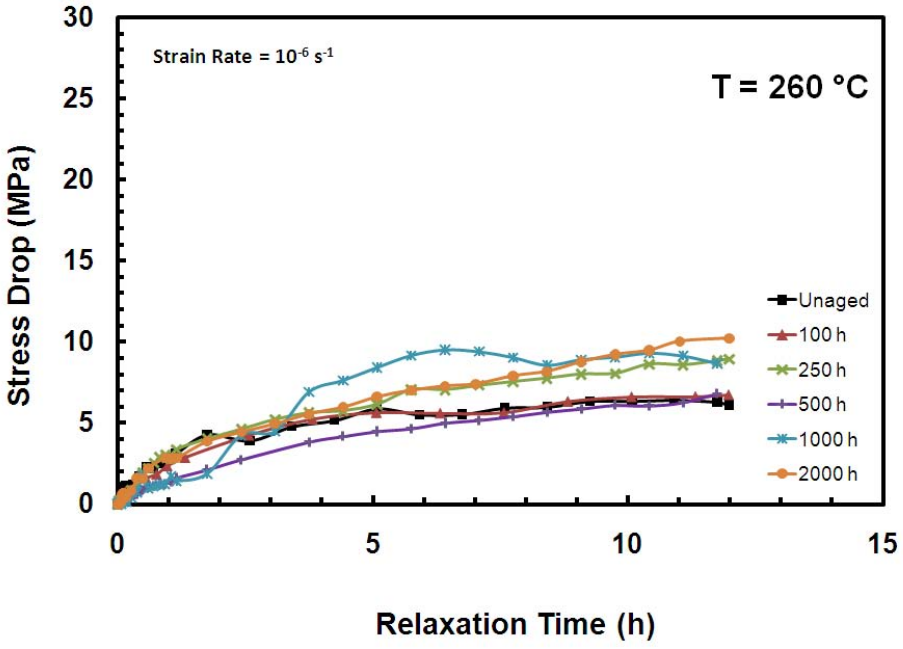

Figure VIII.14: Stress Drop During Relaxation for PMR-15 Specimens Aged at 260 °C in Argon Obtained at Constant Prior Strain Rate of 10^{-6} s^{-1}.

Creep Test

Specimens from each age group were subjected to the creep test described in Chapter V with loading to the creep stress level of 25 MPa at strain rates of 10^{-4} and 10^{-6} s^{-1}. The results of the specimens aged for 100 h are shown in Figure VIII.15. The dependence on prior strain rate is evident. Specimens loaded faster prior to creep result in more strain accumulated during creep.

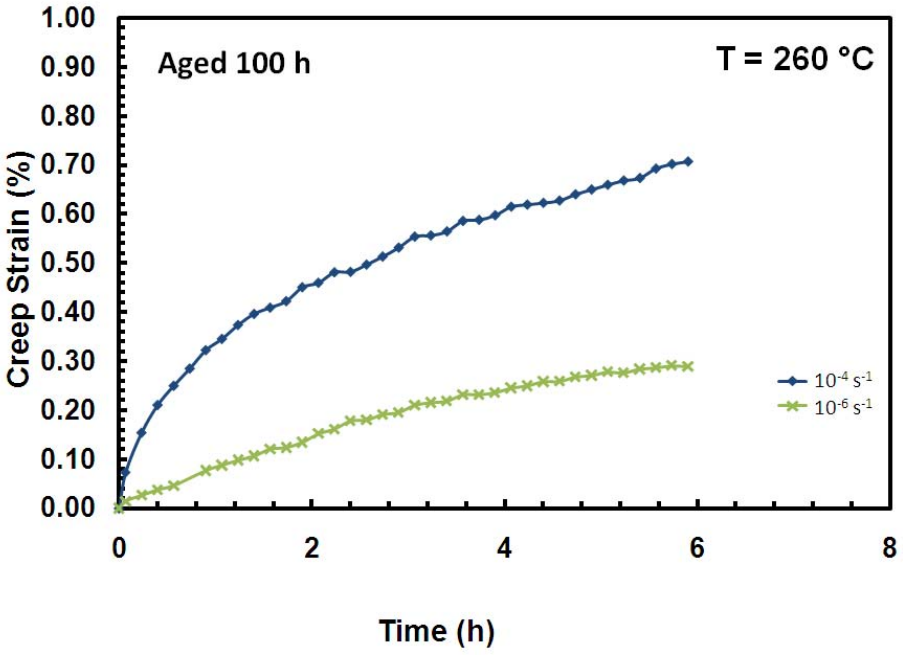

Figure VIII.15: Creep Strain vs Time at 25 MPa and 260 °C for Specimens Aged in Argon at 260 °C for 100 h.

The results of the specimens aged for other durations are shown in Figure VIII.16 - Figure VIII.19. The dependence on prior strain rate is apparent for each age group. Specimens loaded faster prior to creep accumulate more strain during creep. However,

the curves get closer together as the length of prior aging time is increased. This suggests the material stiffens with prior aging.

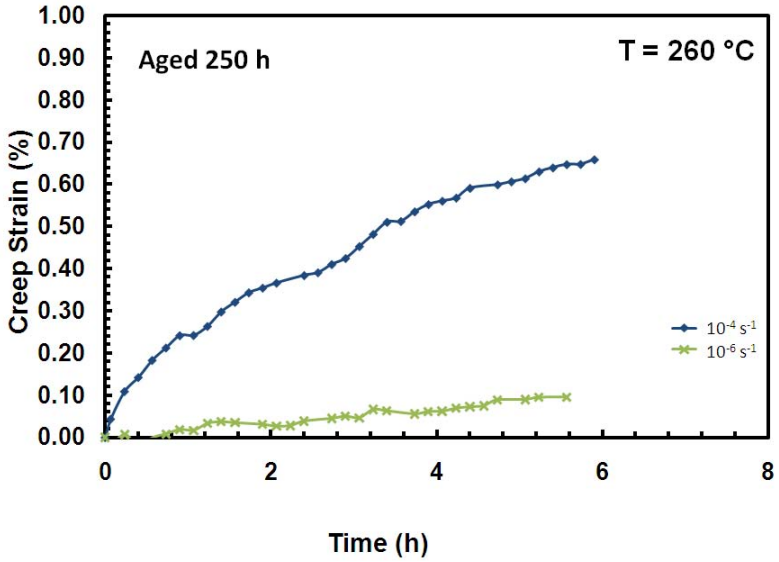

Figure VIII.16: Creep Strain vs Time at 25 MPa and 260 °C for Specimens Aged in Argon at 260 °C for 250 h.

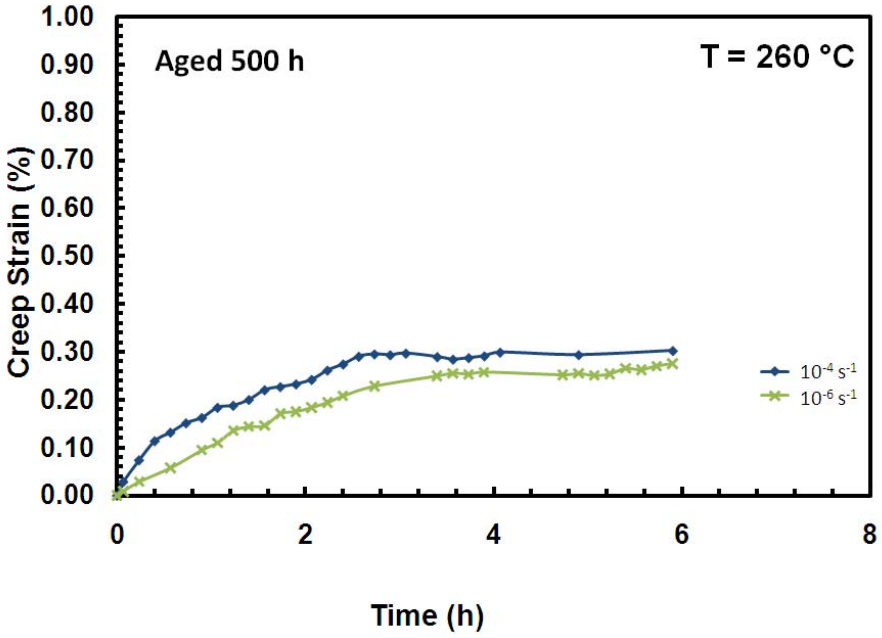

Figure VIII.17: Creep Strain vs Time at 25 MPa and 260 °C for Specimens Aged in Argon at 260 °C for 500 h.

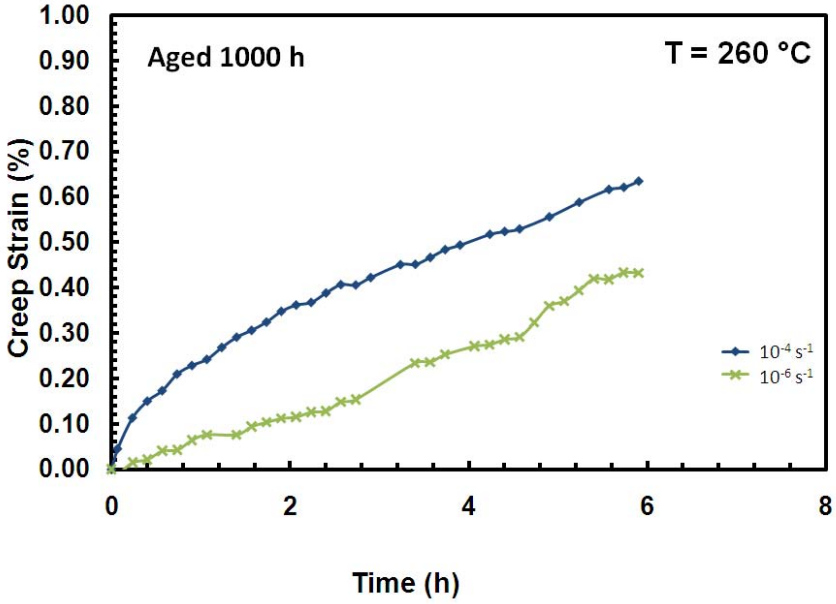

Figure VIII.18: Creep Strain vs Time at 25 MPa and 260 °C for Specimens Aged in Argon at 260 °C for 1000 h.

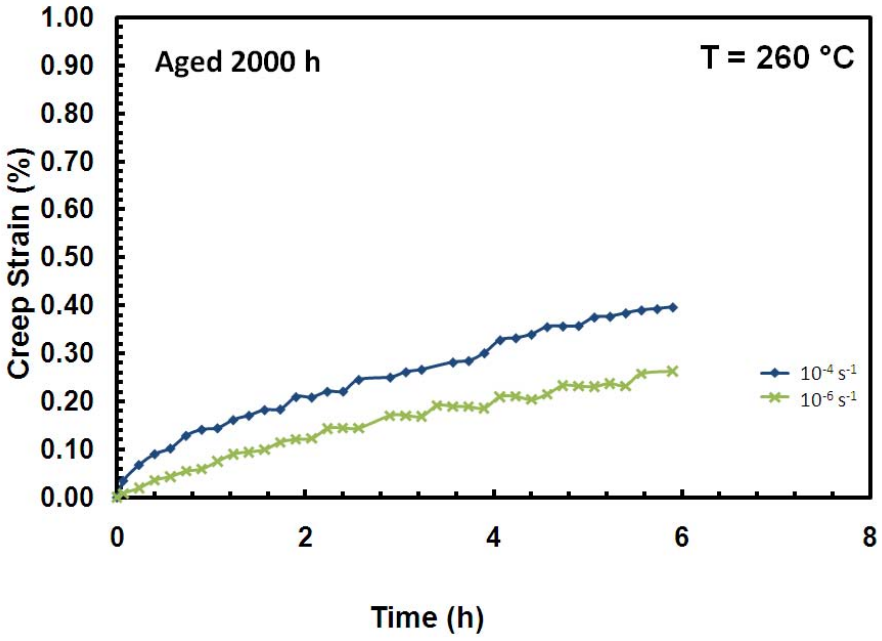

Figure VIII.19: Creep Strain vs Time at 25 MPa and 260 °C for Specimens Aged in Argon at 260 °C for 2000 h.

A comparison of the strain accumulation during creep for each age group subjected to loading with the prior strain rate of 10^{-4} s^{-1} is shown in Figure VIII.20. An increase in prior aging time results in lower creep strain. This further confirms the increased stiffness due to prior aging.

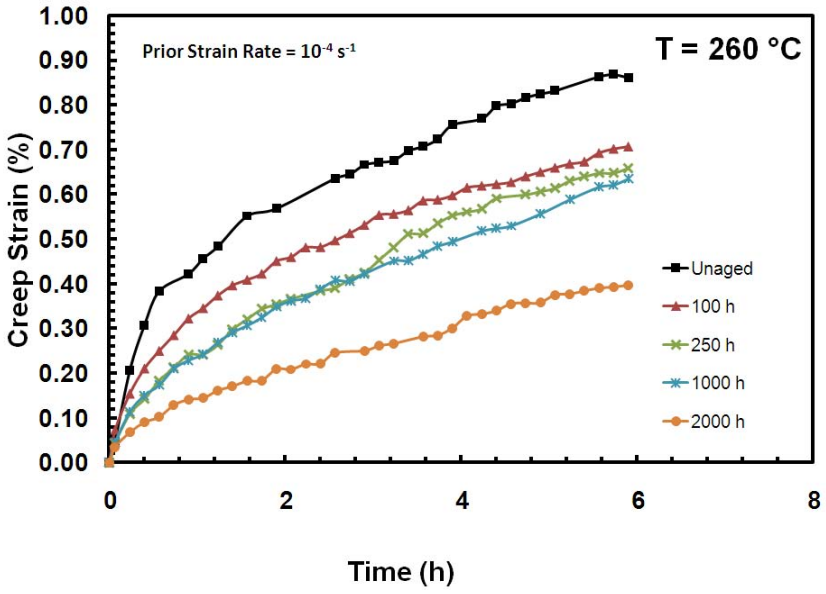

Figure VIII.20: Creep Strain Accumulation for PMR-15 Specimens Aged at 260 °C in Argon Obtained in Creep Tests at 260 °C Conducted at 25 MPa after a Prior Loading Strain Rate of 10^{-4} s^{-1}.

The effect of prior aging on the creep strain obtained for specimens loaded to creep stress at the strain rate of 10^{-6} s^{-1} is not as conclusive (see Figure VIII.21). No distinct trends can be discerned. This could simply be attributed to the lack of any significant creep strain.

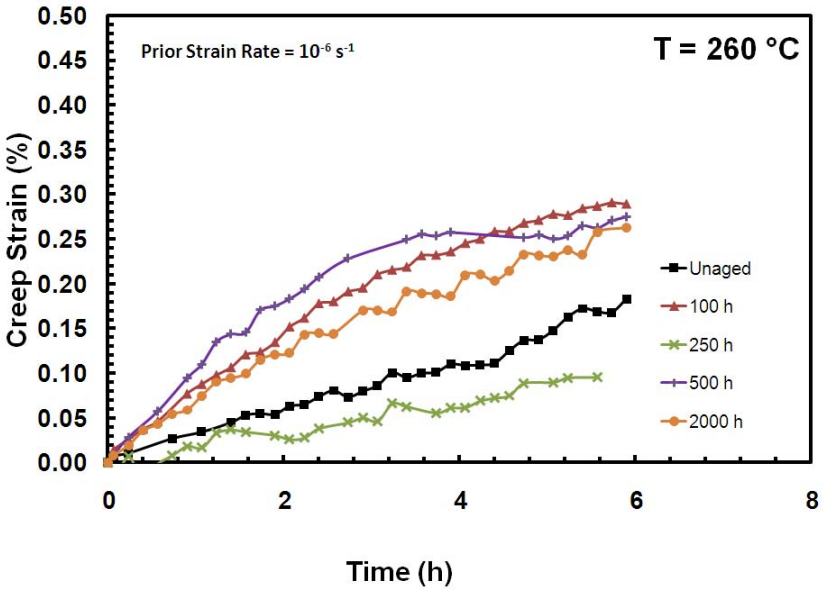

Figure VIII.21: Creep Strain Accumulation for PMR-15 Specimens Aged at 260 °C in Argon Obtained in Creep Tests at 260 °C Conducted at 25 MPa after a Prior Loading Strain Rate of 10^{-6} s^{-1}.

Strain Rate Jump Test

Specimens from each age group were subjected to the strain rate jump test described in Chapter V with strain rates of 10^{-3} and 10^{-5} s^{-1}. The results of the specimens aged for 250 h are shown in Figure VIII.22. The specimen loaded at a strain rate of 10^{-3} s^{-1} first shows a very noticeable change in shape when the loading rate changes to 10^{-5} s^{-1}. It immediately matches up with the curve for the monotonic loading rate of 10^{-5} s^{-1}. This demonstrates the lack of strain rate history effect is still apparent even after being subjected to prior aging. The specimen loaded at a strain rate of 10^{-5} s^{-1} first does show a change in shape after switching to the load rate of 10^{-3} s^{-1}, however it is not as noticeable. It does end up matching the specimen loaded monotonically at a strain rate of 10^{-3} s^{-1}

very well again proving strain rate history has no effect on the loading characteristics of PMR-15 even after prior aging.

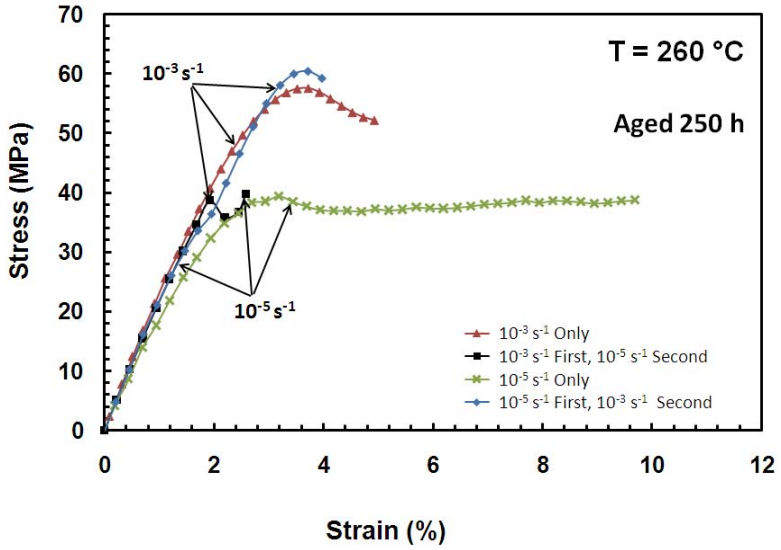

Figure VIII.22: Stress-Strain Curves Obtained for PMR-15 Polymer Subjected to Prior Aging in Argon at 260 °C in Strain Rate Jump Tests and in Constant Strain Rate Tests at 260 °C.

Due to brittleness of the material, the 250 h age group was the only one able to strain far enough past the 2% jump point to clearly demonstrate the lack of a strain rate history effect. However, this is sufficient enough to prove this phenomenon still exists despite prior aging.

Summary of Key Effects of Prior Aging at 260 °C on Deformation Behavior at 260 °C

It has been demonstrated in this chapter that prior aging affects the deformation behavior of PMR-15 at 260 °C. The key effects of prior aging are listed below:

- Increase in modulus of elasticity with increase in prior aging time

- Increased brittleness with increase in prior aging time
- Assumed increase in flow stress with prior aging time. This can be seen somewhat clearly in the data obtained in monotonic tension to failure tests conducted at a strain rate of 10^{-6} s^{-1}
- Stress drop during relaxation is independent of prior aging time
- Decreased strain accumulation in creep with increase in aging time for faster prior strain rates
- No strain rate history effect

Comparison of the Effects of Prior Aging at 260 °C with the Effects of Prior Aging at Other Temperatures

The effect of prior aging in argon was previously determined for specimens tested at 288 °C and 316 °C. Aging temperatures were the same as test temperatures. The following similarities between all three temperatures were noted:

- The modulus of elasticity increased with prior aging time for all three temperatures.
- The flow stress increases with prior aging time for PMR-15 subjected to prior aging at 260 °C (assumed) and 288 °C. However, the specimens aged at 316 °C experienced extremely early failures and never reached the flow stress region. This demonstrates that an increase in aging time results in a more brittle response for all three temperatures.

- Departure from quasi-elastic behavior is delayed with increasing aging time for specimens aged and tested at 288 °C. This is not very clearly seen for specimens aged and tested at 260 °C. This delayed departure from quasi-elastic behavior is not seen at all in specimens aged and tested at 316 °C.
- The effect of prior aging on the tangent modulus of PMR-15 aged and tested at 260 °C and 316 °C cannot be determined since the specimens never attained fully elastic flow. However, specimens aged and tested at 288 °C showed an increase in tangent modulus with increasing prior aging time.

IX. Aged PMR-15 Neat Resin: Constitutive Modeling

This chapter will attempt to apply the VBOP to model the behavior of PMR-15 aged for various durations in argon at 260 °C and tested at 260°C. The model characterization procedure described in Chapter VII will be applied to the 100 h, 250 h, 500 h, and 1000 h age groups. The dependence of each parameter on aging time will be determined and used to predict the model parameters of the 2000 h age group.

Implications for Modeling the Effects of Prior Aging at 260 °C

As discussed in Chapter VIII, there are several key effects of aging on the deformation behavior of PMR-15 tested at 260 °C. These features can be related to parameters in the VBOP.

The increase in the modulus of elasticity with increasing aging time can easily be accounted for in the model by formulating the modulus of elasticity as an increasing function of prior aging time.

The increased brittleness cannot be specifically tied to any parameter in the VBOP. However, the lack of data in the transition region will make the task of defining a shape function, particularly the C_2 value, extremely difficult. The level of difficulty in assigning a shape function to the data may lead to a departure from the model characterization procedure in the specimens aged for longer periods of time.

The increase in flow stress level with aging time can be tied to the isotropic stress. McClung points out that the equilibrium stress is affected by the increase in tangent modulus as well [23]. However, she states the tangent modulus effect on the equilibrium

stress, and subsequently the isotropic stress, is insignificant compared to the effect the isotropic stress has on both of these quantities. Therefore it becomes necessary to have the isotropic stress be an increasing function of prior aging time.

The independence of stress drop during relaxation on prior aging time has a significant effect on the viscosity function. This fact allows the viscosity function to remain unchanged for each age group.

The effect of the decrease in strain accumulation with increasing aging time will hopefully be an artifact of the rest of the changes in the model parameters. This behavior is not directly tied to any parameters in the VBOP.

Characterization of Model Parameters for PMR-15 Neat Resin Subjected to Prior Aging at 260 °C

The model characterization procedure used in Chapter VII was applied to the specimens aged for various durations in argon at 260 °C with some slight changes. The exact approach used is detailed below.

The modulus of elasticity was determined through assessing the initial slope of the stress-strain curve upon leaving the origin as discussed in Chapter VII.

The tangent modulus was determined using the slope of the stress-strain curve in the region of fully established inelastic flow. This determination was very difficult as there is little data in this region. Thus, the tangent modulus value found via the stress-strain curve was compared to the unaged value to ensure the trends seen at 288 °C were being followed. Some slight adjustments to the modulus value may have been made to

ensure the trend was followed, but only if the values still matched the experimental data quite well.

The lack of experimental data in the flow stress region made it nearly impossible to determine an equilibrium stress, and thus, an isotropic stress from experiment. So, a guess and check method was used. The isotropic stress value was found to alter both the flow stress level and relaxation saturation levels. So the relaxation curves and the tension to failure curves were optimized simultaneously.

As discussed earlier, the stress drop during relaxation was determined to be independent of prior aging time. So, the viscosity function found for the unaged material was used for each age group.

The shape function optimization procedure used for the unaged material was used for the aged material as well.

Prior Aging for 100 h

The parameters found for the 100 h age group are listed in Table IX-1.

Table IX-1: Model Parameters Used in the VBOP Predictions of the Deformation Behavior of the PMR-15 Neat Resin at 260 °C Aged in Argon at 260 °C for 100 h.

Moduli	$E = 2400$ MPa, $E_t = 30$ MPa
Isotropic Stress	$A = 37$ MPa
Viscosity Function	$k_1 = 1.0857e+04$ s, $k_2 = 31.18$ MPa, $k_3 = 15.82$
Shape Function	$C_1 = 100$ MPa, $C_2 = 1625$ MPa, $C_3 = 0.22$

The data used for determination of these parameters is plotted against the values predicted by the model in Figure IX.1- Figure IX.5. The relaxation model predictions agree very well with the experimental data. The initial stress drop during relaxation for the prior strain rates of 10^{-3} and 10^{-4} s^{-1} are not modeled extremely well, but the curves converge on their experimental counterparts fairly quickly.

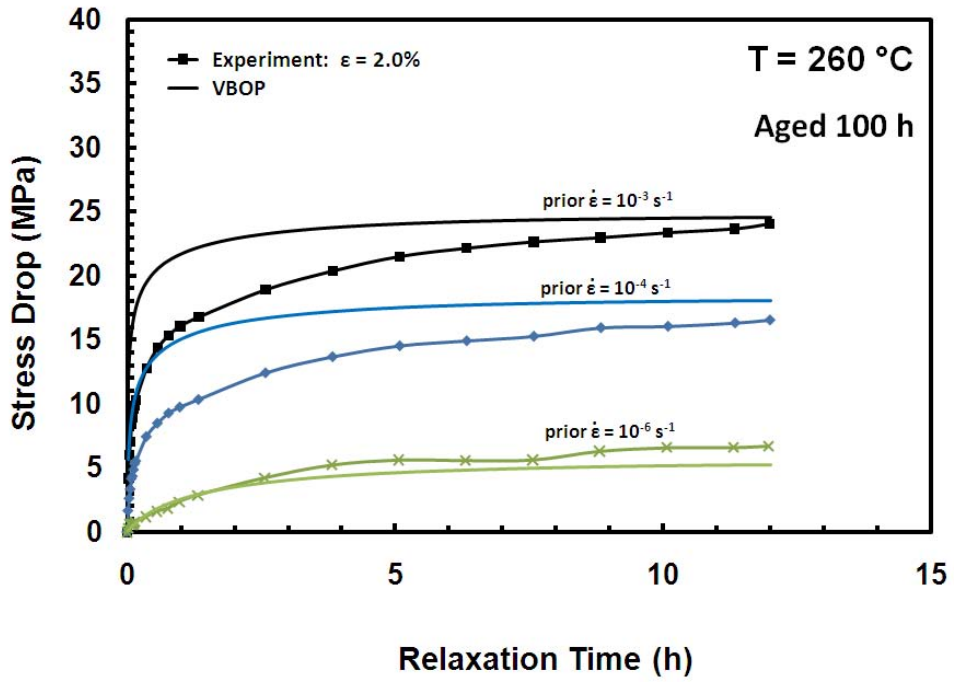

Figure IX.1: A Comparison Between Experimental and Predicted Stress Drop vs Relaxation Time for the PMR-15 Polymer at 260 °C Aged in Argon at 260 °C for 100 h.

The stress-strain curves for the strain rate of 10^{-6} s^{-1} are modeled extremely well. The knee of the stress-strain curve for the strain rate of 10^{-4} s^{-1} is not modeled as well as hoped, but again the experimental and VBOP curves quickly begin to converge. It is assumed this same convergence will occur for the curves obtained for the strain rate of 10^{-3} s^{-1} had the specimen not failed as early as it did. It is quite possible the specimen had

reached the maximum stress and would begin to slightly decrease in stress as is seen in the specimen loaded at a strain rate of 10^{-4} s^{-1}.

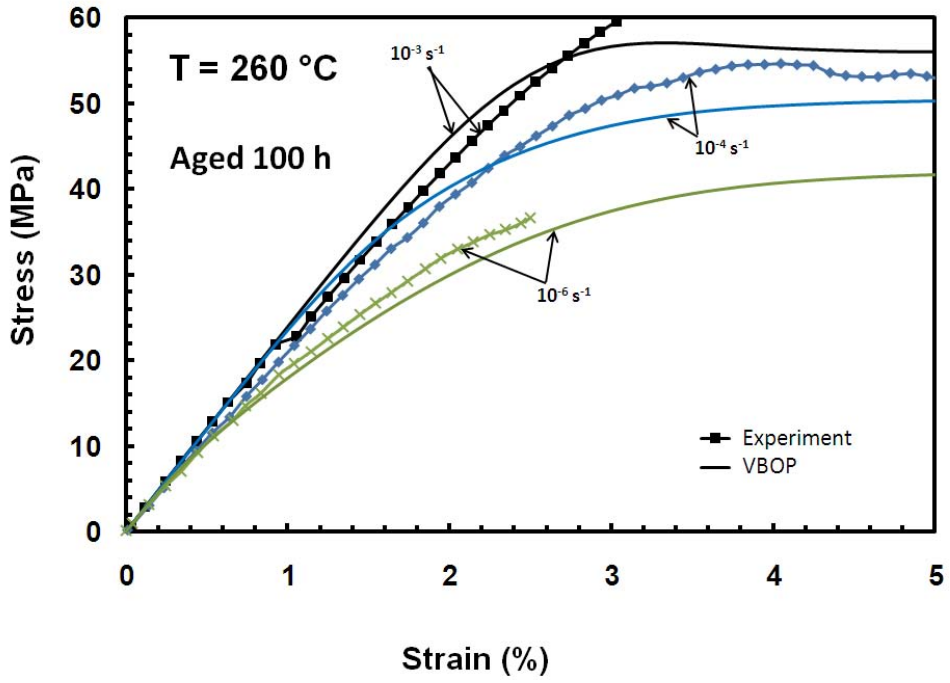

Figure IX.2: A Comparison Between Experimental and Predicted Stress-Strain Curves Obtained for PMR-15 Polymer at Constant Strain Rates of 10^{-3}, 10^{-4}, and 10^{-6} s^{-1} at 260 °C Aged in Argon at 260 °C for 100 h.

As discussed in Chapter VII, a test completely different from the relaxation and monotonic tension to failure tests is needed to verify the model. The creep test was used as this validation test. The results of the creep test using the model parameters from Table IX-1 is compared to the experimental creep test results in Figure IX.3. Qualitatively, the results are excellent. The dependence on prior strain rate is accurately modeled. The quantitative results are not as great. The model predicts the creep behavior well for the prior loading rate of 10^{-6} s^{-1} but loses a great deal of accuracy for the

prior loading rate of 10^{-4} s^{-1}. This can once again be attributed to the lack of data in the flow stress region upon which the model is based.

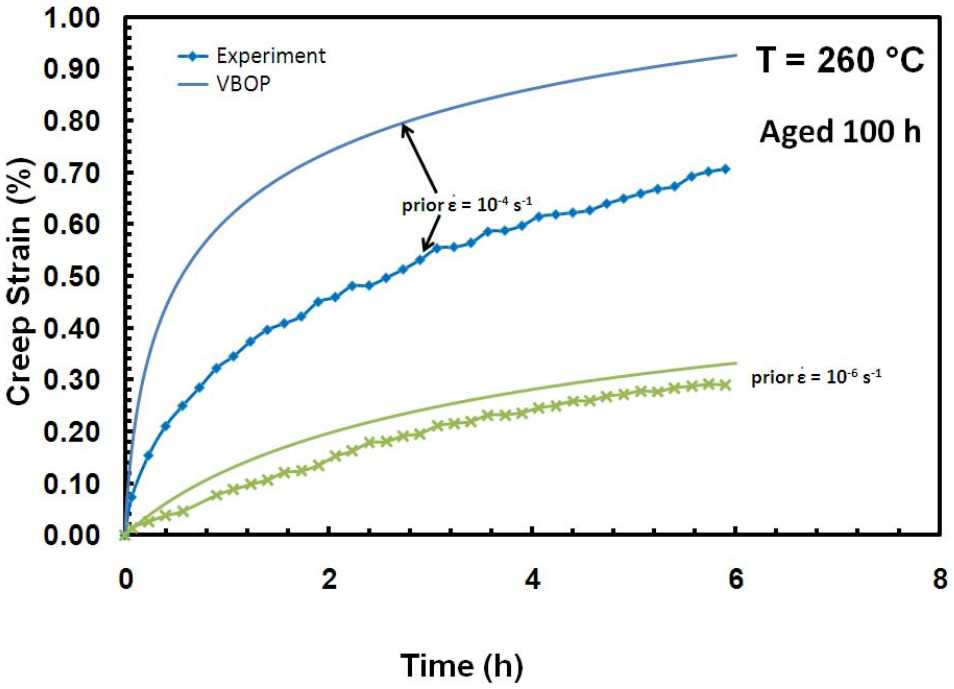

Figure IX.3: Comparison Between the Experimental and Predicted Creep Strain vs Time Curves Obtained for PMR-15 Polymer at 260 °C in Creep at 25 MPa Aged in Argon at 260 °C for 100 h.

The strain rate jump test is another test used to verify the model. The results of the VBOP are plotted against the experimental results in Figure IX.4 - Figure IX.5. The strain rate jump test with the fast loading first matches the VBOP results very well. However, the specimen breaks very soon after entering the second loading, which is at the slower rate. The strain rate jump test with the slower loading first is modeled very well. The distinction between the two load rates is clear. The experimental data seems to be following the loading path described by the model all the way up to failure.

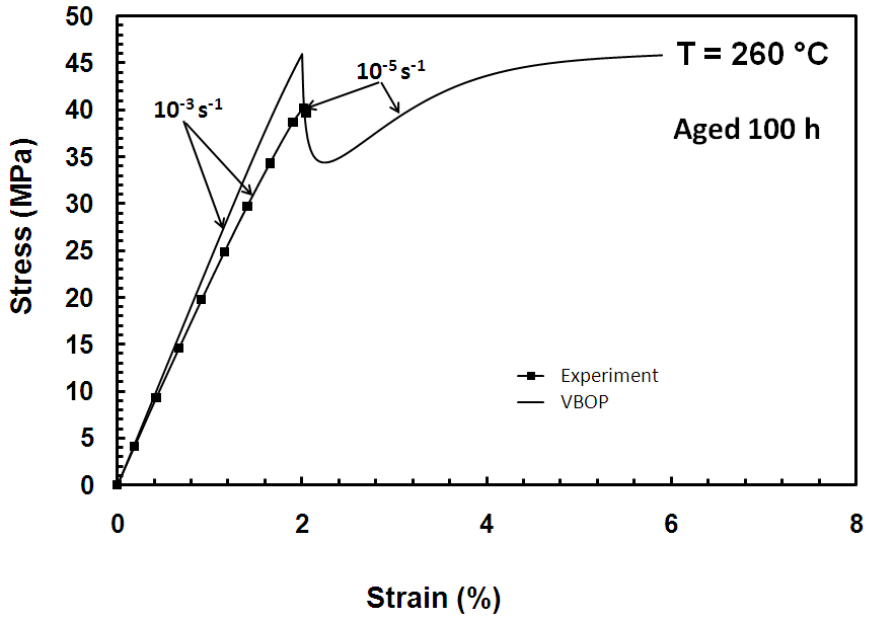

Figure IX.4: A Comparison Between Experimental and Predicted Stress-Strain Curves Obtained for PMR-15 Polymer in the Strain Rate Jump Test at 260 °C with Fast Loading First Aged in Argon at 260 °C for 100 h.

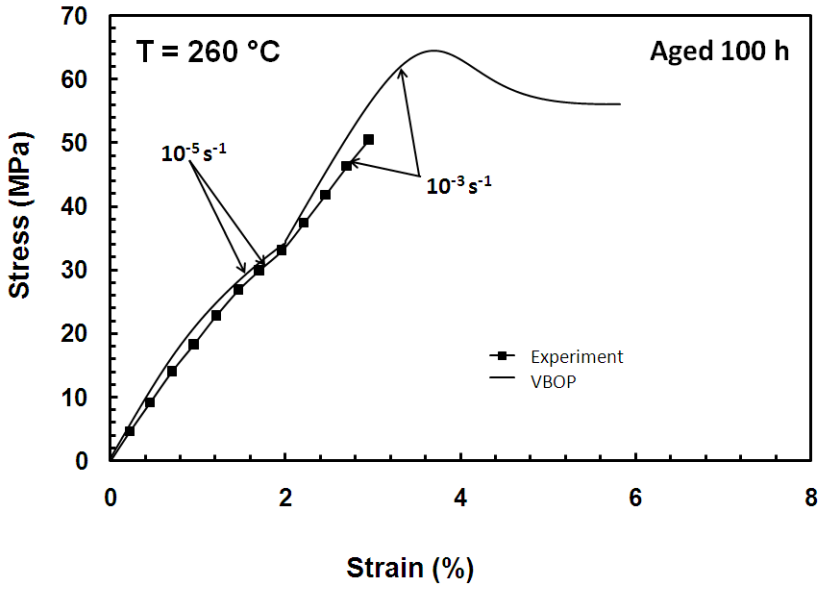

Figure IX.5: A Comparison Between Experimental and Predicted Stress-Strain Curves Obtained for PMR-15 Polymer in the Strain Rate Jump Test at 260 °C with Slow Loading First Aged in Argon at 260 °C for 100 h.

Prior Aging for 250 h

The modified model characterization procedure presented at the beginning of this chapter was used to determine the parameters for PMR-15 aged in argon at 260 °C for 250 h. The parameters for the 250 h age group are listed in Table IX-2.

Table IX-2: Model Parameters Used in the VBOP Predictions of the Deformation Behavior of the PMR-15 Neat Resin at 260 °C Aged in Argon at 260 °C for 250 h.

Moduli	E = 2425 MPa, E_t = 45 MPa
Isotropic Stress	A = 33 MPa
Viscosity Function	k_1 = 1.0857e+04 s, k_2 = 31.18 MPa, k_3 = 15.82
Shape Function	C_1 = 100 MPa, C_2 =1694 MPa, C_3 = 3.56

The results of these parameters applied to the VBOP are plotted against the experimental results in Figure IX.6 - Figure IX.10. Only the relaxation curves obtained in tests with the slower prior strain rates are included. At this length of aging time the material has become brittle enough that loading at the fast strain rates frequently results in early failures. However, as can be seen in Figure IX.6, the stress drops during relaxation for the specimens loaded at a prior strain rate of 10^{-5} and 10^{-6} s^{-1} are modeled very well. The stress strain curves obtained in monotonic tension to failure, shown in Figure IX.7, are modeled very well. The transient behavior, the transition from quasi-elastic to inelastic flow, is not perfectly reproduced. However, the experimental data for all three strain rates shown join back up with the VBOP curves as they approach the flow stress region.

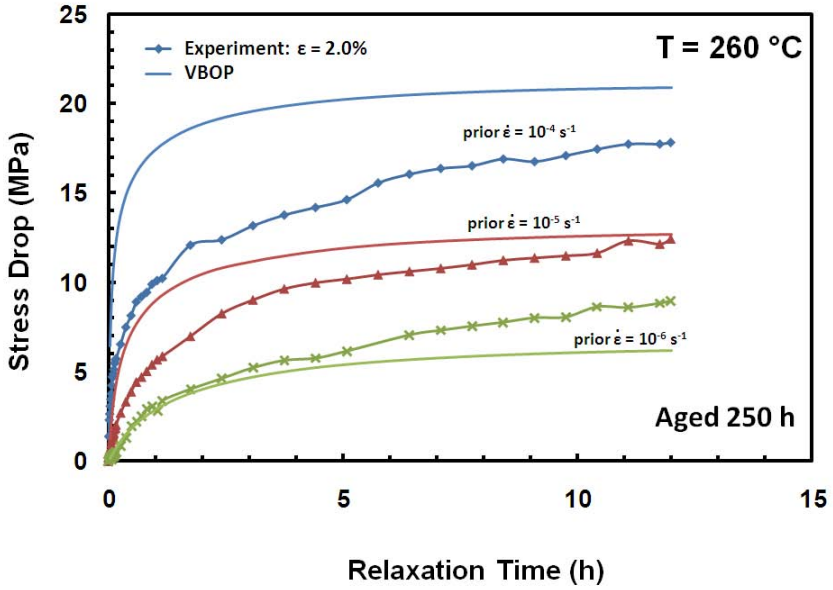

Figure IX.6: A Comparison Between Experimental and Predicted Stress Drop vs Relaxation Time for the PMR-15 Polymer at 260 °C Aged in Argon at 260 °C for 250 h.

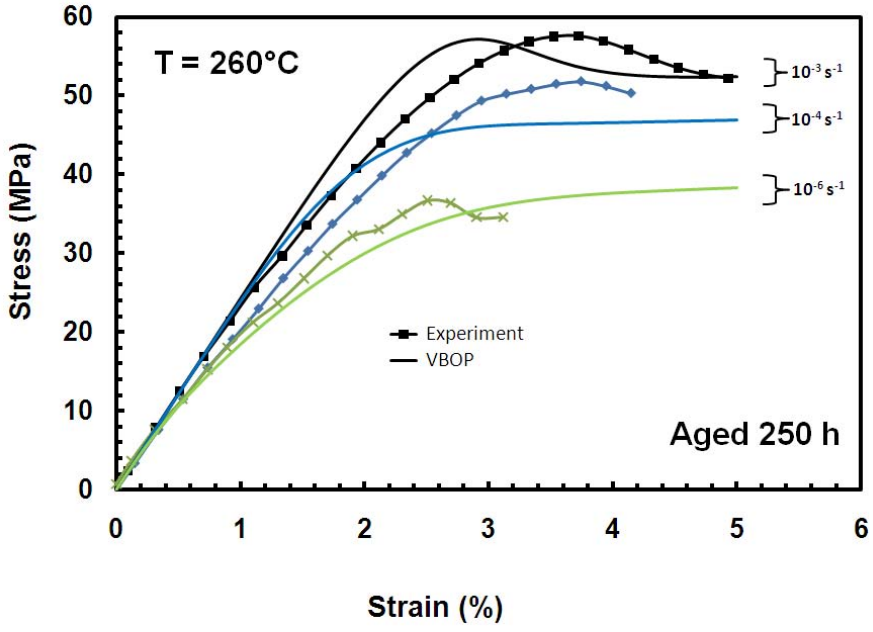

Figure IX.7: A Comparison Between Experimental and Predicted Stress-Strain Curves Obtained for PMR-15 Polymer at Constant Strain Rates of 10^{-3}, 10^{-4}, and 10^{-6} s^{-1} at 260 °C Aged in Argon at 260 °C for 250 h.

The model is again verified using the creep and strain rate jump tests. In creep, the VBOP is only qualitatively correct. Faster prior loading rates result in more strain accumulation during creep. The quantitative results are poor. Again, the parameters were defined using data in the quasi-elastic region. This is contrary to the VBOP formulation, which specifies that model characterization should rely on experimental data obtained in the flow stress region.

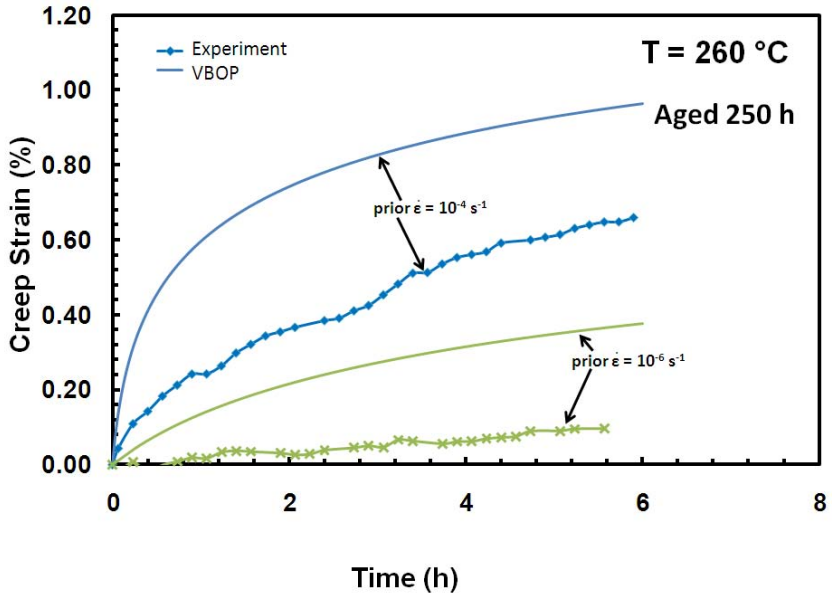

Figure IX.8: Comparison Between the Experimental and Predicted Creep Strain vs Time Curves Obtained for PMR-15 Polymer at 260 °C in Creep at 25 MPa Aged in Argon at 260 °C for 250 h.

The strain rate jump tests were modeled much more successfully. The specimen loaded with the faster strain rate first is qualitatively very accurate. The model and the experimental data both take a dip when the second, slower loading is introduced. The specimen fails before any more observations can be made. The specimen loaded with the

slower strain rate first is both qualitatively and quantitatively accurate. The knee in the stress-strain curve is matched nearly perfectly. This is a very exciting result.

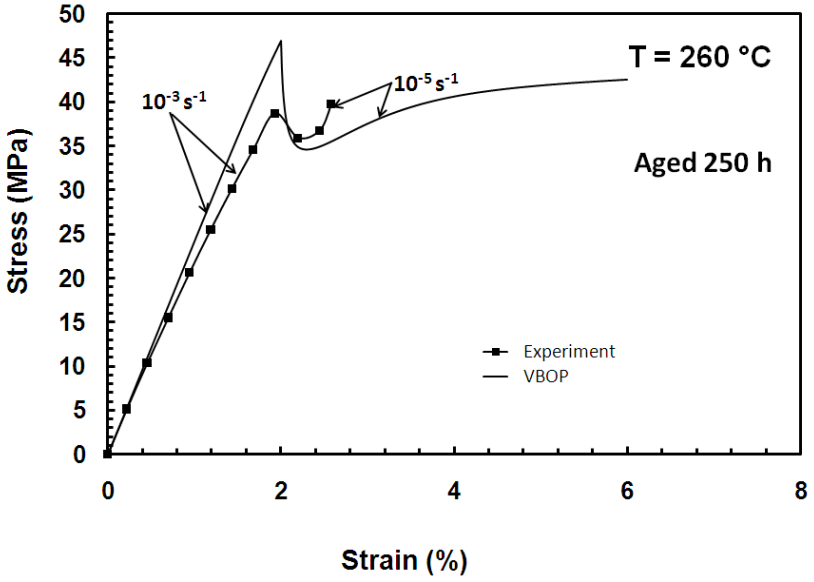

Figure IX.9: A Comparison Between Experimental and Predicted Stress-Strain Curves Obtained for PMR-15 Polymer in the Strain Rate Jump Test at 260 °C with Fast Loading First Aged in Argon at 260 °C for 250 h.

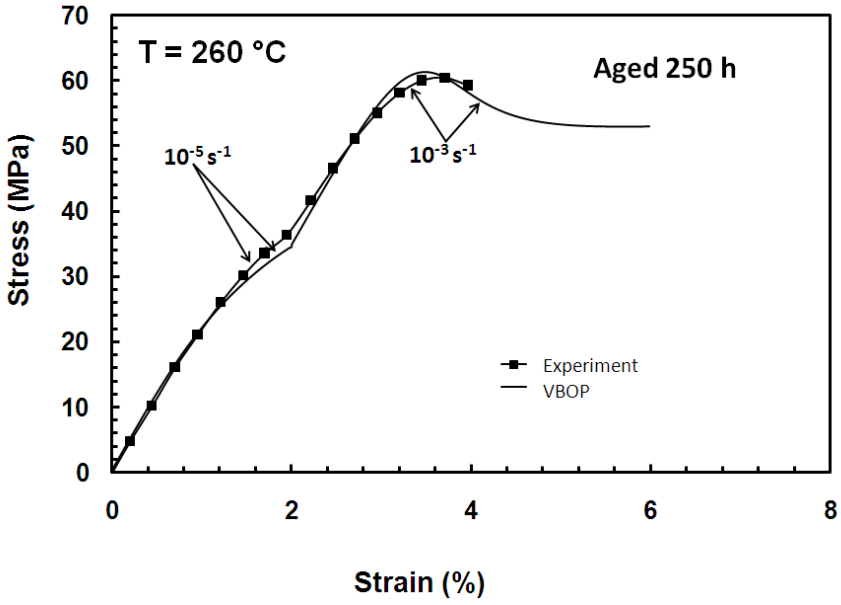

Figure IX.10: A Comparison Between Experimental and Predicted Stress-Strain Curves Obtained for PMR-15 Polymer in the Strain Rate Jump Test at 260 °C with Slow Loading First Aged in Argon at 260 °C for 250 h.

Model Parameters as Functions of Aging Time

The original intention was to model the 500 h and 1000 h age groups in the same manner as the 100 h and 250 h age groups. However, the higher age groups proved to have so little data in the flow stress region that it was nearly impossible to use the same methods. Instead, the parameters found from the unaged, 100 h, and 250 h age groups were analyzed and used to develop predictions for these parameters in the longer aging durations. Each parameter, as was described in the implications for modeling, can be described by an increasing function. To keep consistency with McClung's work, a power law as a function of aging time was fitted to each parameter. The MATLAB code used to complete this task is shown in Appendix C.

The elastic modulus increases with prior aging time as shown in Figure IX.11. The power law curve fit resulted in the modulus of elasticity being defined by

$$E = 15.1t_a^{0.4} + 2304.4, \tag{9.1}$$

where t_a is the prior aging time.

The tangent modulus also increases with prior aging time. Figure IX.12 shows that the tangent modulus can be represented by the equation

$$E_t = 0.022t_a^{1.250} + 23 \tag{9.2}$$

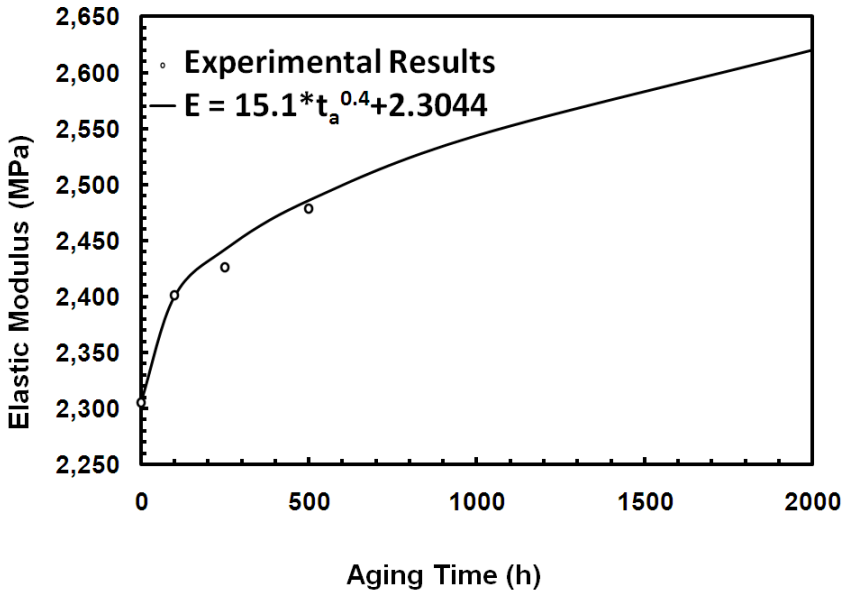

Figure IX.11: Elastic Modulus E at 260 °C as a Continuous Function of Prior Aging Time for the PMR-15 Neat Resin Aged at 260 °C in Argon.

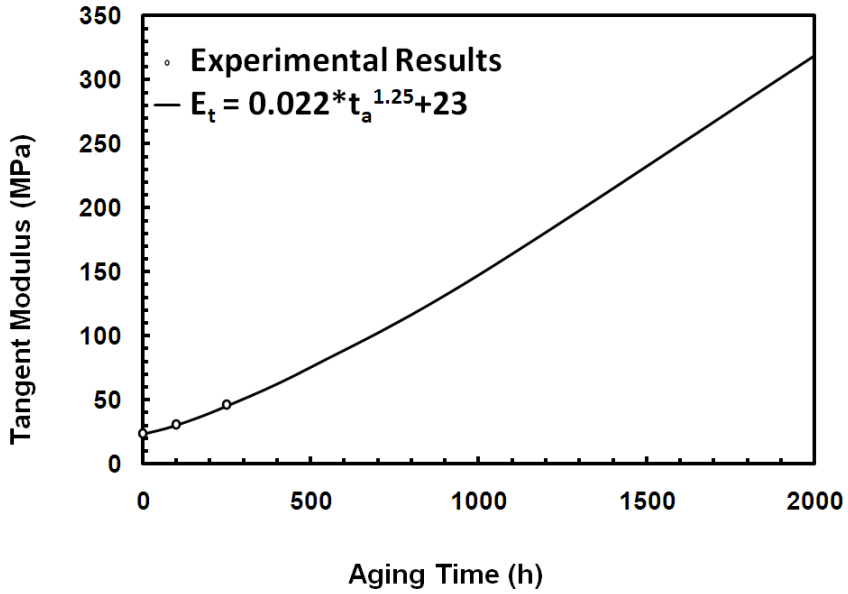

Figure IX.12: Tangent Modulus E_t at 260 °C as a Continuous Function of Prior Aging Time for the PMR-15 Neat Resin Aged at 260 °C in Argon.

The isotropic stress also increases with prior aging time. However, this increase is not nearly as significant. Figure IX.13 shows that the isotropic stress increases initially, but levels off after about 250 h at a value of 35 MPa. The isotropic stress is described by the equation

$$A = 5t_a^{0.0001} + 30 \tag{9.3}$$

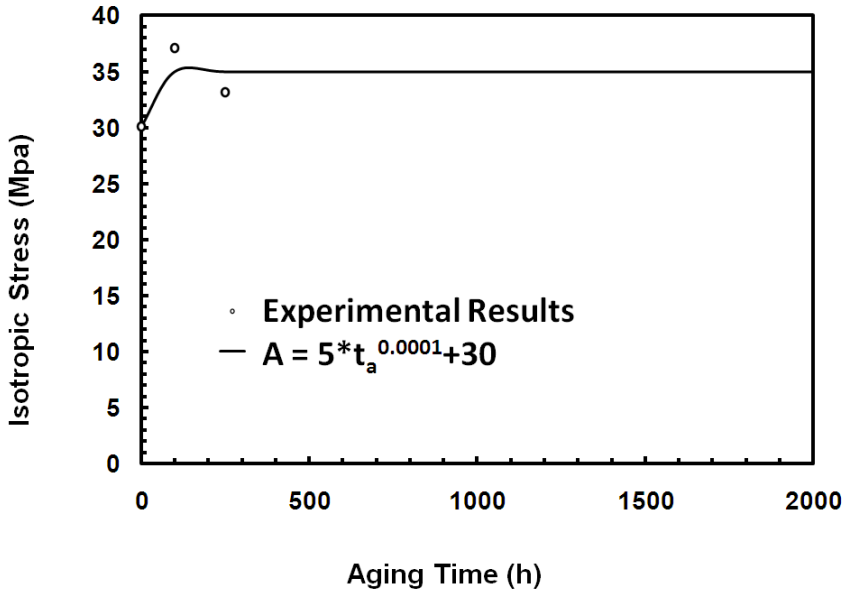

Figure IX.13: Isotropic Stress A at 260 °C as a Continuous Function of Prior Aging Time for the PMR-15 Neat Resin Aged at 260 °C in Argon.

The shape function also has parameters that increase with prior aging time. The shape function parameter C_2 increases with prior aging time as shown in Figure IX.14. It is described by the equation

$$C_2 = 105.3t_a^{0.2} + 1326.8 \qquad (9.4)$$

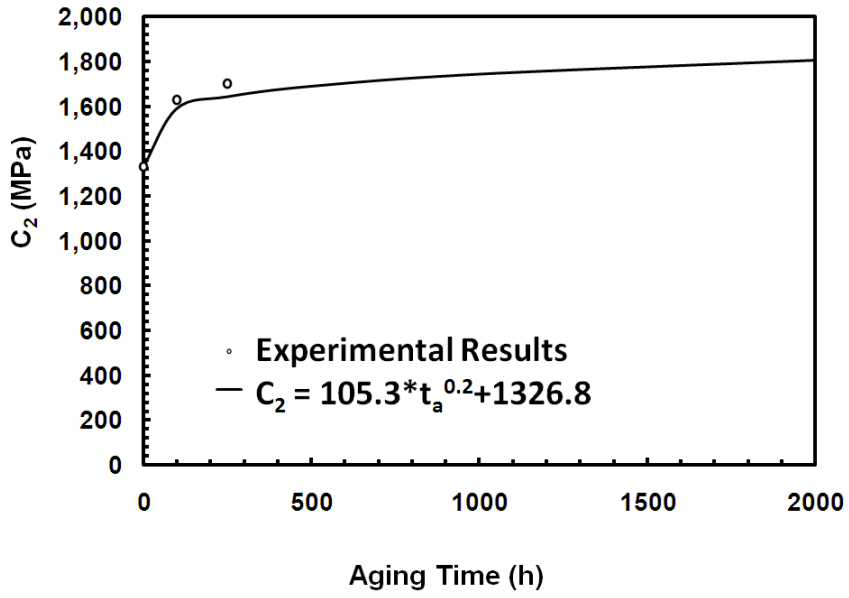

Figure IX.14: Shape Function Parameter, C_2, at 260 °C as a Continuous Function of Prior Aging Time for the PMR-15 Neat Resin Aged at 260 °C in Argon.

Interestingly, the shape function parameter C_3 also increases with prior aging time. This was not the case in the work completed at 288 °C for PMR-15 [23]. It should be noted that the values for C_3 for the unaged group and the 100 h group are close to zero. Only when the specimen has been aged for 250 h does the value of C_3 become significant. Also worth noting is the fact that McClung's value for C_3 never exceeded a value of ten. Thus, this may be a maximum value and the power law function derived for this parameter should level off at the value of ten. Using the available data, an increasing function with prior aging time was developed for the shape parameter C_3 as shown in Figure IX.15 and given by the equation

$$C_3 = 0.0002t_a^{1.767} - 0.207 \tag{9.5}$$

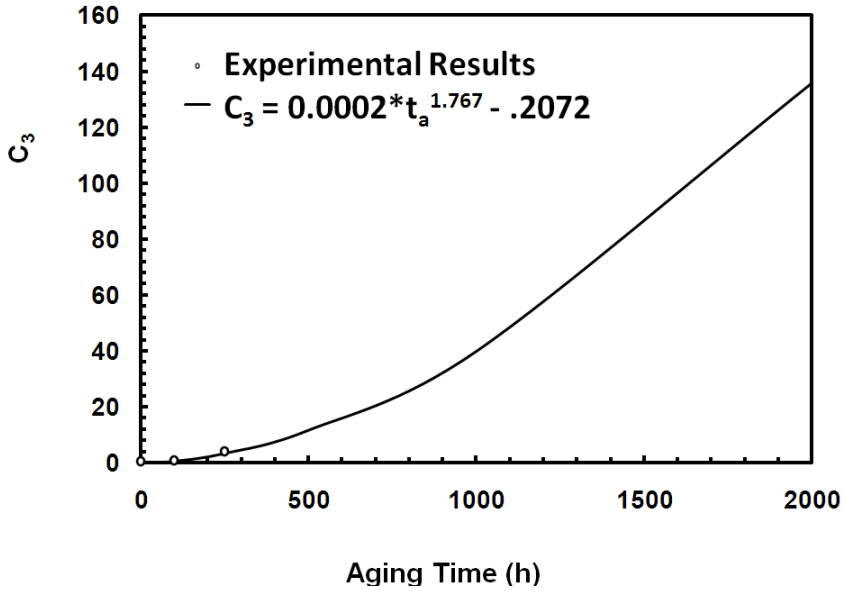

Figure IX.15: Shape Function Parameter, C_3, at 260 °C as a Continuous Function of Prior Aging Time for the PMR-15 Neat Resin Aged at 260 °C in Argon.

The remaining parameters, C_1, k_1, k_2, and k_3, all remained unchanged with increasing aging time.

Predictions of Deformation Behavior of the PMR-15 Neat Resin Subjected to Prior Aging

The continuous functions developed for the model parameters will be used to predict the deformation behavior of PMR-15 tested at 260 °C and aged in argon at 260 °C for 500 h, 1000 h, and 2000 h.

Prior Aging for 500 h

Applying the model parameter continuous functions to the 500 h age group resulted in the parameters listed in Table IX-3.

Table IX-3: Model Parameters Used in the VBOP Predictions of the Deformation Behavior of the PMR-15 Neat Resin at 260 °C Aged in Argon at 260 °C for 500 h.

Moduli	E = 2485.77 MPa, E_t = 75.39 MPa
Isotropic Stress	A = 35 MPa
Viscosity Function	k_1 = 1.0857e+04 s, k_2 = 31.18 MPa, k_3 = 15.82
Shape Function	C_1 = 100 MPa, C_2 =1691.74 MPa, C_3 = 11.54

The stress-strain behavior according to the VBOP is compared to the experimental results for the 500 h age group in Figure IX.16. The strain rate dependence is modeled well. All of the specimens were too brittle to achieve fully established inelastic flow, so it is difficult to say just how well the model predicts the deformation behavior.

The relaxation behavior predicted by the VBOP is compared to the experimental results for the 500 h age group in Figure IX.17. The relaxation behavior for the slower prior strain rates is modeled very well. Results for the higher prior strain rates, however, are not modeled as accurately. The early failures at higher strain rates provide insufficient data making the relaxation behavior of PMR-15 aged for 500 h subjected to a prior strain rate of 10^{-3} s^{-1} inappropriate to model.

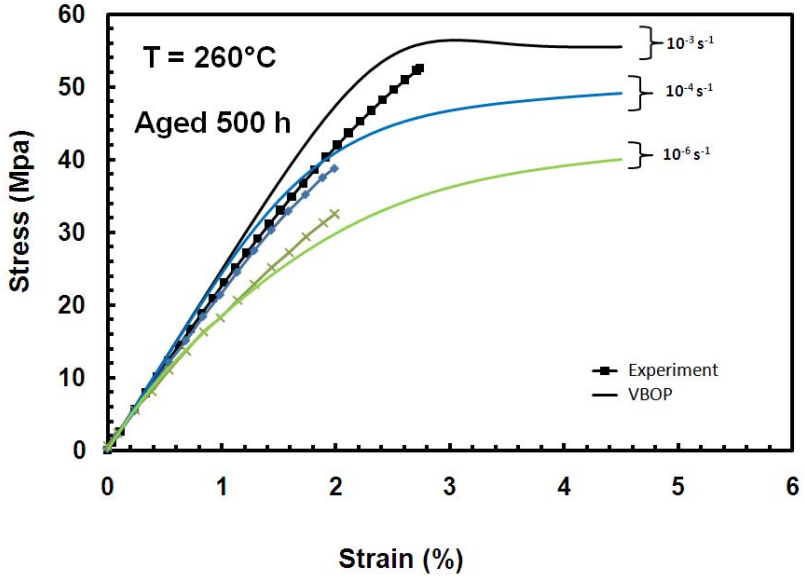

Figure IX.16: A Comparison Between Experimental and Predicted Stress-Strain Curves Obtained for PMR-15 Polymer at Constant Strain Rates of 10^{-3}, 10^{-4}, and 10^{-6} s^{-1} at 260 °C Aged in Argon at 260 °C for 500 h.

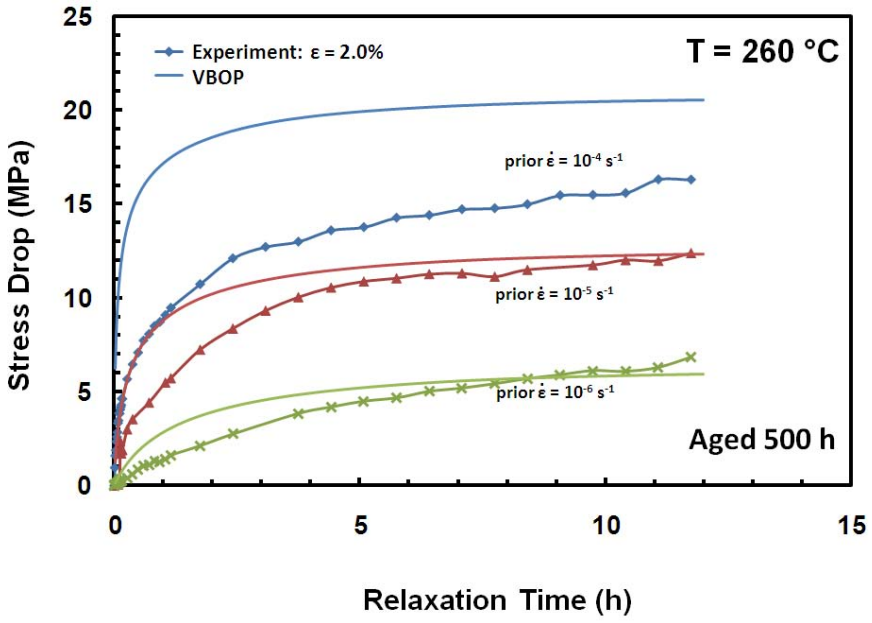

Figure IX.17: A Comparison Between Experimental and Predicted Stress Drop vs Relaxation Time for the PMR-15 Polymer at 260 °C Aged in Argon at 260 °C for 500 h.

The creep curves obtained through this parameter characterization were not nearly as good as previous results. The creep curves from the VBOP and the experimental creep curves are shown in Figure IX.18. The creep curves obtained from a prior strain rate of 10^{-4} s^{-1} are not even close to accurate. It should be noted that the creep curve obtained from the 500 h age group at the prior strain rate of 10^{-4} s^{-1} was not consistent with the rest of the data. So, it is possible that this was an anomaly in testing. Regardless, the VBOP creep curves obtained from a prior strain rate of 10^{-6} s^{-1} match the experimental data surprisingly well.

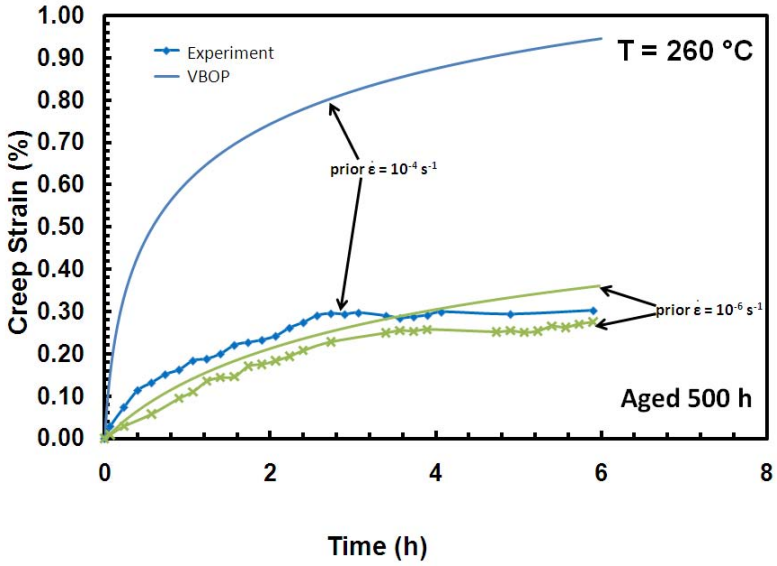

Figure IX.18: Comparison Between the Experimental and Predicted Creep Strain vs Time Curves Obtained for PMR-15 Polymer at 260 °C in Creep at 25 MPa Aged in Argon at 260 °C for 500 h.

The strain rate jump test was also analyzed using the model parameters predicted through the increasing model parameter functions and the values shown in Table IX-3. These results are shown in Figure IX.19. The initial loading is modeled very well. The

specimen fails soon after the strain rate jump occurs. It appears it would join up with the VBOP curve had the failure not occurred. The specimen loaded at the slower strain rate first failed so early after the strain rate jump that it is not even worth showing. This is another tribute to the brittleness of PMR-15 subjected to prior aging for 500 h in argon at 260 °C.

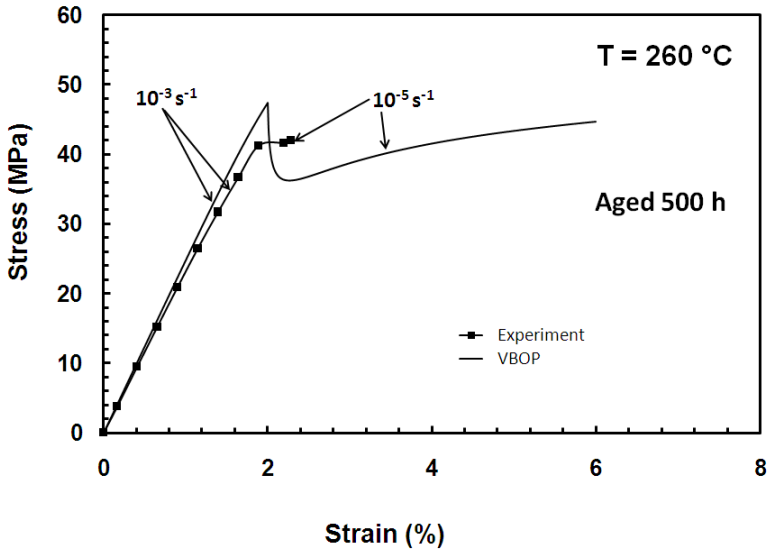

Figure IX.19: A Comparison Between Experimental and Predicted Stress-Strain Curves Obtained for PMR-15 Polymer in the Strain Rate Jump Test at 260 °C with Fast Loading First Aged in Argon at 260 °C for 500 h.

Prior Aging for 1000 h

Applying the model parameter continuous functions to the 500 h age group resulted in the parameters listed in Table IX-4.

Table IX-4: Model Parameters Used in the VBOP Predictions of the Deformation Behavior of the PMR-15 Neat Resin at 260 °C Aged in Argon at 260 °C for 1000 h.

Moduli	E = 2543.72 MPa, E_t = 147.58 MPa
Isotropic Stress	A = 35 MPa
Viscosity Function	k_1 = 1.0857e+04 s, k_2 = 31.18 MPa, k_3 = 15.82
Shape Function	C_1 = 100 MPa, C_2 =1746.01 MPa, C_3 = 39.79

The stress-strain behavior according to the VBOP using the model parameters from Table IX-4 is compared to the experimental results for the 1000 h age group in Figure IX.20. The strain rate dependence is modeled well. The experimental results for the specimen loaded at a strain rate of 10^{-6} s^{-1} shows that the tangent modulus for the model is probably a bit high. However, the shape of the knee of the stress-strain curve is modeled as well as it has been for previous age groups. The specimens loaded at faster strain rates may well follow the VBOP curves had they not failed as early as they did.

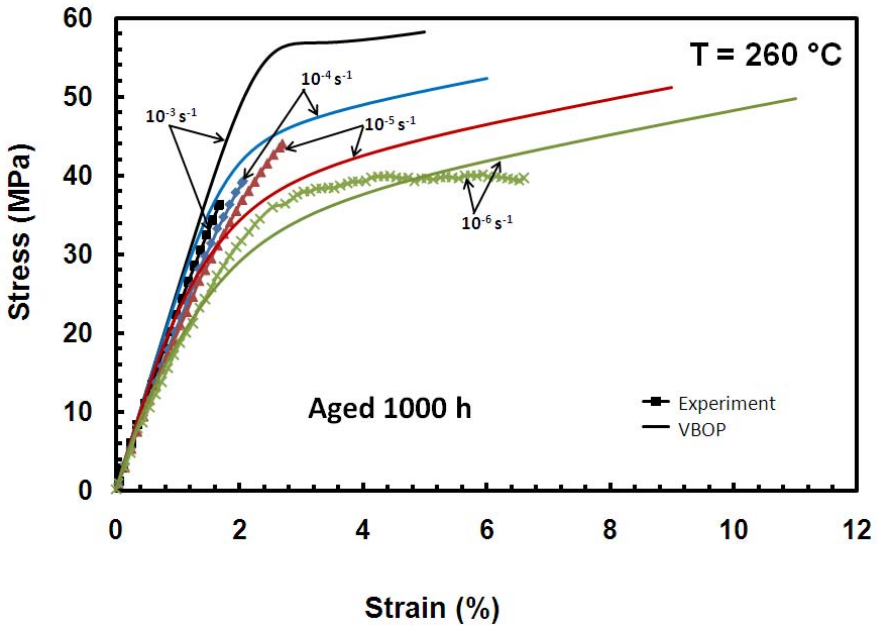

Figure IX.20: A Comparison Between Experimental and Predicted Stress-Strain Curves Obtained for PMR-15 Polymer at Constant Strain Rates of 10^{-3}, 10^{-4}, 10^{-5}, and 10^{-6} s^{-1} at 260 °C Aged in Argon at 260 °C for 1000 h.

The relaxation behavior according to the VBOP is compared to the experimental results for the 1000 h age group in Figure IX.21. The strain rate dependence is again modeled very well. However, the quantitative accuracy of the modeled is not very good. The model is beginning to show its limitations.

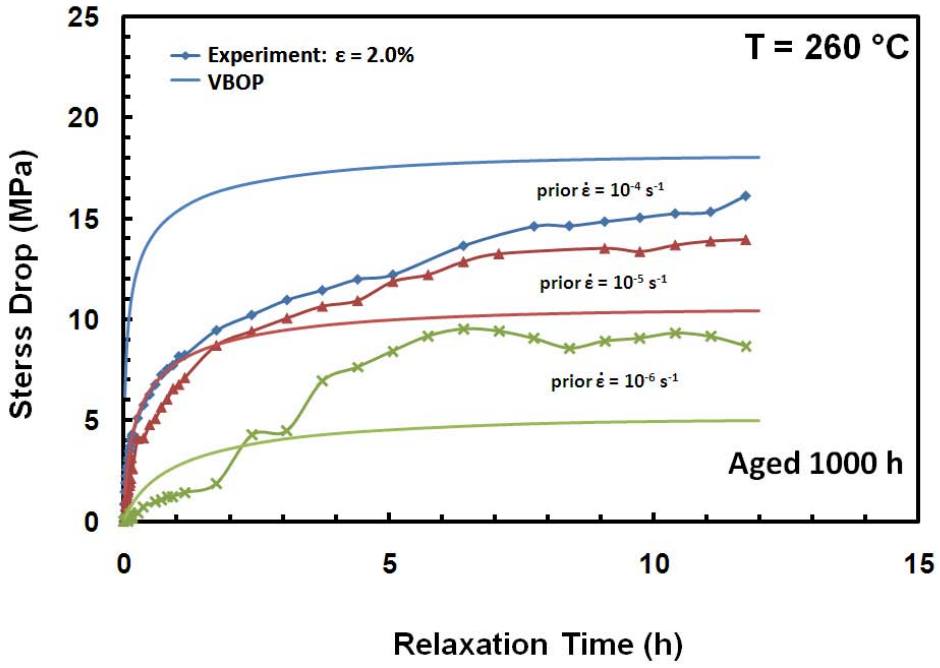

Figure IX.21: A Comparison Between Experimental and Predicted Stress Drop vs Relaxation Time for the PMR-15 Polymer at 260 °C Aged in Argon at 260 °C for 1000 h.

The creep curves for the specimens aged for 1000 h in argon at 260 °C are modeled much better than those obtained for the specimens aged for 500 h. The creep curves from the VBOP and the experimental creep curves for the 1000 h age group are shown in Figure IX.22. The qualitative aspect of creep is modeled well. The strain rate dependence is clearly modeled. The quantitative accuracy is acceptable in the case of the prior strain rate of 10^{-6} s^{-1}, but is not very good for the prior strain rate of 10^{-4} s^{-1}. It is still remarkable that the VBOP is performing as well as it is considering the parameters were defined using insufficient data.

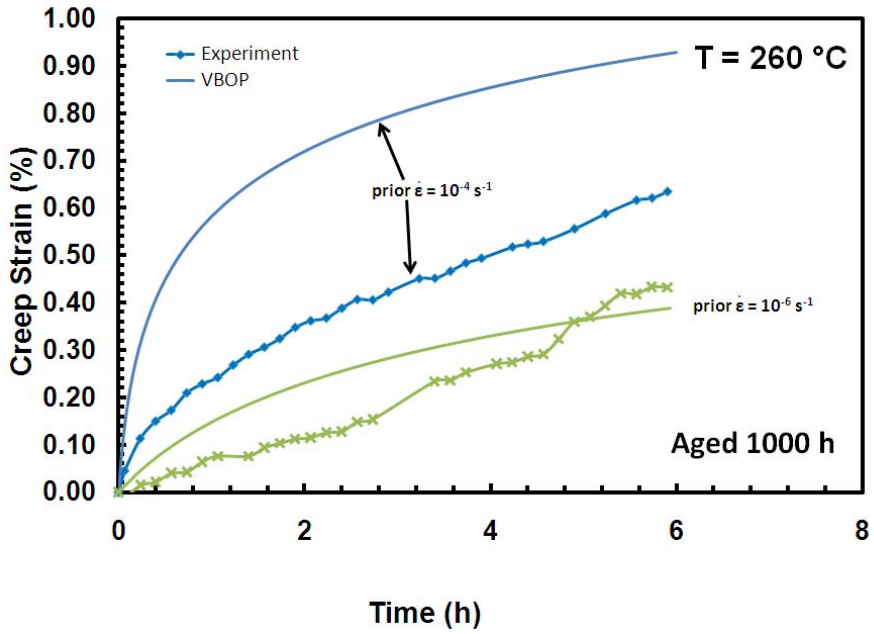

Figure IX.22: Comparison Between the Experimental and Predicted Creep Strain vs Time Curves Obtained for PMR-15 Polymer at 260 °C in Creep at 25 MPa Aged in Argon at 260 °C for 1000 h.

Prior Aging for 2000 h

Applying the model parameter continuous functions to the 2000 h age group resulted in the parameters listed in Table IX-5. Judging from the results of the 1000 h age group, it is assumed that the tangent modulus is probably too high. However, these values will still be used since there is no data to prove otherwise.

Table IX-5: Model Parameters Used in the VBOP Predictions of the Deformation Behavior of the PMR-15 Neat Resin at 260 °C Aged in Argon at 260 °C for 2000 h.

Moduli	E = 2620.18 MPa, E_t = 319.24 MPa
Isotropic Stress	A = 35 MPa
Viscosity Function	k_1 = 1.0857e+04 s, k_2 = 31.18 MPa, k_3 = 15.82
Shape Function	C_1 = 100 MPa, C_2 =1808.34 MPa, C_3 = 135.92

The stress-strain behavior according to the VBOP using the model parameters from Table IX-5 is compared to the experimental results for the 2000 h age group in Figure IX.23. The model clearly shows strain rate dependence. The specimens loaded at strain rates of 10^{-3}, $10^{-4}$and 10^{-5} s^{-1} all failed before departing from quasi-elastic behavior. Therefore, the strain rate dependence is not seen. This does not mean the model is inappropriate. The model is simply showing data corresponding to specimens which might survive higher strains. The specimen loaded at a strain rate of 10^{-6} s^{-1} does enter a region of inelastic flow. And it actually shows that the tangent modulus value is quite appropriate. The slope at the end of the stress-strain curve for the specimen loaded at a strain rate of 10^{-6} s^{-1} appears to be close to parallel with the final slopes of the curves predicted by the VBOP. The flow stress for the specimen loaded at a strain rate of 10^{-6} s^{-1} is higher than the VBOP predicts. This suggests that an increase in the isotropic stress should be considered.

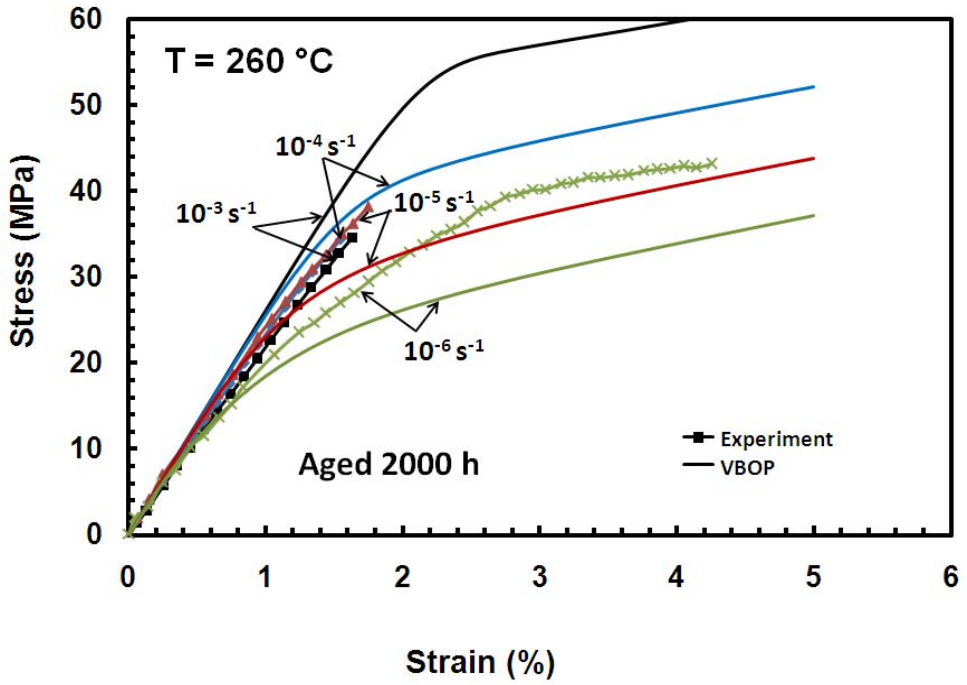

Figure IX.23: A Comparison Between Experimental and Predicted Stress-Strain Curves Obtained for PMR-15 Polymer at Constant Strain Rates of 10^{-3}, 10^{-4}, 10^{-5}, and 10^{-6} s^{-1} at 260 °C Aged in Argon at 260 °C for 2000 h.

The relaxation behavior of the 2000 h age group is shown with its corresponding VBOP model in Figure IX.24. It should be noted that the only specimen to achieve the 2% strain required for relaxation was loaded at a strain rate of 10^{-6} s^{-1}. Thus, it is the only experimental data shown in Figure IX.24. The model predictions for the other strain rates are included in this figure to show what is expected had the specimens not failed early. The VBOP appears to under predict the stress drop during relaxation for the specimen loaded at a strain rate of 10^{-6} s^{-1}. However, an increase in the isotropic stress would fix this problem. This confirms the isotropic stress predicted from the continuous function is too low.

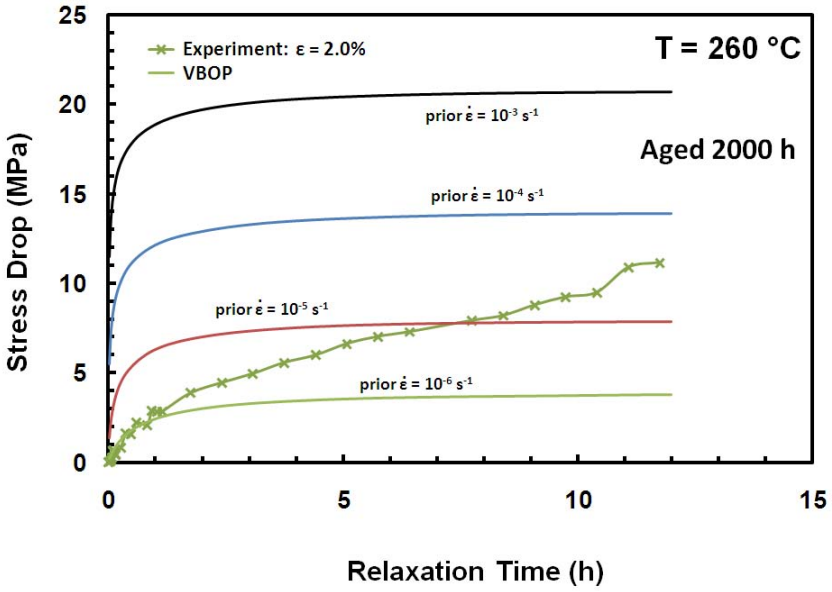

Figure IX.24: A Comparison Between Experimental and Predicted Stress Drop vs Relaxation Time for the PMR-15 Polymer at 260 °C Aged in Argon at 260 °C for 2000 h. Experimental Data is for Prior Strain Rate 10^{-6} s^{-1}.

The creep behavior of the 2000 h age group is plotted against the VBOP predictions for creep in Figure IX.25. The model seems to be decreasing in its accuracy. The strain rate dependence is still modeled, but the quantitative results are not very good. One should exercise caution in using the presented model for the 2000 h age group.

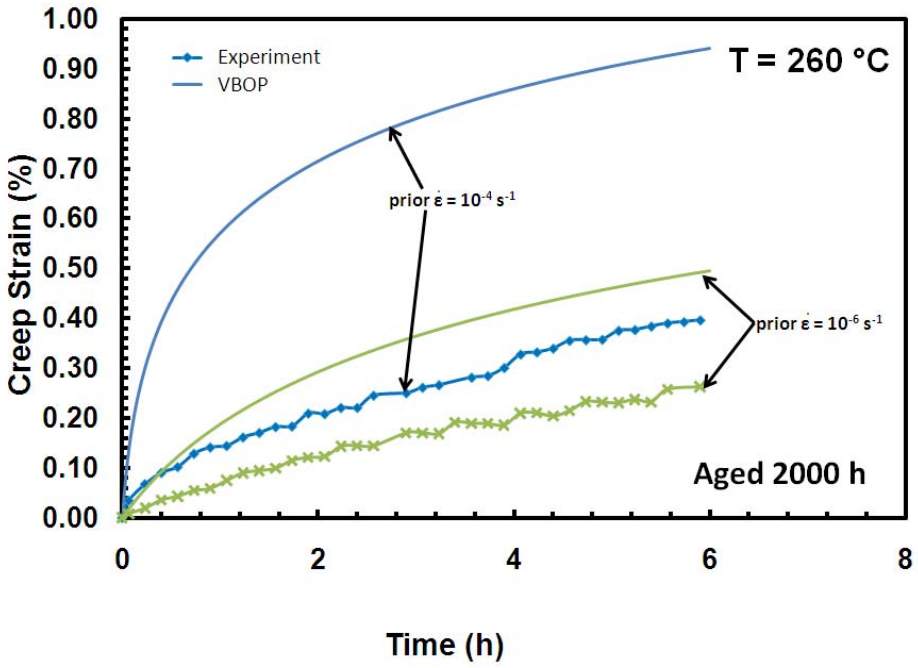

Figure IX.25: Comparison Between the Experimental and Predicted Creep Strain vs Time Curves Obtained for PMR-15 Polymer at 260 °C in Creep at 25 MPa Aged in Argon at 260 °C for 2000 h.

X. Conclusions and Recommendations

Concluding Remarks

The deformation behavior of unaged PMR-15 neat resin was investigated at 260 °C. The experimental results confirmed the rate dependence of PMR-15. Positive, nonlinear strain rate sensitivity was seen for monotonic loading and unloading. Because the material often failed before the inelastic flow could be fully established, changes in the flow stress with changes in strain rate could not be always measured. However, it can be inferred from experimental results that the flow stress increases with increasing strain rate.

The relaxation behavior of unaged PMR-15 neat resin at 260 °C is significantly influenced by the prior strain rate. An increase in prior strain rate leads to an increase in stress drop during relaxation. It appears the stress values at the end of relaxation come to rest below the stress-strain curve for the slowest loading rate suggesting the existence of an equilibrium stress and an equilibrium stress-strain curve. This equilibrium stress-strain curve would have the same shape as the curve produced at a strain rate of 10^{-6} s^{-1} and would be located below the stress-strain curve obtained for the strain rate of 10^{-6} s^{-1}. All specimens tested failed shortly after the loading was resumed following the relaxation period. The inelastic flow was not fully established during reloading.

Recovery strain and creep strain are also significantly influenced by prior strain rate. Both strain recovered at zero stress and strain accumulated during creep increase

with increase in prior strain rate magnitude. Results obtained in the strain rate rate jump test demonstrated that there was no strain rate history effect.

All of the features described for the unaged PMR-15 neat resin suggest the usefulness of the overstress constitutive model in modeling the deformation behavior of this material. The Viscoplasticity Based on Overstress for Polymers (VBOP) was chosen for constitutive modeling. The model characterization procedure developed by McClung [23] was applied to the case of PMR-15 at 260 °C. This procedure was developed to eliminate the necessity of a "guess and check" method of determining the parameters for the VBOP. It was specifically developed using data from the region of fully established inelastic flow. This region can be seen in Figure X.1.

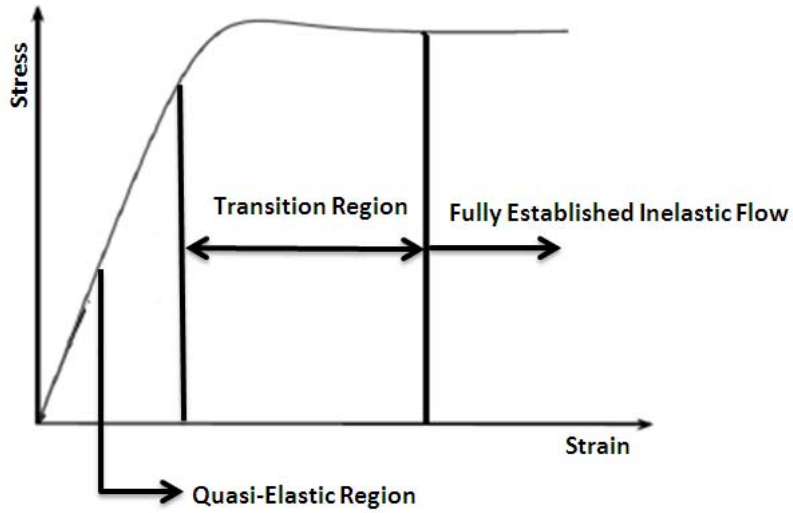

Figure X.1: Stress- Strain Behavior of Viscoplastic Material

As specified before, fully established inelastic flow was not attained at 260 °C. Some specimens even failed before entering the transition region. Therefore modeling

efforts became much more complicated. The isotropic stress, in particular, was not easily calculated as described by McClung. Instead, the very "guess and check" method McClung was attempting to avoid was necessary to determine a value for the isotropic stress. The rest of the parameters were determined using McClung's method. The agreement between model predictions and experimental results was surprisingly good despite the lack of data in the inelastic flow region which is required for the model characterization. In particular, relaxation was modeled very well. The stress-strain response in monotonic loading was adequately modeled. It is impossible to tell just how well the model performs in the transition region since the specimens all failed before the inelastic flow becomes fully established. Conversely, the creep behavior is not represented very well. However, the qualitative aspect of an increase in creep strain accumulation with an increase in prior strain rate is modeled well. The unloading behavior of PMR-15 was modeled with a fair amount of accuracy.

The effects of prior aging in argon at 260 °C on the time-dependent behavior of PMR-15 at 260 °C were also examined. Prior aging does not significantly affect the relaxation behavior of PMR-15. Prior aging does increase the stiffness of the material, but this increase is not very significant. An increase in brittleness is clearly seen with the long aging durations of 500 h, 1000 h and 2000 h as the aged specimens begin to fail earlier than the unaged specimens. The flow stress appears to increase with prior aging time. The increased stiffness due to prior aging is much more apparent in the creep test with a prior loading rate of 10^{-4} s^{-1}. Less strain is accumulated during creep for

specimens aged in argon for longer periods of time. The lack of a strain rate history effect is still shown through the strain rate jump tests.

The VBOP parameters were determined for specimens subjected to prior aging. The model characterization procedure developed by McClung was attempted, but without success. The lack of experimental data in the flow stress region required adjustments in the model characterization procedure. The tangent modulus and the isotropic stress were determined from a "guess and check" method instead of the systematic procedure developed by McClung. This worked well for the prior aging durations of 100 h and 250 h, but was no longer achievable for specimens aged for longer periods of time. Instead, the model parameters determined for the unaged material and for specimens aged for 100 h and 250 h were extended as functions of prior aging time to determine the model parameters for specimens aged for 500 h, 1000 h, and 2000 h. Accurate predictions were obtained with the model parameters found for specimens aged for 500 h. As the model parameters for longer aging times were extrapolated, however, the predictions became less satisfactory.

Comparison with Previous Efforts

PMR-15 was also tested at 288 °C and 316 °C. The most obvious difference between the results obtained for PMR-15 at 260 °C and those obtained at other temperatures was the lack of data in a fully established flow stress region. This made modeling efforts difficult.

Several similarities between the deformation behavior of the unaged PMR-15 at the three temperatures can be noted:

- Positive, nonlinear strain rate sensitivity in monotonic loading
- Dependence of recovery behavior on prior strain rate
- Dependence of creep strain accumulation on prior strain rate
- No strain rate history effect
- Dependence of relaxation behavior on prior strain rate

PMR-15 aged and tested at 316 °C exhibited extreme brittleness [24]. This led to the termination of testing and modeling efforts. Several key effects of prior aging at 288 °C on the inelastic behavior of the PMR-15 resin at 288 °C were similar to those observed for the PMR-15 aged and tested at 260 °C:

- Increase in elastic modulus with prior aging time
- An increase in tangent modulus with prior aging time
- Delayed departure from quasi-elastic behavior with increase in prior aging time
- An increase in the flow stress level with an increase in prior aging time

A key difference in modeling the rate-dependent behavior of PMR-15 at 260 °C and at 288 °C was the shape parameter C_3, which did not remain constant with increase in prior aging time at 260 °C. The value of C_3 for PMR-15 aged and tested at 260 °C was also significantly smaller from the value determined at 288 °C. This is most likely due to the near glassy behavior seen at the lower temperature.

Recommendations

It is recommended that a temperature range be determined where inelastic flow is fully developed for PMR-15 consistently. Then testing and aging can be conducted within the aforementioned temperature range. Data obtained at these additional temperatures will allow the VBOP to be extended to capture the effect of temperature. Ideally, the effect of temperature and prior aging time on the deformation behavior of PMR-15 can be combined into one constitutive model.

Appendix A: MATLAB Scripts for Optimizing Viscosity Function

```
%kfun_full

%Written by Amber McClung
%Modified by Bradley Diedrick

%curve fit the k function

%initial guess based off of previous results
xo=[1.28,3.16,1.2];

%time in hours where data from relaxation at 1e-6, 1e-4, and 1e-3
%will be taken
xdata=[10,10.5,11,11.5,11.983,...
       10,10.5,11,11.5,11.983,...
       10,10.5,11,11.5,11.983];

%time in seconds
xdata=xdata*3600;

%experimental stress drop values for 1e-6, 1e-5, 1e-4, 1e-3
ydata=[6.262,6.303,6.108,6.281,6.112,...
       13.675,13.694,13.663,13.960,13.605,...
       20.788,20.640,20.492,19.991,20.525];

optsnew = optimset('DiffMinChange',1.0e-4);
x =lsqcurvefit(@k_opt_full,xo,xdata,ydata,[0,3,0],[2,5.0,2],optsnew);
k1 = x(1)*1e4 %sec
k2 =x(2)*1e1 %MPa
k3 = x(3)*1e1



function  F = k_opt_full(x,xdata)
%Optimization function

%Written by Amber McClung
%Modified by Bradley Diedrick

%Insert parameters into .dat file
E=2304;
Et=23;

%Isotropic Stress Function Constants
Ac=0;
```

```
Af = 0;
Ao= 30;

%Viscosity Function Constants
k1 = x(1)*1e4 %sec
k2 =x(2)*1e1 %MPa
k3 = x(3)*1e1
 k4 = 0; %Not used
 k5 = 0; %Not used


 %Shape Function Constants (seed values)
C1=  100; %MPa
C2 = 1000; %MPa
C3 = 2; %1/MPa


save('parameters.dat', 'E', 'Et', 'Ac', 'Af', 'Ao', 'k1', 'k2', 'k3',
'k4', 'k5', 'C1', 'C2', 'C3','-ascii')
save('../load/parameters.dat', 'E', 'Et', 'Ac', 'Af', 'Ao', 'k1', 'k2',
'k3', 'k4', 'k5', 'C1', 'C2', 'C3','-ascii')

%Run Function that Calculates the Objective Function
cd ../load/
Load
cd ../relax_stiff
Relax

run_d_2=csvread('run_6_2_relax.csv',1,0);
%run_c_2=csvread('run_5_2_relax.csv',1,0);
run_b_2=csvread('run_4_2_relax.csv',1,0);
run_a_2=csvread('run_3_2_relax.csv',1,0);

%These values are being compared to the experimental values to
determine
%the optimization.  Column 2 represents stress values.  To find the
stress
%drop, subtract the stress value calculated in the run_#_#_relax.csv
file
%at the times determined in kfun_full (xdata) from the first stress
value
%(beginning of relaxation) in the run_#_#_relax.csv file
y=[run_d_2(1,2)-run_d_2([ 36000 37800 39600 41400 43139],2).',...
    run_b_2(1,2)-run_b_2([ 36000 37800 39600 41400 43139],2).',...
    run_a_2(1,2)-run_a_2([ 36000 37800 39600 41400 43139],2).'];

F=y;

return
```

```
%Load

% %VBOP follows Khan and Krempl, JEMT, 2006
%
% %Qualitative Creep at 20 MPa loading at 1Mpa/sec
%
% %Written by: Amber McClung, Feb, 2007 to create VBOP from VBO
%
% %units:
% %stress: MPa
% %strain: mm/mm

%Strain rate four
fprintf('Begin 1.E-6 Rate.\n');
[z,z,z,z,Ai] = materialparams();

lr = 1E-6; %Strain rate that you load at(1/s)
Y0 = [0,0,0,Ai,0,0,lr]; %Initial State Variable Vector
send = 0.11; %Strain that the program stops at
dt = send/lr/1E7;    %Timestep
dts = 1; %Save increment
t = 0;  %Simulation time
ts = 0; %Save timer

options = optimset('FunValCheck','on','MaxIter',10);
[t,Y] = ode45(@VBOEqnsEC,[0:1000:110000],Y0,options);

data=[t(1:dts:end),Y(1:dts:end,1:6)];
csvwrite('run_6_load.csv',data);

Y0=Y(end,:);
clear t Y



%Strain rate three
fprintf('Begin 1.E-5 Rate.\n');

lr = 1E-5; %Strain rate that you load at(1/s)
Y0 = [0,0,0,Ai,0,0,lr]; %Initial State Variable Vector
send = 0.05; %Strain that the program stops at
dt = send/lr/1E7;    %Timestep
t = 0;  %Simulation time
ts = 0; %Save timer

options = optimset('FunValCheck','on','MaxIter',10);
[t,Y] = ode45(@VBOEqnsEC,[0:100:9000],Y0,options);
```

```
data=[t(1:dts:end),Y(1:dts:end,1:6)];
csvwrite('run_5_load.csv',data);

Y0=Y(end,:);
clear t Y


%Strain rate two
fprintf('Begin 1.E-4 Rate.\n');

lr = 1E-4; %Strain rate that you load at(1/s)
Y0 = [0,0,0,Ai,0,0,lr]; %Initial State Variable Vector
send = 0.04; %Strain that the program stops at
t = 0;  %Simulation time
ts = 0; %Save timer

options = optimset('FunValCheck','on','MaxIter',10);
[t,Y] = ode45(@VBOEqnsEC,[0:10:600],Y0,options);


data=[t(1:dts:end),Y(1:dts:end,1:6)];
csvwrite('run_4_load.csv',data);

Y0=Y(end,:);
clear t Y




%Strain rate one
fprintf('Begin 1.E-3 Rate.\n');

lr = 1E-3; %Strain rate that you load at(1/s)

Y0 = [0,0,0,Ai,0,0,lr]; %Initial State Variable Vector
send = 0.06; %Strain that the program stops at
t = 0;  %Simulation time
ts = 0; %Save timer


options = optimset('FunValCheck','on','MaxIter',10);
[t,Y] = ode45(@VBOEqnsEC,[0:1:50],Y0,options);


data=[t(1:dts:end),Y(1:dts:end,1:6)];
csvwrite('run_3_load.csv',data);
```

```
Y0=Y(end,:);
clear t Y



function [E, Et, Ac, Af, Ao, k1,k2,k3,k4,k5,C1,C2,C3] =
materialparams()
%Written by: Aaron Schinder summer 2006

%Modified by: Amber McClung, Feb. 2007
%Modified by: Bradley Diedrick, Nov 2009
%The 11 main material parameters that govern traditional
%VBO behavior
%Ai - initial Isotropic Stress
%This function acts as a series of global variables. It is called
within
%various functions to get the material properties of what you're
%simulating.
%

load('parameters.dat', 'E', 'Et', 'Ac', 'Af', 'Ao', 'k1', 'k2', 'k3',
'k4', 'k5', 'C1', 'C2', 'C3');
%Modulus
E=parameters(1);
Et=parameters(2);

%Isotropic Stress Function Constants
Ac=parameters(3);
Af = parameters(4);
Ao= parameters(5);

%Viscosity Function Constants
k1 = parameters(6); %sec
k2 =parameters(7); %MPa
k3 = parameters(8);
 k4 = parameters(9); %Not used
 k5 = parameters(10); %Not used

 %Shape Function Constants
C1=  parameters(11); %MPa
C2 = parameters(12); %MPa
C3 = parameters(13); %1/MPa


 return



%Relax
```

```
% %VBOP follows Khan and Krempl, JEMT, 2006
%
% Relaxation during constant strain rate jump tests with relaxation
%
% %Written by: Amber McClung, Feb, 2007 to create VBOP from VBO
% %Modified by:  Bradley Diedrick, Nov 2009 to use relaxation values at
2%
%
% %units:
% %stress: MPa
% %strain: mm/mm

%Strain rate four
fprintf('Begin 1.E-6 Rate.\n');
 [z,z,z,z,Ai] = materialparams();
%Y(1) = sig - mechanical stress
%Y(2) = g   - equilibrium stress
%Y(3) = eta - strain
%Y(4) = A   - Isotropic Stress
%Y(5) = f   - Kinematic Stress
%Y(6) = p   - Accumulated Inelastic Stress (used in Beta Function)

%relaxation at 2%
lr = 1E-6; %Prior Strain rate that you load at(1/s)
dt = 0.1;    %Timestep  (arbitrarily chosen, may need to be refined)
dts = 1; %Save increment

tend=12*3600;%12 hours
%Relaxation at 2%
Y0 = [csvread('../load/run_6_load.csv',20,1,[20 1 20 6])]; %Initial
State Variable Vector 45000,
23.9784,19.3934,0.045,20,0.604471,0.0335817

options = optimset('FunValCheck','on','MaxIter',10);
odeset('BDF','on');
[t,Y] = ode15s(@VBOEqnsEC,[0:1:tend],Y0,options);

data=[t(1:dts:end),Y(1:dts:end,1:6)];
csvwrite('run_6_2_relax.csv',data);

 clear t Y

% %Strain rate three
 fprintf('Begin 1.E-5 Rate.\n');

% %relaxation at 2.%
  lr = 1E-5; %Prior Strain rate that you load at(1/s)

%Relaxation at 2.%
```

```
Y0 = [csvread('../load/run_5_load.csv',20,1,[20 1 20 6])]; %Initial
State Variable Vector  4600,
29.6958,19.7164,0.046,20,0.573465,0.0318592

options = optimset('FunValCheck','on','MaxIter',10);
odeset('BDF','on');
[t,Y] = ode15s(@VBOEqnsEC,[0:1:tend],Y0,options);

data=[t(1:dts:end),Y(1:dts:end,1:6)];
csvwrite('run_5_2_relax.csv',data);

 clear t Y

 %Strain rate two
 fprintf('Begin 1.E-4 Rate.\n');
 lr = 1E-4; %Prior Strain rate that you load at(1/s)

% % %
% %Relaxation at 2.%
 Y0 = [csvread('../load/run_4_load.csv',20,1,[20 1 20 6])]; %Initial
State Variable Vector 450, 37.2992,20.147,0.045,20,0.490293,0.0272385

options = optimset('FunValCheck','on','MaxIter',10);
odeset('BDF','on');
[t,Y] = ode15s(@VBOEqnsEC,[0:1:tend],Y0,options);

data=[t(1:dts:end),Y(1:dts:end,1:6)];
csvwrite('run_4_2_relax.csv',data);

 clear t Y

 fprintf('Begin 1.E-3 Rate.\n');
 lr = 1E-3; %Prior Strain rate that you load at(1/s)

% % %
% %Relaxation at 2.%
 Y0 = [csvread('../load/run_3_load.csv',20,1,[20 1 20 6])]; %Initial
State Variable Vector 450, 37.2992,20.147,0.045,20,0.490293,0.0272385

options = optimset('FunValCheck','on','MaxIter',10);
odeset('BDF','on');
[t,Y] = ode15s(@VBOEqnsEC,[0:1:tend],Y0,options);

data=[t(1:dts:end),Y(1:dts:end,1:6)];
csvwrite('run_3_2_relax.csv',data);

 clear t Y
```

Appendix B: MATLAB Scripts for Optimizing Shape Function

```
%shapefun_full.m
%curve fit the shape function

%initial guess at C1, C2, C3
xo=[10,10,.01];

%strain in mm/mm
xdata=[0.0101,0.0132,0.0173,0.0202,...
    0.0254,0.0274,0.0294,0.0314,...
    0.0207,0.0226,0.0256,0.0275];

%Experimental stress values at given strains.  These correspond to the
%knees of the stress strain curves.
ydata=[14.45,18.13,22.50,23.56,...
    38.86,40.20,41.24,41.40,...
    40.85,43.68,47.35,49.35];

optsnew = optimset('TolFun',1e-5,'DiffMinChange',1.0e-4);
x
=lsqcurvefit(@shape_opt_full,xo,xdata,ydata,[0,11,0],[100,15,.1],optsne
w);

C1 = x(1)*1e1
C2 =x(2)*1e2
C3 = x(3)*1e2

load('parameters.dat', 'E', 'Et', 'Ac', 'Af', 'Ao', 'k1', 'k2', 'k3',
'k4', 'k5', 'C1', 'C2', 'C3');
%Modulus
E=parameters(1);
Et=parameters(2);

%Isotropic Stress Function Constants
Ac=parameters(3);
Af = parameters(4);
Ao= parameters(5);

%Viscosity Function Constants
k1 = parameters(6); %sec
k2 =parameters(7); %MPa
k3 = parameters(8);
 k4 = parameters(9); %Not used
 k5 = parameters(10); %Not used

 %Shape Function Constants
```

```
C1=  parameters(11); %MPa
C2 = parameters(12); %MPa
C3 = parameters(13); %1/MPa


function  F = shape_opt_full(x,xdata)
%Optimization function

%Insert parameters into .dat file
E=2304;
Et=23;

%Isotropic Stress Function Constants
Ac=0;
Af = 0;
Ao= 30;

%Viscosity Function Constants
k1 =  1.0857e+004;
k2 =   31.1751;
k3 =   15.8197;
k4 = 0; %Not used
k5 = 0; %Not used


 %Shape Function Constants
C1=  x(1)*1e1 %MPa
C2 = x(2)*1e2 %MPa
C3 = x(3)*1e2 %1/MPa

save('parameters.dat', 'E', 'Et', 'Ac', 'Af', 'Ao', 'k1', 'k2', 'k3',
'k4', 'k5', 'C1', 'C2', 'C3','-ascii')

%Run Function that Calculates the Objective Function

Load

run_6=csvread('run_6_load.csv',1,0);
run_4=csvread('run_4_load.csv',1,0);
run_3=csvread('run_3_load.csv',1,0);


y=[ run_6([10,13,17,20],2).',...
    run_4([25,27,29,31],2).',...
    run_3([20,23,25,28],2).'];

F=y;

return
```

```
%Load.m
% %VBOP follows Khan and Krempl, JEMT, 2006

%
% %Written by: Amber McClung, Feb, 2007 to create VBOP from VBO
%
% %units:
% %stress: MPa
% %strain: mm/mm

%Strain rate four
fprintf('Begin 1.E-6 Rate.\n');
[z,z,z,z,Ai] = materialparams();

lr = 1E-6; %Strain rate that you load at(1/s)
Y0 = [0,0,0,Ai,0,0,lr]; %Initial State Variable Vector
send = 0.11; %Strain that the program stops at
dt = send/lr/1E7;    %Timestep actually not used
dts = 1; %Save increment
t = 0;  %Simulation time
ts = 0; %Save timer

options = optimset('FunValCheck','on','MaxIter',10);
odeset('BDF','on');
[t,Y] = ode15s(@VBOEqnsEC,[0:1000:110000],Y0,options);

data=[t(1:dts:end),Y(1:dts:end,1:6)];
csvwrite('run_6_load.csv',data);

Y0=Y(end,:);
clear t Y



%Strain rate three
fprintf('Begin 1.E-5 Rate.\n');

lr = 1E-5; %Strain rate that you load at(1/s)
Y0 = [0,0,0,Ai,0,0,lr]; %Initial State Variable Vector
send = 0.05; %Strain that the program stops at
```

```
dt = send/lr/1E7;    %Timestep
t = 0;  %Simulation time
ts = 0; %Save timer

options = optimset('FunValCheck','on','MaxIter',10);
odeset('BDF','on');
[t,Y] = ode15s(@VBOEqnsEC,[0:100:9000],Y0,options);

data=[t(1:dts:end),Y(1:dts:end,1:6)];
csvwrite('run_5_load.csv',data);

Y0=Y(end,:);
clear t Y


%Strain rate two
fprintf('Begin 1.E-4 Rate.\n');

lr = 1E-4; %Strain rate that you load at(1/s)
Y0 = [0,0,0,Ai,0,0,lr]; %Initial State Variable Vector
send = 0.04; %Strain that the program stops at
t = 0;  %Simulation time
ts = 0; %Save timer

options = optimset('FunValCheck','on','MaxIter',10);
odeset('BDF','on');
[t,Y] = ode15s(@VBOEqnsEC,[0:10:600],Y0,options);


data=[t(1:dts:end),Y(1:dts:end,1:6)];
csvwrite('run_4_load.csv',data);

Y0=Y(end,:);
clear t Y




%Strain rate one
fprintf('Begin 1.E-3 Rate.\n');

lr = 1E-3; %Strain rate that you load at(1/s)

Y0 = [0,0,0,Ai,0,0,lr]; %Initial State Variable Vector
send = 0.06; %Strain that the program stops at
t = 0;  %Simulation time
ts = 0; %Save timer
```

```
options = optimset('FunValCheck','on','MaxIter',10);
odeset('BDF','on');
[t,Y] = ode15s(@VBOEqnsEC,[0:1:50],Y0,options);


data=[t(1:dts:end),Y(1:dts:end,1:6)];
csvwrite('run_3_load.csv',data);

Y0=Y(end,:);
clear t Y
```

Appendix C: MATLAB Scripts for Power Law Curve Fitting of Model Parameters

```
clc
clear all
close all

ta = [0,100,250,500];

ta = ta(:); %makes ta a column vector

E = [2304,2400,2425,2477];

Starting = [.5, 2, 1300];
options = optimset('Display','iter');
Estimates = fminsearch(@power_law,Starting,options,ta,E)

plot(ta,E,'*')
hold on
plot(ta,Estimates(1)*ta.^Estimates(2)+Estimates(3),'r')



function sse=power_law(params,Input,Actual_Output)
A_1 = params(1); %coefficient on time
A_2 = params(2); %exponent on time
A_3 = params(3); %vertical shift component

Fitted_Curve = A_1*Input.^A_2+A_3;
Error_Vector = Fitted_Curve - Actual_Output(:);

sse = sum(Error_Vector.^2);

return
```

Bibliography

1. Baker, Alan, S. Dutton and D. Kelly, *Composite Materials for Aircraft Structures.* 2nd Edition. Reston: American Institute of Aeronautics and Astronautics, 2004.

2. Black, S. "Are High-Temp Thermosets Ready to Go Commercial?" *High Performance Composites* (2004).

3. Bordonaro, C.M. and E. Krempl. "A state Variable Model for High Strength Polymers." *Polymer Engineering and Science* 35.4 (1995): 310-316.

4. Bordonaro, Christine Marie. *Rate Dependent Mechanical Behavior of High Strength Plastics: Experiment and Modeling.* Rensselaer Polytechnic Institute. Troy, NY, 1995.

5. Bowles, K. J., et al. "Longtime Durability of PMR-15 Matrix Polymer at 204, 260, 288, and 316 °C." TM 210602 2001.

6. Broeckert, J. L. and M.B. Ruggless-Wrenn. "Effects of Prior Aging at 288 °C in Air and in Argon Environments on Creep Response of PMR-15 Neat Resin." *Journal of applied Polymer Science* 111 (2009): 228-236.

7. Broeckert, Joseph L. *Effects of Prior Aging at Elevated Temperature in Air and in Argon Environments onCreep Response of PMR-15 Neat Resin at 288 °C.* Master's thesis. Air Force Institute of Technology. Wright-Patterson Air Force Base, Ohio, 2007.

8. Chuang, K. "Development of DMBZ-15 High-Glass-Transition-Temperature Polyimides as PMR-15 Replacements Given R&D 100 Award." (n.d.).

9. Daniel, I.M. and O Ishai. *Engineering Mechancis of Composite Materials.* Oxford: Oxford University Press, 1994.

10. Falcone, C. M. and M. B. Ruggles-Wrenn. "Rate Dependence and Short-Term Creep Behavior of a Thermoset Polymer at Elevated Temperature." *Journal of Pressure Vessel Technology* 131 (2009).

11. Falcone, Christina. *Some Aspects of the Mechanical Response of PMR-15 Neat Resin at 288 °C: Experiment and Modeling.* Master's Thesis. Air Force Institute of Technology. Wright-Patterson Air Force Base, Ohio, 2006.

12. Green, J.A.S et al. *New Materials for Next Generation Commercial Transports.* Washington DC: National Academies Press, 1996.

13. Ho, K. *Application of the Viscoplasticity Theory Based on Overstress to the Modeling of Dynamic Strain Aging of Metals and to the Modeling of the Solid Polymers, Specifically to Nylon 66.* Ph.D. Thesis. Rensselaer Polytechnic Institute. Troy, NY, 1998.

14. Kelley, Anthony and Carl Zweben, *Comprehensive Composite Materials.* New York: Elsevier, 2000.

15. Krempl, E, J.J. McMahon and D. Yao. "Viscoplasticity Based on Oversterss with a Differential Growth Law for the Equilibrium Stress." *Nonlinear Constitutive Relations for High Temperature Application-1984 Symposium Proceedings.* Cleveland, OH: NASA Conference Publication 2369, 1984. 25-50.

16. Krempl, E. "Cyclic Creep: An Interpretive Literature Survey." *Weld. Res. Counc. Bull.* no. 195 (1974): pp. 63-123.

17. Krempl, E. *Unified Constitutive Laws of Plastic Deformation.* San Diego: Academic Press, 1996.

18. Krempl, Erhard and F. Khan. "Rate (time)-Dependent Deformation Behavior: An Overview of some Proiperties of Metals and Solid Polymers." *International Journal of Plasticity* 19 (2003): 1069-1095.

19. Krempl, Erhard. "From the Standard Linear Solid to the Viscoplasticity Theory Based on Overstress." *Proceedings of the International Conference on Computational Engineering science.* Ed. S.N. Atluri, G. Yagawa and T.A. Cruse. Hawaii: Springer, 1995. 1679-1684.

20. Krempl, Erhard. "The Role of Aging in the Modeling of Elevated Temperature Deformation." *Proceedings of the International Conference.* Ed. Wilshire B. and D. R. J. Owen. Swansea, Wales: Pineridge Press, 1981. 201-211.

21. McClung, A. J. W. and M. B. Ruggles-Wrenn. "Strain Rate Dependence and Short-Term Relaxation Behavior of a Thermoset Polymer at Elevated Temperature: Experiment and Modeling." *Journal of Pressure Vessel Technology* 131 (2009).

22. McClung, A. J. W. and Ruggles-Wrenn M. B. "The Rate (Time)-Dependent Mechanical Behavior of the PM-15 Thermoset Polymer at Elevated Temperature." *Polymer Testing* 27 (2008): 908-914.

23. McClung, Amber J. W. *Extension of Viscoplasticity Based on Overstress to Capture the Effects of Prior Aging on the Time Dependent Deformation of a High-Temperature Polymer: Experiments and Modeling.* PhD Dissertation. Air Force Institute of Technology. Wright-Patterson Air Force Base, Ohio, 2008.

24. Ozmen, Ozgur. *Effects of Prior Aging at 316 °C in Argon on Inelastic Deformation Behavior of PMR-15 Polymer at 316 °C: Experiment and Modeling.* Master's Thesis. Wright Patterson AFB, OH: Department of Aeronautics and Astronautics, Air Force Institute of Technology, 2009.

25. Riande, Evaristo et al, ed. *Polymer Viscoelasticity: Sterss and strain in Practice.* Marcel Dekker, Inc, 2000.

26. Schapery, R.A. "On the Characterizatin of Nonlinear Viscoelastic Materials." *Polymer Engineering and Science* 9 (1969): 295-310.

27. Tsuji, L.C., H. L. McManus and K. J. Bowles. "Mechanical Properties of Degraded PMR-15 Resin." TM 208487 1998.

28. Westberry, Candice M. *Rate Dependence and short-Term reep Behavior of PMR-15 Neat Resin at 23 and 288 °C.* Master's Thesis. Air Force Institute of Technology. Wright-Patterson Air Force Base, Ohio, 2005.

REPORT DOCUMENTATION PAGE		*Form Approved* *OMB No. 0704–0188*

1. REPORT DATE (DD–MM–YYYY)	2. REPORT TYPE	3. DATES COVERED *(From — To)*
05-03-2010	Master's Thesis	Sept 2008 – Mar 2010

4. TITLE AND SUBTITLE	5a. CONTRACT NUMBER
Effectsof Prior Aging at 260 °C in Argon on Inelastic Deformation Behavior of PMR-15 Polymer at 260 °C: Experiment and Modeling	5b. GRANT NUMBER
	5c. PROGRAM ELEMENT NUMBER
6. AUTHOR(S) Bradley K. Diedrick, 2nd Lt, USAF	5d. PROJECT NUMBER
	5e. TASK NUMBER
	5f. WORK UNIT NUMBER
7. PERFORMING ORGANIZATION NAME(S) AND ADDRESS(ES) Air Force Institute of Technology Graduate School of Engineering and Management (AFIT/ENY) 2950 Hobson Way WPAFB OH 45433-7765	8. PERFORMING ORGANIZATION REPORT NUMBER AFIT/GAE/ENY/10-M08
9. SPONSORING / MONITORING AGENCY NAME(S) AND ADDRESS(ES) Dr. Joycelynn Harrison Air Force Office of Scientific Research (AFOSR) 875 N Randolph St. Suite 325 Rm. 3112 Arlington, VA 22203	10. SPONSOR/MONITOR'S ACRONYM(S) AFOSR
	11. SPONSOR/MONITOR'S REPORT NUMBER(S)

12. DISTRIBUTION / AVAILABILITY STATEMENT
APPROVED FOR PUBLIC RELEASE; DISTRIBUTION UNLIMITED

13. SUPPLEMENTARY NOTES

14. ABSTRACT

The inelastic deformation behavior of PMR-15 neat resin, a high-temperature polymer, was investigated at 260 °C. The experimental program was designed to explore the influence of strain rate on loading and unloading behaviors. In addition, the effect of prior strain rate on creep, relaxation, and recovery responses was evaluated. The material exhibits positive, nonlinear strain rate sensitivity in monotonic loading. Early failures occur before inelastic flow is fully established. The creep, relaxation, and recovery responses are significantly influenced by prior strain rate. The experimental data were modeled using the Viscoplasticity Based on Overstress for Polymers (VBOP) theory. The effects of prior aging in argon at 260 °C on the time (rate)-dependent behavior of the PMR-15 polymer were evaluated in a series of strain controlled experiments. Several of the VBO material parameters were expanded as functions of prior aging time. The resulting model was used to predict the behavior of PMR-15 subjected to various prior aging durations.

15. SUBJECT TERMS
Polymer, PMR-15, creep, recovery, relaxation, prior strain rate, nonlinear viscoplastic theory, aging

16. SECURITY CLASSIFICATION OF:			17. LIMITATION OF ABSTRACT	18. NUMBER OF PAGES	19a. NAME OF RESPONSIBLE PERSON Marina B. Ruggles-Wrenn, PhD
a. REPORT	b. ABSTRACT	c. THIS PAGE	UU	163	19b. TELEPHONE NUMBER (Include Area Code) (937)255-3636, ext 4641
U	U	U			

Standard Form 298 (Rev. 8–98)
Prescribed by ANSI Std. Z39.18